UNIVERSITAT DE BARCELONA

Cytoskeletal modulation of single-cell branching

Delia Ricolo

Programa de Doctorado del Departamento de Genética
Facultad de Biología
Universidad de Barcelona (UB)

Cytoskeletal modulation of single-cell branching

Memoria presentada por

Delia Ricolo

Para optar al grado de

Doctor por la Universidad de Barcelona

La Directora	La alumna	La tutora
Dra. Sofia Araùjo	Delia Ricolo	Dra. Montserrat Corominas

Barcelona, Marzo 2017

Cover: ganglionic terminal cell and stalk st14 from btl>shotCGFP stained with anti GFP(gray), CBP (cyan) and anti CP309 (red).

The research in this PhD was carried out under the supervision of Dra. Sofia Araújo at the laboratory of Morphogenesis in *Drosophila*, headed by Prof. Jordi Casanova, belonging to the Research Program of Cell and Developmental Biology of the Institute for Biomedical Research of Barcelona (IRB) and the Department of Developmental Biology of the Molecular Biology Institute of Barcelona (IBMB).

This research was funded by Ministerio de Educacion Cultura y Deporte by means of Ph.D. FPU fellowship to the author of this thesis.

I feel that, in a sense, the writer knows nothing any longer. He offers the reader the contents of his own head, a set of options and imaginative alternatives. His role is that of a scientist, whether on safari or in his laboratory, faced with an unknown terrain or subject. All he can do is to devise various hypotheses and test them against the facts.
— J. G. Ballard

Cuarta ley de las revisiones:
Después de cuidadísimos y exactísimos análisis de una muestra, siempre resulta que no era esa la que se tenía que analizar.
— Arthur Bloch

A Sofia

Jordi y Nico

INDEX

1 INTRODUCTION

1 INTRODUCTION

1.1 Inside the Cell

In the 17th century, in the first important work on microscopy, "Micrographia", Robert Hooke wrote:

> *"I took a good clear piece of Cork and with a Pen -Knife Sharpen'd as keen as a Razor, I cut a piece of it off, and thereby left the surface of it exceeding smooth, then examining it very diligently with microscope, me thought I could perceive it to appear a little porous".*

He named such little porous (**Fig. 1**) "**cells"**, from latin *cella,* meaning small room. Since 1665, scientists and philosophers have been intrigued to know the function and the contents that define such small rooms. Today, we know that inside the cell tremendous and complex systems interact between them, giving rise to the basal unit of life. In this thesis, I report my journey through a special cell type of *Drosophila melanogaster* that is able to generate a capillary tube within its cytoplasm. The journey was mainly done through its cytoskeleton components, which are instrumental in inducing the morphogenetic events responsible for the formation of this type of unicellular tube. In this introductory section I am going to describe some general aspects of the cytoskeleton, then I give a general overview about how cells are able to form tubular structures, and in particular I describe the model system used during my work, the *Drosophila* tracheal system. Lastly, I describe the "inside" of embryonic terminal cell, and the state of art about its ability to make a subcellular lumen.

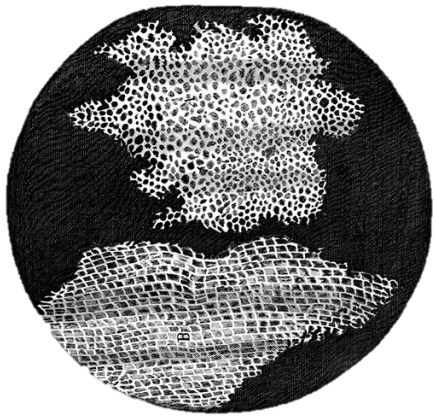

Figure 1. First cell description. Robert Hooke's drawing of the cellular structure from a thin cutting of cork. Figure adapted from Micrographia, 1665.

1.1.1 Cytoskeleton

The cytoskeleton is a dynamic three-dimensional structure that fills the cytoplasm of all cells from all domains of life (Wickstead and Gull, 2011).

The cytoskeleton spatially organizes the contents of the cell, connects the cell physically and biochemically to the external environment and generates coordinated forces that enable the cell to move and change shape. To achieve these functions, the cytoskeleton integrates the activity of a multitude of cytoplasmic proteins and organelles. Despite the connotations of the word 'skeleton', the cytoskeleton is not a fixed structure whose function can be understood in isolation. Rather, it is a **dynamic and adaptive structure** whose component polymers and regulatory proteins are in constant flux (Fletcher and Mullins, 2010).

Microtubules (MTs), intermediate filaments (IFs) and microfilaments (MFs) are the three main structural components of the cytoskeleton in eukaryotic cells. Because in *Drosophila melanogaster*, the model used in this thesis, IFs are not present (or their presence is controversial), I will focus on the microtubules and the microfilaments. Both are polymers formed by basic unit proteins, tubulin for microtubules and actin for microfilaments. The polymerization and depolymerisation of microtubules and actin filaments generate forces that drive changes in cell shape and that, together with associated cytoskeleton protein, guide the organization of cellular components. Many classes of regulatory proteins control the activity of cytoskeleton polymers. In general, we can distinguish nucleation factors, which catalyse the initial formation,

polymerization and depolymerisation factors that promote fast growth and disassembly of filaments, cross-linkers and stabilizing proteins which reinforce the higher order structure, capping proteins that terminate filament growth and finally, "communicator" proteins that integrate information between different cytoskeleton components.

1.1.2 Microtubules

Microtubules participate in many aspects of cell physiology; they serve as "rails" for intracellular transport, are involved in cell division and regulate many aspects of morphogenesis. MTs are hetero-polymers of **α and β tubulin** organized in head to tail configuration. The repetition in tandem of these subunits makes lineal proto-filaments that associate laterally to form the wall of a microtubule cylindrical structure (**Fig. 2**). MTs are characterized by an intrinsic polarity with two distinct ends: a faster growing plus end (at which β-tubulin is exposed) and the slower growing `minus' end (at which α-tubulin is exposed). MTs switch between phases of growth, and disassembly and such process is named "dynamic instability". Such behaviour allows MTs to explore cellular regions and retract in case they do not find the proper environment (Kapitein and Hoogenraad, 2015).

The dynamic properties of the two ends are markedly different. The **plus ends**, which often extend the cell periphery and explore the cellular space, represents the core of MT dynamicity, displaying phases of rapid growth and shortening. However, microtubule plus ends can also be stabilized, with their dynamics reduced due to attachment to different cellular structures, such as the cell cortex. It is generally accepted that MTs **minus ends** in cells never grow, possibly due to capping by specific factors, such as the γ-tubulin ring complex (Akhmanova and Hoogenraad, 2015), (described below).

The MTs dynamic behaviour is orchestrated by several factors. An important group are **microtubule plus-end tracking proteins** (+TIPs), which are structurally and functionally diverse proteins, distinguished by their specific and dynamic accumulation at microtubule plus ends. This dynamic localization (which has also been called 'surfing' on the plus ends) was initially discovered by observing the live behaviour of the CLIP-170–green fluorescent protein (GFP) fusions, which appeared as comet-like structures coinciding with the tips of polymerising MTs (Akhmanova and Hoogenraad, 2005). Some +TIPs like XMAP215, recruit tubulin dimers and increase the rate of tubulin addition to the plus end. Other +TIPs, such as the end-binding proteins (EBs), can

increase MT polymerization rates recruiting other +TIPs and modulating the structure of MT ends. Another important function of some +TIPs is to modulate the interaction between the MT plus end and other cellular components such as membranes and actin (Akhmanova and Steinmetz, 2015; Galjart, 2010). The dynamic instability of MT not only depends on +TIPs but also requires the coordinated actions of many additional regulatory factors named **microtubule-associated proteins** (MAPs). In the classical view MAPs bind tubulin at multiple binding sites and stabilize microtubules by suppressing dissociation of the subunits. Currently in the literature, the "denomination" microtubule associated protein is linked to a large group of proteins that in general interact with microtubules: for example motor proteins (e.g., kinesins and dynein) that use the energy from ATP hydrolysis to step along microtubule tracks to transport cargo (Goshima and Vale, 2003); another group includes crosslinking proteins that align filaments with a specific geometry and stabilize structures (Bratman and Chang, 2008); the third set comprises proteins that modulate the amount of microtubule bundles that interact with nucleation proteins (Luders and Stearns, 2007; Subramanian and Kapoor, 2012).

One of the best-studied MAPs are MAP2/Tau. They are mainly neuronal proteins, responsible for microtubule bundle assembly and stabilization. It has been proposed that this class of proteins induces rigidity by inhibiting depolymerisation (Butner and Kirschner, 1991; Dehmelt and Halpain, 2005).

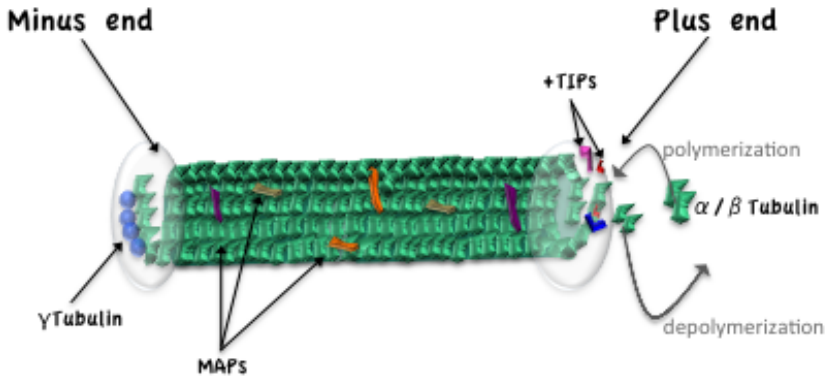

Figure 2. Schematic representation of a microtubule. Heterodimers of α and β tubulin are organized in linear proto-filaments that associate laterally, giving rise to cylindrical structure. α and β tubulin polymerize and depolymerize at the plus end where +TIPs are accumulated. MAPs bind proto-filaments along the microtubule in different binding site. The minus end faces proteins involved in nucleation like γ-tubulin.

It should be emphasized that, due to the intrinsic dynamism of MTs, there is not a clear border between the different activity of MT-interacting proteins, so stabilizing proteins can influence the polymerization/depolymerisation and proteins involved in plus end growth can influence the degree of MT stabilization.

The many different function of MTs are possible also by regulation of **post-transcriptional modification** (PTMs), which allows significant variability in dynamics and remodelling of the microtubule network. For example, acetylation of tubulin is fairly common and can be found on stable microtubules in most cell types. The tyrosination is associated with the new tubulin incorporated at the plus end. So, also tubulin PTMs influence the stability and structure of MT assemblies. Whether this is a direct effect of tubulin modification on microtubule structure or an indirect effect due to regulation of microtubule associated proteins, is an open question (Hammond et al., 2008).

1.1.3 Microtubule Organizing Centers

As mentioned before, the minus ends of MTs in cells do not growth and are often densely clustered in central regions of the cell, where they can be stabilized through attachment to nucleation sites. **γ-tubulin**, the third main member of the tubulin superfamily, as described below, is a primer player in MT nucleation and organization in all eukaryotes (Lin et al., 2015). The cellular site or the "discrete foci" from where microtubules are generated is named microtubule organizing center (MTOC) (Brinkley, 1985).

In nature, different kinds of MTOCs are found but the best-documented MTOC in eukaryotic cells is the **centrosome**, localized in the cytoplasm, during interphase or at the poles of mitotic spindle in dividing cells. The centrosome consists in an area where two orthogonally, 'mother' and 'daughter' centrioles are embedded in a matrix, formed by a dynamic collection of proteins, named **pericentriolar material** (PCM) (**Fig.3**). During cell cycle, centrioles are synthetized in new daughter cells by duplication from pre-existing centrioles from the mother cell. Centrosome duplication occurs during G1/S transition and must be coupled to the events of nuclear cell cycle; failure to coordinate duplication and mitosis results in abnormal number of centrosomes and aberrant mitosis (Lacey et al., 1999).

Between the several hundred of proteins making the PCM there are scaffold proteins, involved in forming the foundations of the PCM. In many cases, such proteins are involved in centriole duplication, as well as assembly and maintenance of the PCM core.

For example, *Drosophila* Asterless (Als), the homolog of human Centrosomal protein 152 (Cep152), is a protein required for the initiation of centriole duplication as well as for maintenance and assembly of PCM (Blachon et al., 2008). Other proteins in the PCM are exclusively involved in centriole duplication like *Drosophila* Spindle assembly abnormal 4 (Sas-4), related to the human microcephaly protein Centromere Protein J (CenpJ) and the *C. elegans* centriolar protein SAS-4 (Leidel and Gonczy, 2003). *Drosophila* Sas-4 is essential for centriole replication in flies; *sas-4* mutants start to lose centrioles and centrosomes during embryogenesis and later in development no centrioles and centrosomes are detectable (Basto et al., 2006). On the other hand, the overexpression of *sas-4*, induces the de novo formation of centriole-like structures in *Drosophila* (Peel et al., 2007). Another PCM component, essential during centriole duplication is the *Drosophila* serine/threonine protein kinase PLK4/SAK, a Polo-like kinase whose human homolog is PLK4. Several studies show that down-regulation of *SAK*, by genetic mutation or RNAi, leads to loss of centrioles (Bettencourt-Dias et al., 2005). Moreover, *SAK* overexpression conditions have been associated with centriole over-duplication (Peel et al., 2007). Within the PCM-scaffold proteins there are also organizer components such as Cp309, also known as Pericentrin-like protein (PLP) that associates with centrioles and is required for efficient recruitment of other PCM components.

In the centrosome area, more peripherally localized, there are effector pericentriolar proteins involved directly in MT nucleation (**Fig.3**). γ-tubulin is the prime component in microtubule nucleating material that catalyses the initiation of α and β tubulin polymerization (Luders and Stearns, 2007). The γ -tubulin associates with defined partner proteins named γ -tubulin ring proteins (Grip). In *Drosophila,* Dgrip84 and Dgrip91 together with γ -tubulin assemble into the γ -tubulin small complex (γ -TuSC) then, outer Dgrip subunits (like Dgrip75, Dgrip128, and Dgrip163) associate with the γ -TuSC, to form the large γ tubulin complex, referred as γ tubulin ring complex (γ –TuRC) because of its characteristic ring shape observed by electron microscope (Luders and Stearns, 2007). The γ –TuRC is the functional core of the microtubule organizing centre because acts as a scaffold for α / β tubulin dimers to initiate polymerization (Brodu et al., 2010).

Accumulating evidence suggests that, in addition to the well-characterized centrosomal MT nucleation, cells also employ **acentrosomal MTOCs**, which also require the γ-TuRC, but utilize different recruiting factors to target to different MT nucleation sites. Acentrosomal arrays of MTs are frequently generated in differentiated polarized cells, like neuronal or epithelial cells (Bartolini and Gundersen, 2006). An example of

acentrosomal MTOC exists in the context of the tracheal system and I will describe it below.

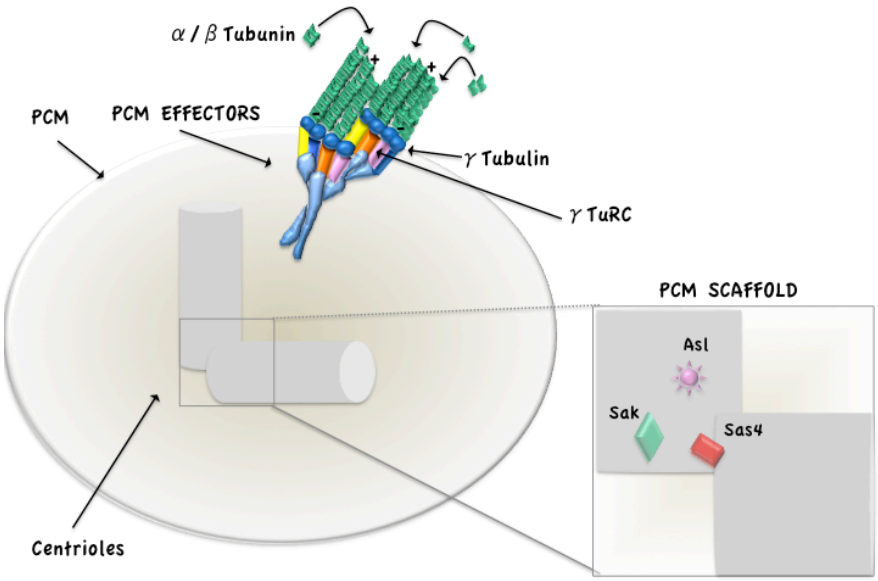

Figure 3. The centrosome is the major Microtubule Organizing Centre (MTOC). Two orthogonal centrioles (in grey) are surrounded by pericentriolar material (PEM) forming the centrosome area (in light beige). Internal PCM Proteins like Asl, SAK and Sas-4 are involved in duplication and maintenance of centrioles. Effector proteins, peripherally localized, like components of γ-tubulin ring complex (γTuRC) act nucleating microtubules (in green). Figure adapted from Conduit P. et al., 2016.

1.1.4 Actin

Microfilaments are other components of the cytoskeleton. Because during the course of this work, I have studied, albeit only tangentially, such components, I will make a brief overview about actin and related higher- order structures.

Actin is involved in motility, trafficking, generation and maintenance of cell morphology and polarity. Individual actin molecules (actin monomers) are globular proteins having tight binding sites that mediate head-to-tail interactions with two other actin monomers, so that they polymerize to form filaments (**F-Actin**). A myriad of proteins, generally named **actin binding protein** (**ABPs**) orchestrate the dynamics of actin filaments. Like MTs, there are proteins involved in polymerization, assembly/disassembly, stabilization, nucleation and crosslinking with other cellular structures. The actin filament network is

organized in a higher-order structure forming two-dimensional or three-dimensional networks with the properties of semisolid gels (Cooper, 2000).

A rich area of actin filaments in the cell localizes in the *cortex,* a narrow zone just beneath the plasma membrane. In this region, most actin filaments are arranged into a network that excludes most organelles from the cortical cytoplasm (**Fig. 4 i)**). Several ways to organize the cortical actin are observed in distinct cell types. In epithelial cells, cortical actin filaments are part of a three-dimensional network that fills the cytosol and anchors the cell to the substratum. The cell cortex is organized and maintained by different kind of factors including the Ezrin, Radixin and Moesin (ERM) proteins, which have the ability to interact with both the plasma membrane and filamentous actin.

The most important higher-order structure formed by actin is found at the edge of moving or spreading cells. These cells dynamically interact with and probe their environment by growing finger-like structures named **filopodia** (**Fig. 4 iv)**) composed of unbranched bundled actin filaments oriented with their growing ends toward the membrane (Blanchoin et al., 2014). The dynamics of filopodia are mainly caused by the actin rich core or shaft, which sits inside the filopodial membrane and continuously undergoes changes like growth, shrinking, bending, and rotation (Leijnse et al., 2015). ENA/VASP proteins, which are found at the filopodial tip, are important organizing factors that promote actin filament elongation and elaboration of filopodial structure (see below), (Lebrand et al., 2004). The other actin higher-order structure found in moving and spreading cells, is the lamellipodia (**Fig. 4 iii)**), which consists in a quasi-two-dimensional actin network formed via the assembly filaments beneath the leading edge membrane. Excluded from the lamellipodia/filopodia region, but present throughout the rest of the cell are the contractile fibres (**Fig. 4 ii)**). These structures are bundles of unbranched actin filaments of mixed polarity.

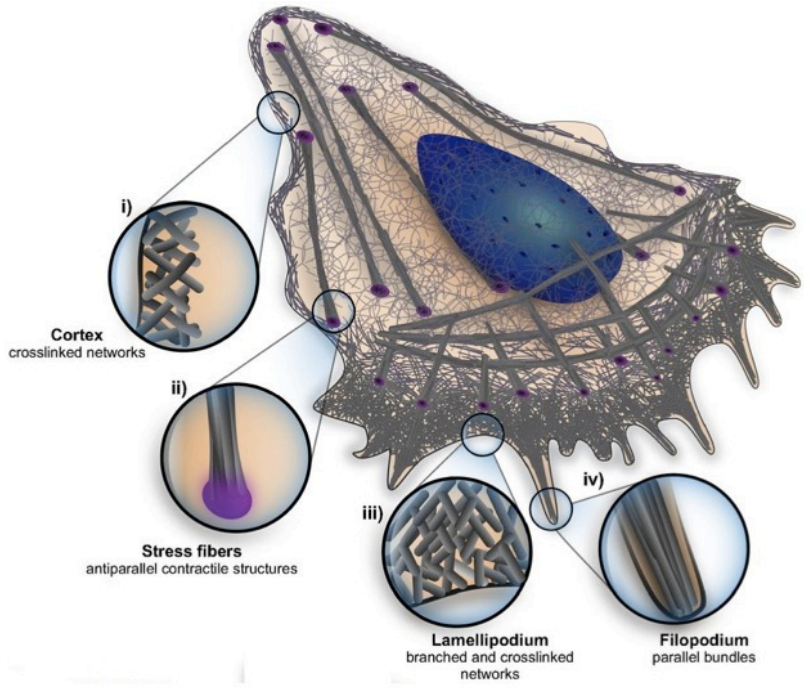

Figure 4. Schematic representation of the cell with the different actin organization architectures : *i*) the cell cortex; *ii*) an example of a contractile fiber, the stress fiber; *iii*) the lamellipodium; and *iv*) filopodium. The zoom regions highlight architectural specificities of different regions of the cell. Figure from Blanchoin L. et al., 2013.

1.1.5 Actin microtubules crosstalk

Although actin and microtubules have distinct properties and form different networks, they are intricately linked together. The organization of these links and the resultant architecture of the cytoskeletal networks have a central role in transmitting compressive and tensile stresses and in sensing the mechanical microenvironment. When the cell divides, changes shape, polarizes and migrates the connection between actin and MTs is critical (Fletcher and Mullins, 2010). An important instance of actin-MTs coordination in cells consists in guidance of MT growth by bundles of F-actin. This occurs in migratory cells where growing MTs ends are targeted at actin filaments in focal adhesion to regulate their turnover or in extending cells like axons of neuronal cells where the plus end of MTs extends inside filopodia consolidating the direction of cell growth. Primary players in actin/microtubule crosstalk are spectraplakins.

1.1.6 Spectraplakins; the giants

Spectraplakins are evolutionarily conserved enormous proteins with up to 9000 amino acids (aa) able to bind, regulate and integrate the function of all classes of cytoskeleton components and link them at other cell components (**Fig. 5**). The best-studied spectraplakins to date are **Short-stop** (**Shot**) in *Drosophila*, the two human and mouse spectraplakins Bullous Pemphigoid Antigen 1 (BPAG1/dystonin/BP320) and Microtubule–Actin Cross-linking Factor 1 (MACF1/Actin Cross-linking Family 7/ACF7), as well as VAB-10 in *Caenorhabditis elegans*. Even if in *Drosophila and in C. elegans* is present only one gene and in mammals (human and mouse) just two, all the genomic loci of spectraplakins generate **numerous isoforms** characterized by different combination of conserved functional domains related with Spectrin, Plakin and GAS2 like proteins, for this reason, spectraplakins are often considered belonging to all these three protein families (**Fig. 5**), (Hahn et al., 2016).

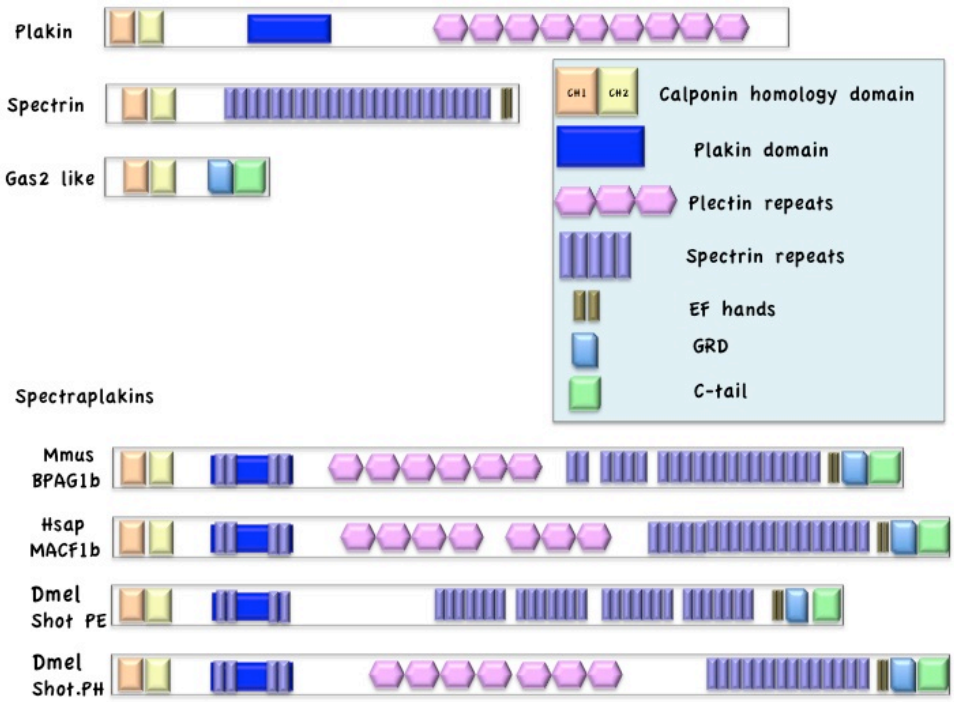

Figure 5. Family association and functional domains of spectraplakins. Plakin, spectrin and GAS2-like protein families share functional domains with spectraplakin protein superfamily. The functional domains are represented in boxes and running from N-terminal to C-terminal; two calponin domain CH1 and CH2 form the actin binding domain (ABD). The plakin homology domain interacts with integrins and trans-membrane protein. The spectrin repeats act as spacer regions and dimerization domains. Plectin domains generally bind intermediate filaments. The two helix–loop–helix EF-hand motifs bind calcium to regulate

actin network and MT association. The Gas2-related domain (GRD) binds MTs and together with C-tail protects them against destabilization. The flexible positively charged C-tail region binds end-binding proteins (EB1) and induces MTs polymerization.
On the bottom are shown the longest isoform of mouse BPAG1, the longest isoform of human MACF1, and the long Shot-PE and Shot-PH isoforms. Figure adapted from Hahn., 2015

1.1.6.1 Domains in spectraplakins

Most spectraplakins harbour at their N-terminal an actin binding domain composed by two **calponin domains** CH1 and CH2. The CH1-CH2 actin-binding domains of mammalian ACF7/MACF1, BPAG1 and *Drosophila* Shot spectraplakins bind to F-actin strongly and with similar dissociation constants (Roper et al., 2002; Yang et al., 1996). The CH1 domain by itself binds actin, although with a lower affinity than a CH1–CH2 tandem domain. The CH2 domain by itself has an even weaker affinity for actin. It has been described that some isoforms of mammalian and invertebrate spectraplakins have only CH2 domain and these isoforms interact only weakly with F-actin (Karakesisoglou et al., 2000; Leung et al., 1999).

The **spectrin repeats**, folded in α-helices, provide flexibility to the spectrin and spectraplakin proteins and enable them to respond elastically to applied extensions or mechanical forces. It has been proposed that spectrin repeats acts as a spacer region between functional domains at the NH_2 and COOH termini. In *Drosophila,* it has been proposed that Shot is able to switch between an opened and a closed state. In the "opened state", Shot cross links actin and microtubules and in a "closed state" Shot is folded through interactions between its NH_2-terminal actin-binding domain and COOH-terminal EF-hand-GAS2 domain. This inactive conformation is targeted to the growing microtubule plus end by EB1. The spectrin repeats are responsible for the protein folding required for the interaction between N-terminus and C-terminus and consequent intramolecular inhibition (Applewhite et al., 2013). Data from spectrin proteins suggest that spectrin repeats are also involved in dimerization (Begg et al., 2000).

The **plakin domain**, characterized by a high α-helical content, is a region for protein-protein interaction. Such domain is typically involved in the interaction with membrane proteins, in particular with integrin and trans-membrane collagens (Jefferson et al., 2004).

Plectin repeat domain (PRD) generally confers the ability to bind IF and is present in few spectroplakin isoforms. *Drosophila* lacks cytoplasmic IFs, but an isoform of Shot

containing conserved plectin repeats exists, so the PRD may have functions that extend beyond IF binding (Hahn et al., 2016).

The two helix–loop–helix **EF-hand** motifs are formed by one hand that binds calcium and another hand, which is independent of calcium. The calcium binding EF hand motif is involved in regulating the association between MTs and Actin. In particular, it has been proposed to regulate switching between open and close conformation (Applewhite et al., 2013). Moreover the EF-hand is also involved in interaction with actin and its regulation (Sanchez-Soriano et al., 2009).

In the proximity of the C-terminus there are the domains interacting with MTs. The **GAS2** related domain (GRD) is present in all spectraplakins. It was initially found in MACF, as a microtubule-binding region. Isolated GAS2 domain of Shot, MACF and BPAG1 colocalizes with bundles of MTs (Jefferson et al., 2004). Some studies in muscle-tendon junction cells suggest that GRD interacts with plus end of MTs supporting polymerization (Subramanian et al., 2003). However, work in neurons supports the idea that the GRD is involved in protecting MTs against destabilization by cooperating with the nearby flexible and positively charged region **C-terminal tail** (C-tail) (Alves-Silva et al., 2012). The C-tails of all Spectraplakins and Gas2-like proteins are poorly conserved at the sequence level but despite sharing a high content in glycines, serines, and arginine. In *Drosophila* neurons and fibroblasts it has been described that the GRD and C-tail together confer to Shot the ability to stabilize MT bundles, like the classical MAPs. Interestingly, the C-tail in addition to interacting with MT shafts, strongly accumulates at their polymerizing plus ends and interacts with EB1, encouraging MT polymerization (Alves-Silva et al., 2012). All spectraplakin functional domains are represented in **Fig.5**.

1.1.6.2 Short-stop: one gene many proteins with different functions

In *Drosophila*, the *shot* gene consists of 78kb placed in position 50C6-11 of chromosome 2R and it has been predicted to give rise to 22 RNA/protein isoforms. This high number of isoforms is due to the presence of **multiple alternative transcription start sites** and through the **alternative splicing** of 43 coding exons (Hahn et al., 2016). Four transcription start points (*P1-P4*) generate four families of Shot isoforms differing between them in the N-termini and classified as Shot -L(A), -L(B), -L(C) and -L(D) (Lee et al., 2000), (**Fig. 6**). Isoforms A and B contain both CH1 and CH2 domains, but they differ in unique sequences upstream of the calponin domain (143 aa for isoform A and

32aa for isoform B). Isoform C contains only the CH2 of calponin domain and a unique sequence of 210 aa at the N-termini. Finally, isoform D does not contain a calponin domain at all. Alternative splicing in the middle and at the C-terminal domain can introduce additional diversity (Lee et al., 2000) (**Fig. 6**). The impressive variety of Shot isoforms reflects its tremendous functional diversity.

Shot acts in a wide range of cellular processes, in which **different domains play context-specific functions**. The first documented phenotype associated with *shot* was published in the 90s regarding neuromuscular connectivity (Vactor et al., 1993). During the last two decades *shot* null alleles or severe loss-of function mutants have been related to different defective aspects of nervous system, epidermis, muscle attachment, foregut, wing, oocyte and tracheal system development.

The role of Shot has been widely investigated in neurons (**Fig. 7**). To build a neural network, neurons send out processes in a regulated manner, to contact target tissues. Neuronal growth is characterized by local sprouting of neurites in the target areas and terminal arborisation on the surface of target cells. Neurite growth and movement is carried out by specialized migrating structures named **growth cones**. Growth cones extend filopodia and distinct changes in the actin cytoskeleton cause newly assembling MTs to accumulate at the base of these filopodia, consolidating a new part of the axon or dendrite. *shot* mutations affect terminal branch formation of embryonic motoneurons and local sprouting of their dendrites in the central nervous system (Prokop et al., 1998a). Also dendrites of sensory neurons in *shot* mutants are greatly shorter, (Bottenberg et al., 2009; Gao et al., 1999; Prokop et al., 1998a) and many structural neuronal proteins like Futsch and Fas2 fail to compartmentalise in *shot* mutant (Bottenberg et al., 2009; Lee et al., 1999; Prokop et al., 1998a). Interestingly, not all neurons require Shot function in fact in *shot* null allele some central and neuro-muscular neuron seem to develop normally (Lohr et al., 2002).

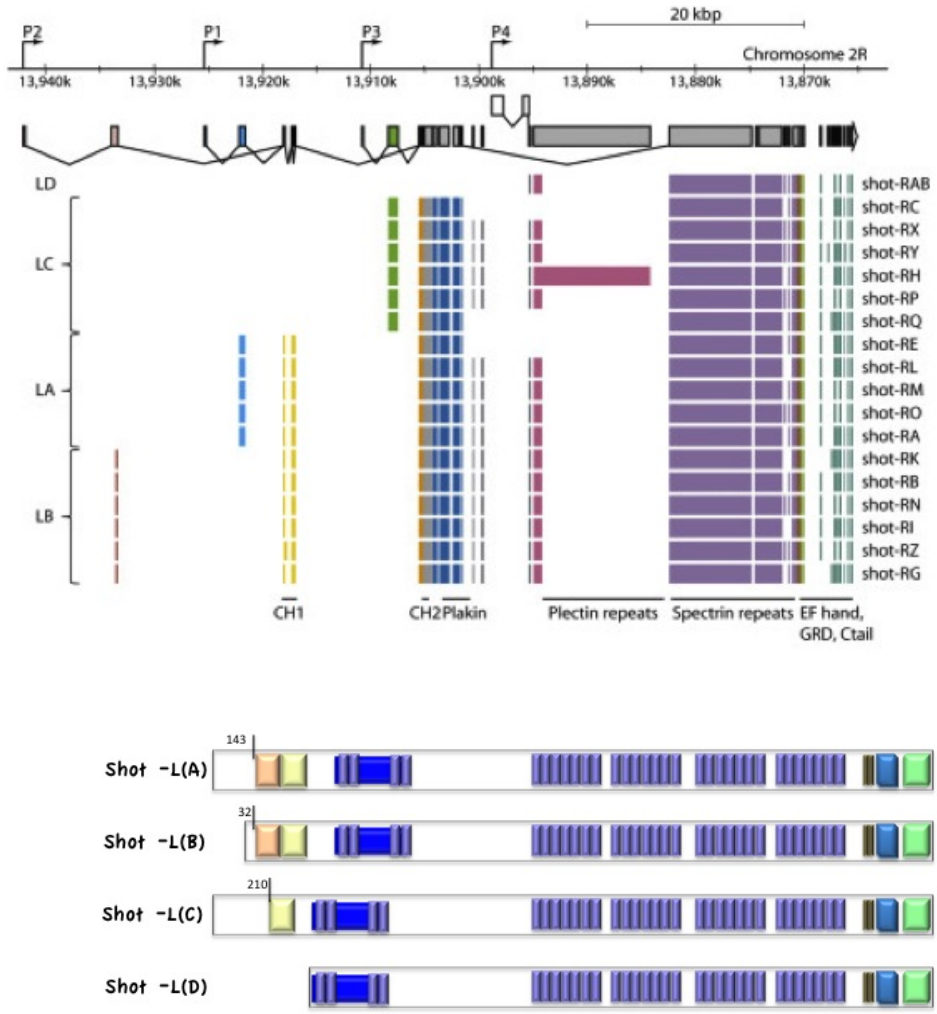

Figure 6. *shot* locus and Shot family isoforms. In the first panel the organisation of the *shot* genomic locus is shown (~80kb) and four alternative transcriptional start sites are depicted (*P1*, *P2*, *P3*, *P4*). Coloured boxes represent exons and splicing is only shown for alternative starts or where exons are bypassed. The resulting different transcripts are shown below the gene. The colours of the exons indicate the domain they encode, consistent with the bottom panel and fig.5. The different isoform are referred as R/P A-Z (R is for transcript and P for protein). It is not experimental evidence that all isoform predicted are transcribed.

The panel on the bottom represents longest members from the four isoforms family (Shot –Long A-D). Shot L (A) (represented Shot PE) and Shot L (B) (represented Shot PB) contain CH1 and CH2 calponin domain, Shot (L) C (represented Shot P C) contain only CH1 and Shot L (D) (represented Shot R RAB) lacks actin binding domain. Figure adapted from Hahn I. et al., 2015.

It has been described that shorter axons in *shot* mutant are associated with an important disorganization of MTs bundles and reduction of filopodia. The MT disorganization observed in *shot* mutant has been primarily associated to defective **actin and MT linkage**. This function depends on three different simultaneous mechanism: (1) binding

of N-terminal calponin homology domains to F-actin, (2) association of MTs through the Gas2-related domain and the positively charged C-terminal tail, and (3) binding of C-terminal tail to EB1 (End-Binding protein 1) at the MT plus ends (Alves-Silva et al., 2012; Bottenberg et al., 2009; Lee and Kolodziej, 2002b; Sanchez-Soriano et al., 2009). Therefore, Shot with its C-tail binds EB1 at the plus ends of polymerising MTs, and at the same time binds actin through its calponin domain and guides MTs along actin structures in the direction of axon growth (**Fig. 7, box 1**). Therefore the isoform -L (A), specifically expressed in the neuronal cells, is necessary for correct axonal extension. (Lee and Kolodziej, 2002b; Sanchez-Soriano et al., 2009). Reduction in filopodia number does not depend on actin and MT linkage but it has been demonstrated that the EF-hand domain is required for **proper filipodia formation**, probably due to its interaction with other proteins involved in the growth cone organization (**Fig. 7 Box 2**) (Lee et al., 2007; Sanchez-Soriano et al., 2009).

Like MAPs, Shot is also able to **stabilize microtubules** in neurons because the GRD domain, together with the positive charged C-terminal tail, stabilises MTs against depolymerisation (**Fig. 7 box 3**). The domains at the C-terminal jointly mediate a robust association along the shaft and at the tip of MTs that is required for both MT guidance and stabilisation (Alves-Silva et al., 2012; Prokop et al., 2013).

Recent studies demonstrate that Shot and Tau have an overlapping role in stabilizing MTs during development and maintenance of synapsis. Loss of *tau* and *shot* induce defects in MTs and trigger an internal stress-signalling pathway known as the JNK pathway. Activating JNK signalling blocks the transport of synaptic materials along axons, which prevents the formation of new synapses and starves existing synapses leading to their decay (Voelzmann et al., 2016). So, Shot and Tau act upstream of a regulatory cascade ensuring adequate delivery of synaptic proteins.

Shot has also been extensively analysed in specialized epidermal cells, called tendon cells.

Drosophila has an exoskeleton formed by an extracellular matrix (ECM) called cuticle, which is secreted from the apical surface of the epidermis (Broadie et al., 2011). Muscle tips anchor to the opposite basal surface of the epidermis via integrin and ECM-dependent junctions (Prokop et al., 1998b). To support the muscular pulling forces, the epidermis forms specialized tendon cells at these anchor points which contain dense arrays of actin and MT filaments linking the basally attached muscles to the apical cuticle on the other side. In this context, Shot is required for linking the basal, integrin-dependent

junctional complexes to the cytoskeleton, and their functional loss causes intracellular rupture at these junctions. Studies in tendon cells, so far, revealed that Shot is required for the integrity of MT arrays but not actin arrays (Alves-Silva et al., 2008). This function is absolutely dependent on the MT-binding C-terminal GRD and C-tail, partly the spectrin-repeats, but not at all the ABD or plakin-like domain (Bottenberg et al., 2009).

Shot is involved in many other developmental processes. These include development of the foregut, where Shot is involved in Notch signalling (Fuss et al., 2004); salivary gland organization, where Shot anchors minus ends of MTs (Booth et al., 2014); the compound eye, where Shot is involved in junctional morphogenesis (Mui et al., 2011); oocytes where Shot is required for MT linkage to an internal membrane structure, the fusome, and where Shot together with Patronin is involved in assembling noncentrosomal MTOC (Nashchekin et al., 2016) and polarises MTs to direct membrane trafficking and microvilli formation (Khanal et al., 2016). Shot is also involved in the embryonic development of tracheal system as described below.

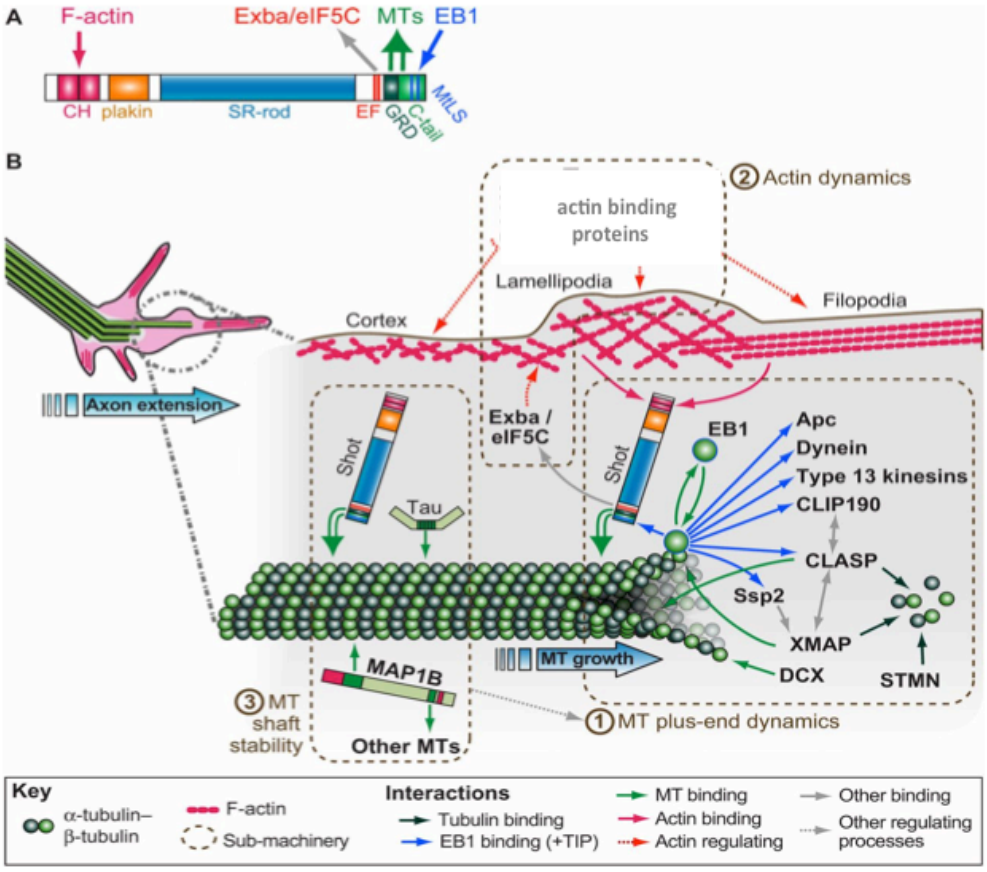

Figure 7. Role of Shot during axon extension. (**A)** Schematic representation of Shot L (A) and its functional domains. (**B)** A single MT and different organization of actin filaments within a growth cone of

a neuronal cell. Three different Shot functions related with cytoskeleton machinery are highlighted and numbered. **(1) Regulation of MT plus-end dynamics**; Shot binds EB1, which directly binds MT plus ends and recruits others +TIPs (blue arrows). When bound to EB1, it links MT plus ends to F-actin via its N-terminal CH domains and guides polymerising MT plus ends in the direction of axon growth. The proper localisation of Shot at MT plus ends requires direct association with MTs through its GRD and C-terminal tail. **(2) Actin dynamics**; The Shot–actin linkage is influenced by actin regulators (red stippled arrows) that coordinate the dynamics and structure of F-actin networks (cortex, lamellipodia, filopodia). In the context of filopodia formation, Shot contributes to the regulation of F-actin through binding of Exba/eIF5C at its EF-hand motifs. **(3) MTs shaft stabilization**; Shot with GRD and C-tail binds along MT shaft and stabilizes them like Tau and others MAPs. The stabilization of MTs is independent of its linkage to F-actin. Figure adapted from Prokop A. et al. 2013.

1.2 Cells making tubes

Understanding how complex organ structure is generated within multicellular organisms is a fascinating topic in developmental biology. A commonly tissue design is **a network of cellular tubes**, which functions in the transport of liquids and gases throughout the body. Tubes are the fundamental structural units of many organs, including the vascular system, exocrine glands, digestive tract, lung and kidney. Through evolution, as metazoans evolved into larger creatures, tubes became essential for transporting and distributing metabolites. Biological tubes are characterized by a remarkable diversity of sizes and complexity. Many tubular organs develop from the organization of polarized epithelial cells of ectodermal, mesodermal and endodermal origin like the neuronal tube, the vascular system and the respiratory system. Tubes can be very large, but with relatively simple organization, as demonstrated by the massive multicellular tube of the intestine. They can also form organs of extreme complexity, such as the human lung, which includes some of hundreds conducting and respiratory airways. Tubes can be small, such as small vertebrate capillaries, the *C. elegans* kidney cell or the *Drosophila* tracheal terminal cell tube. Many key components in tube formation and branching are conserved throughout evolution (Iruela-Arispe and Beitel, 2013).

1.2.1 Tube architecture; seamed and seamless

The first feature of a tube is a **lumen** (from Latin *lūmen*, meaning "an opening"); the space in the interior of a hollow tubular structure. Different cell solutions to make a lumen are described and conserved in vertebrates as well as in invertebrates (Lubarsky and Krasnow, 2003).

Tubes can be organized essentially in “seamed “ or “seamless”. Seamed tubes can be multicellular or unicellular and are characterized by intercellular or auto-cellular junction. The main morphology of big size tubes is a multicellular structure where several cells are organized around the lumen resulting in an extensive network of junctions connecting these cells. In this structure, polarized cells face the lumen with the apical membrane and the basal membrane defines the outline of the tube (**Fig. 8A**). The mammalian lung, and the main branch in *Drosophila melanogaster* tracheal system are examples of these kinds of tubes.

Then there are tubular structures formed by several unicellular seamed tubes in which cells intercalate and fold themselves, with their apical membrane facing towards the lumen to form a unicellular tube with an auto-cellular junction (**Fig. 8B**). Such tubes are found in the tracheal system of *Drosophila melanogaster* and in some cells of the excretory tract in *C. elegans* (Nelson et al., 1983). Tubes named **seamless**, lack junctional seams and instead possess a luminal space surrounded by a continuous **subcellular apical membrane** (**Fig. 8C**). Although not as richly documented in the literature as larger seamed tubes, seamless tubes have been described in the vertebrate vascular system, the fly respiratory system, and the nematode renal system (Sundaram and Cohen, 2016).

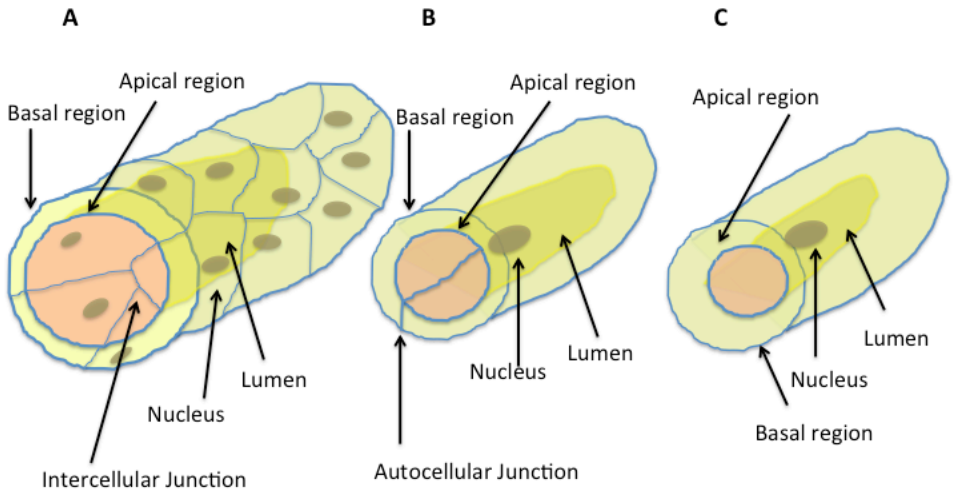

Figure 8. Different tube organizations; (**A**) Several cells interact between them through intercellular junctions, giving rise to a multicellular seamed lumen. (**B**) A single cell folds itself and forms a unicellular seamed tube generating an auto-cellular junction. (**C**) A single cell generates a subcellular lumen without junction along the tube resulting in a seamless tubular structure.

1.2.2 Cellular mechanisms of seamless tube formation

Three different mechanisms of seamless tube formation are described in literature (Sigurbjornsdottir et al., 2014; Sundaram and Cohen, 2016), (**Fig. 9**). "**Cell hollowing**" is a mechanism of seamless tube formation based on pinocytosis. The cell internalizes basal plasma membrane in the form of vesicles and generates an apical domain subcellularly by vesicle coalescence. Subcellular lumen initiates because small cytoplasmic vesicles fuse to each other (**Fig. 9A**). This seamless tube mechanism formation is observed in endothelial cell culture, like human umbilical vein endothelial cells HUVEC cells grown in 3-D matrices (Davis et al., 2000). Cell hollowing has been also described for several models in vivo like the *C. elegans* single excretory kidney cell (Buechner, 2002), and zebrafish blood vessels (Kamei et al., 2006). Second mechanisms is "**wrapping model**" in which the cell first folds up itself generating an auto-junction and then, probably by a mechanism of fusion membrane, melts the junction (**Fig. 9B**). This mechanism is found in some mammalian kidney cells and in zebrafish vasculature. Another mechanism described is "**apical membrane invagination**". In this case the lumen is generated by the invagination and growth of new apical membrane inside the cell. The process of subcellular lumen formation is associated with elongation of the cell (**Fig. 9C**). Both subcellular lumen formation and cell elongation depend by vesicles trafficking guided by a specific **rearrangement of cytoskeleton** (see below). This model of seamless tube generation came out from studies in *Drosophila* tracheal system (Gervais and Casanova, 2010).

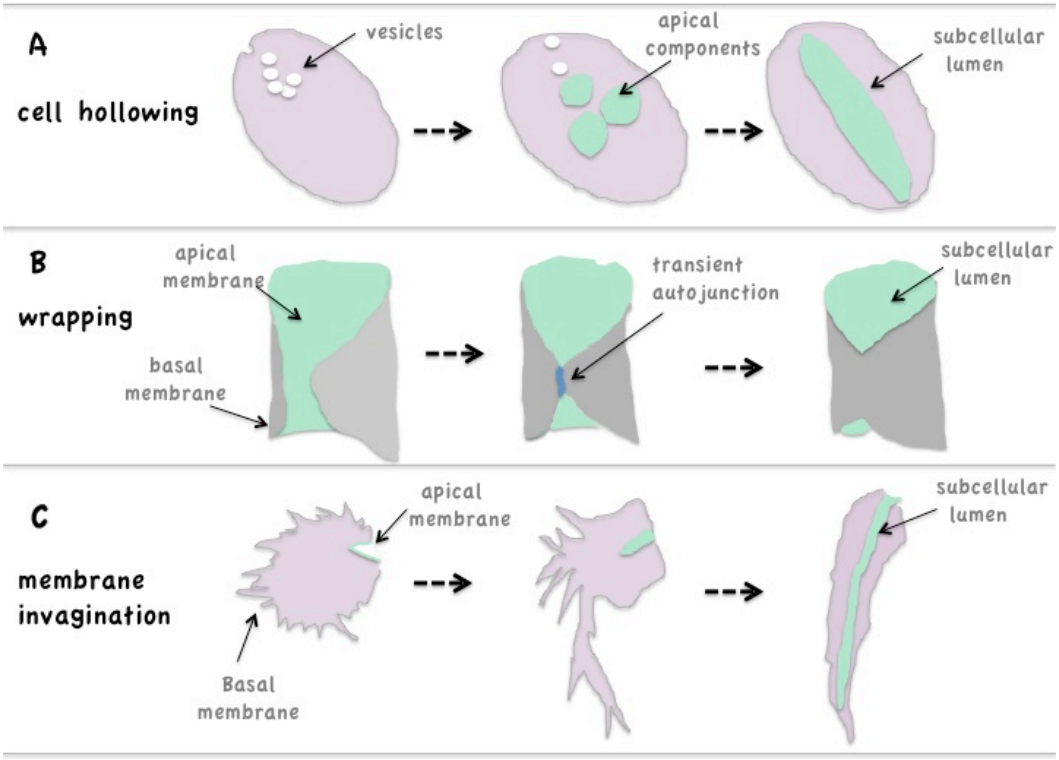

Figure 9. Models for seamless tube formation (**A**) Cell hollowing (**B**) Wrapping model (**C**) membrane invagination. Basal membrane is in grey, apical domain/ lumen in green cytoplasm in purple.

1.2.3 Seamless tubes in physiology and pathology

Many **capillaries** in the vertebrate vascular system are seamless tubes. Endothelial capillary architecture differs significantly from one organ to another. Generally the circumference of capillaries is made up of one (seamless) or 2/more endothelial cells (seamed). For example, single cell seamless tubes make up to 78% of all brain capillaries. In contrast, in other systems like the mesentery or in the urinary bladder seamless capillaries are a minority group. In other organs, both types of capillary are found in the same ratio. Generally, seamless tubes localize in anastomoses and branch points and intercalate most frequently in those capillaries that develop last in the terminal vascular bed (Bar et al., 1984). Abnormalities in capillary development and maintenance are involved in many diseases. For example, some **Mendelian syndromes** like Cerebral Cavernous Malformation (CCM), Cerebral Autosomal Recessive Arteriopathy with subcortical infarcts and leukoencephalopathy (CARASIL) and Osler–Weber–Rendu

disease are related with defects in smaller blood vessels. Genes involved in these hereditary diseases are associated with dysfunctional behaviours in growth factor signalling, vesicle trafficking and cytoskeleton organization (Sundaram and Cohen, 2016). Seamless tubes are importantly implicated in **angiogenesis**. Angiogenesis is a developmental process consisting in the growth of new capillary blood vessels in the body and is an important natural process used for healing and reproduction. However, angiogenesis is now recognized as a "common denominator" underlying many deadly and debilitating conditions, including cancer, skin diseases, age-related blindness, diabetic ulcers, cardiovascular disease, stroke, and many others (Adair and Montani, 2010). For example, angiogenesis can be induced by **hypoxia**, a condition in which tissues undergo a reduction of oxygen. Hypoxia induces the sprouting of vascular tip cells (many of which later form seamless tubes) that lead the outgrowth of new vessels into under-vascularized tissue. Hypoxia is a feature of many tumours and plays an important role in tumour progression and resistance to therapy (Wilson and Hay, 2011).

1.3 *Drosophila melanogaster* and its respiratory system

The first documented use of *Drosophila melanogaster* in laboratory was by William Castle's group at Harvard in 1906 (Castle, 1906). From then to now the fruit fly has been used productively in research to study a broad range of developmental processes and between them *Drosophila* has proven to help on the analysis of the cellular and molecular mechanisms of tubulogenesis.

1.3.1 Fruit fly as model organism

Drosophila is a small animal, inexpensive to culture in laboratory, its whole genome has been sequences and it can be genetically modified in several ways. Furthermore, the life cycle is short (around 10 days), (**Fig. 10**) and produces a large numbers of externally laid embryos. Once fertilized, the embryo develops in the egg for around one day (at 25 °C), through several embryonic stages (from stage 1 to stage 17) before hatching as a larva. The larva eats and grows (going through three molts) over five days until it pupates and undergoes metamorphosis into the adult fly over the course of four days. During metamorphosis, most of the embryonic and larval tissues are destroyed. Some adult tissues (e.g., wing, leg, eye) develop from groups of cells known as "imaginal discs" that have been set-aside since early embryonic development. Others, like the nervous system

and tracheal system do not depend on imaginal origin for their development until adult stages.

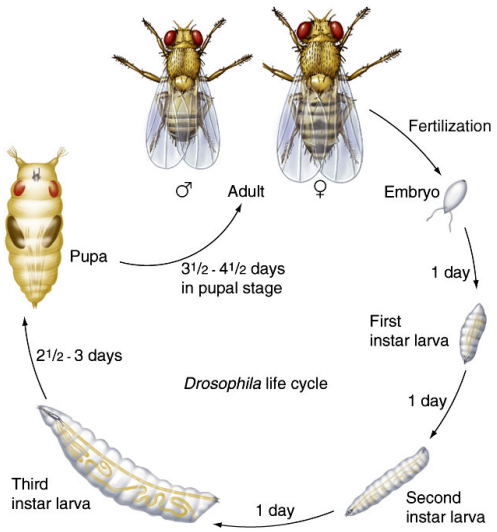

Figure 10. Life cycle of *Drosophila melanogaster.* At 25° the *Drosophila* generation time is about 10 days and consist in 1 day of embryogenesis, 1day first instar larvae, 1 day second instar larvae, 2-3 days third instar larvae and about 4 days pupal stages (adapted from Flybase).

1.3.2 *Drosophila* tracheal system as tubulogenesis model

In *Drosophila melanogaster*, a combined cellular and genetic approach is possible and has begun to elucidate the cellular mechanisms and molecules that govern formation of several organs. The tracheal (respiratory) system of *Drosophila*, a **branched tubular epithelium**, is a very well described system useful for understanding the mechanisms that orchestrate tube formation. Many genetic tools and cellular analysis are available to elucidate in detail how during development the tracheal system is formed in all its complexity. The availability of a large battery of molecular cell markers for the tracheal system provides an excellent system to define the mechanisms of branching morphogenesis (Samakovlis et al., 1996). Furthermore, several mutants in tracheal morphogenesis have been identified and the structure and physiology of the insect trachea have been extensively studied and reviewed. So, the *Drosophila* tracheal system is a powerful model useful to obtain molecular and cellular understanding of different intriguing steps that lead to the formation of tubes.

1.3.3 Embryonic development of tracheal system

The tracheal system is the respiratory organ of the fly. In the adult, it is a complex tubular epithelial network that ramifies throughout the body of the animal. The oxygen enters from the spiracles, external openings repeated segmentally on either side of the thorax and abdomen and terminates in enlargements called air sacs where gas exchange takes place. The tracheal system develops embryonically from a defined set of **ectodermal precursor cells** (**Fig. 11**). At stage (st.) 10 of embryogenesis, groups of lateral ectodermal cells in each side of the para-segments, acquire the tracheal **placode** fate. They undergo two more rounds of mitosis to generate approx. 80 cells. From this stage the tracheal system develops **without any further cell division** and very little cell death (Affolter and Caussinus, 2008). At st. 11 these placode cells start to i**nvaginate** (**Fig. 11A**) to form the sac–like tracheal structures (**Fig. 11B**). This structure generates the **luminal cavity**, which is subsequently expanded and remodelled during the branching process (**Fig.11 C, C'**). Some cells in this sac-like invagination, respond to chemoattractant cues, adopt migratory properties and migrate while remaining attached to their tracheal neighbours. At st. 13-14 (**Fig. 11D**), through extensive cell rearrangements and cell shape changes, tracheal cells elongate to form branches of distinct cellular architecture, ranging from multicellular tubes to fine unicellular branches. At st. 15, an **interconnection** of the tracheal metameres at distinct fusion points occurs. Meanwhile, specialized **tracheal tip-cells** at the periphery of the tracheal system extend the luminal space into individual cell extensions, to reach virtually every tissue in the embryo (**Fig. 11E**), (Affolter and Caussinus, 2008; Wilk et al., 1996). At the end of embryonic development the tracheal system appears as an intriguing complex structure of interconnected metameric units of different-sized tubes that extend over the entire embryo. From the initial metameric tracheal sac, six branches are generated (**Fig. 11 C'**). The main branch of the tracheal system, the **dorsal trunk** (**DT**) arises from cells moving anteriorly and posteriorly that join with those in the adjacent segment and fuse between them. Other cells migrate ventrally and anteriorly forming the **lateral trunk** (**LT**) by the fusion of the anterior and posterior lateral trunk branches. Some cells in each segment migrate towards the dorsal midline generating **dorsal branches** (**DB**). DBs of each side fuse with their contralateral ones at the dorsal midline. Other cells, forming the **ganglionic branches** (**GB**), migrate ventrally reaching the nervous system. **Visceral Branches** (**VB**) migrate internally into the embryo, to provide internal tissues with

oxygen. Finally, groups of cells that remain near the site of invagination form the **spiracular branches** (**SB**) (Manning and Krasnow, 1993).

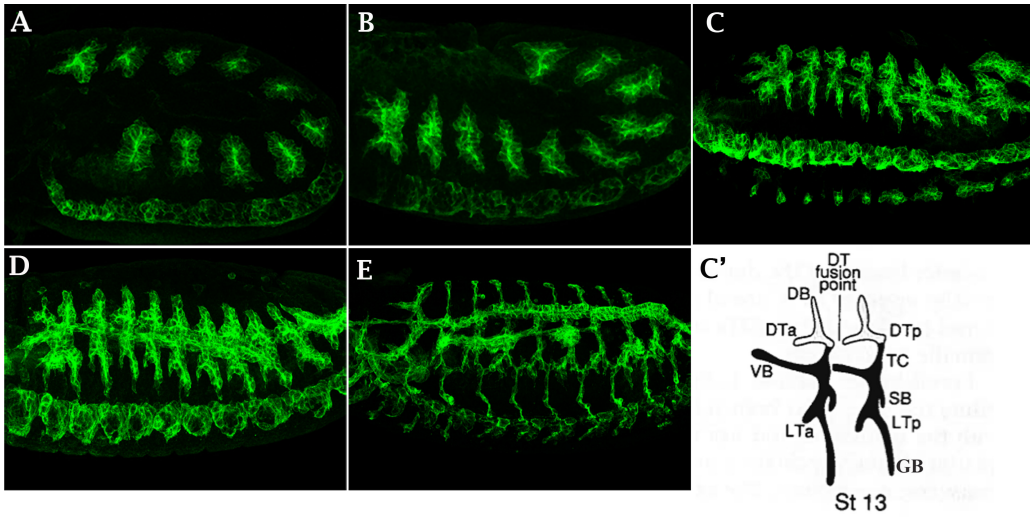

Figure 11. Embryonic tracheal system development. (A-E) Confocal projections of fixed embryos from st. 11 to st. 16 expressing GFP in the tracheal system (by the tracheal driver *btl-GAL4*), stained with anti-GFP antibody. Anterior side of the embryo is on the left; dorsal, up. Individual clusters of tracheal cells invaginate and start to form the sac-like structures from where different luminized branches are generated and extended in stereotyped directions. (B) (C). Tracheal branches elongate (D) and fuse between them to form an interconnected network (E). In (**C'**) is represented a scheme of a tracheal metamere at st. 13 (**a** anterior, **p** posterior, **DB** dorsal branch, **DT** dorsal trunk, **VB** visceral branch, **SB** spiracular branch, **LT** lateral trunk **GB** ganglionic branch).

1.3.4 Tracheal specification

The genetic program and signalling pathways that orchestrate tracheal system development have been very well described during the last decades. The earliest events are controlled by global patterning genes, including the dorsal-ventral, homeotic, and segment polarity genes (Kerman et al., 2006). Patterning genes both limit the number of segments in which trachea develops and determine the anterior-posterior and dorsal-ventral location of the primordia within each segment. Three known transcription factors are specifically expressed early in the cells that will develop as trachea: ***trachealess (trh)***, *ventral veinless (vvl)* and *knirps/knirps-related (kni/ knrl)*. It has been demonstrated that Trh plays a major role in activation and maintenance of tracheal gene expression and Vvl and Kni/ Knrl have only minor roles compared to Trh. In the absence of *trh*, tracheal cells fail to invaginate and to form tubes. Expression of many tracheal-specific genes depends on *trh*, but all of the known targets have relatively minor phenotypes compared to loss of *trh* (Chung et al., 2011). The most important target of *trh* is ***breathless*** (***btl***), the *Drosophila* homolog of the mammalian **fibroblast growth factor receptor** (FGFR), whose expression is induced just before branching. At the same time, the expression of the **FGF ligand**, **Branchless** (**Bnl**) turns on in specific subset of cells nearby the tracheal cells, exactly at each point toward the branches will bud (Sutherland et al., 1996). Activation of Btl, by the binding of the Bnl, induces the activation of the canonical **Ras/MAPK pathway**, which regulates the expression of several targets genes. The cells at the tip of the branches have a higher FGFR pathway activity and lead the migration of branches (Caussinus et al., 2008). The Bnl/Btl pathway induces tracheal motility through the formation of the dynamic filopodia at the tip/leading cells, thereby regulating the cytoskeletal dynamics (Okenve-Ramos and Llimargas, 2014a; Okenve-Ramos and Llimargas, 2014b; Wolf et al., 2002).

1.3.5 Microtubules in tracheal system

During their specification, tracheal cells change shape, change position, migrate and establish contact between themselves. MT organization contributes widely in organizing and modulating tracheal cell behaviour during tubulogenesis. It has been reported that MT depolymerisation in tracheal cells, by the overexpression of Spastin (Spas), a member of the microtubule-severing AAA ATPase superfamily, at early developmental

stages, generates abnormalities in placode invagination (Brodu et al., 2010). Moreover, MT depolymerisation induces defects in cell elongation. While the branch extends, an over-elongation of branch cells ultimately leads to branch break. MT depolymerisation also induces defects in lumen formation, as indicated by the low and abnormal deposition of chitin (Le Droguen et al., 2015). From placode invagination and during tracheal tree development MTs bundles are organized in networks mostly concentrated in apical surface (Brodu et al., 2010; Lee and Kolodziej, 2002a). **Non-centrosomal microtubule networks** are found in tracheal cells; Brodu and co-workers demonstrated that between st. 11 to st. 12/13, MTOC components re-localize from the centrosome to apical domain of tracheal cells (**Fig. 12**). At placode stages centrosomes are detectable in a sub-apical domain. Short new MTs are apically organized into a meshwork, from where some larger MTs elongate pointing the basal-lateral membrane (**Fig. 12A**). At st. 11 γ-tubulin and **γ–TuRC c**omponents co-localize with **centrioles** but gradually they move and **re-localize to the apical membrane**. At the end of placode invagination most centrioles are depleted in γ–TuRC components and the apical membrane is active as a MT nucleation centre (**Fig. 12B)**. The mechanism that controls γ –TuRC re-localization has been described; first Spas, relases γ–TuRC from centrioles, subsequently, γ-TuRC is transported, probably by a MT-dependent mechanism, toward the apical membrane. Here Piopio (Pio), a MT anchor protein, links γ –TuRC to the apical membrane. All this process is orchestrated by *trh*, involved both in Spastin activation and *pio* gene expression (Brodu et al., 2010).

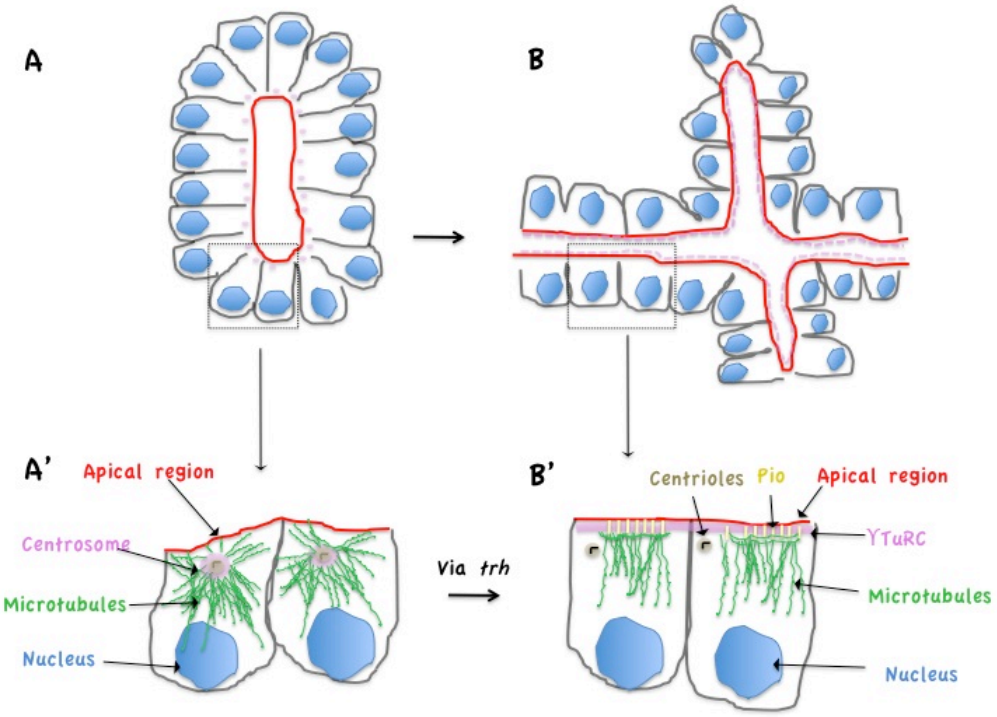

Figure 12. Microtubule organization changes during tracheal system development. (A) Cartoon of tracheal placode at st. 11; centrosomes (in pink) are localized next to the apical region (in red). Nuclei (in blu) are at the basal region. **(A')** Cartoon of a close up of two placode tracheal cells; MT (in green) are organized at the apical side where centrosomes (in pink) are also placed. The nucleus is at the basal side (in blue). (**B**) Cartoon of tracheal cells at st. 13; the apical region (in red) is facing the lumen, nuclei (**in blue**) are placed in the basal region. (**B'**) Cartoon of a close up of two tracheal cells at st. 13; MTs are now organized in non-centrosomal arrays. γ-TuRC components (in pink) do not co-localize with centrioles (in brown) but they are placed near to the apical membrane where Piopio acts as anchor. γ TuRC relocalization takes place toward st. 11 (not shown in the picture) when *trh* orchestrates Spas activity and *pio* expression Figure adapted from Brodu et al., 2010.

1.3.6 Short stop during tracheal system development

Tracheal cells adhere to each other by adherens junction (AJs) where the cell-adhesion molecule E-Cadherin is present. During tracheal system development, new E-cadherin contacts must be made or broken for cells to change shape or move. These remodelling processes require the AJ to organize the cytoskeleton. MTs play a critical role in sustaining E-cadherin and apical membrane components at the AJ. Furthermore, E-cadherin interacts with the F-actin cytoskeleton via the β-catenin/α-catenin complex and regulates F-actin assembly (Lampugnani et al., 2002; Lee et al., 2003). **Short-stop** has been described to be critical during the fusion process (or anastomosis) when a new E-

cadherin contact forms between fusion cells. Loss of function alleles of *shot* display destroyed anastomoses sites in the DT, LT and across the dorsal midline (**Fig. 13** panel **1**) and the apical cytoskeleton of tracheal cells appears disorganized (**Fig. 13** panel **2**), (Lee and Kolodziej, 2002a). F-actin in *wild-type* (*wt*) DT is apically localized all around the lumen (**Fig. 13** panel **2 A**, **C**, **G** and **K**). In *shot* null allele actin appears disorganized at anastomosis sites (**Fig. 13** panel **2 D**, **F**, **I** and **L**). Also, in *wt* conditions MTs localize apically (**Fig. 12** panel **2 B**, **C** and **H**), but in *shot*^{3} mutant they remain largely at the cell periphery (**Fig. 12** panel **2 E**, **F** and **J**). It has been proposed that **Shot interacts with the cytoskeleton machinery in fusion cells** and is required for E-cadherin contacts essential for lumen formation (Lee et al., 2003; Lee and Kolodziej, 2002a).

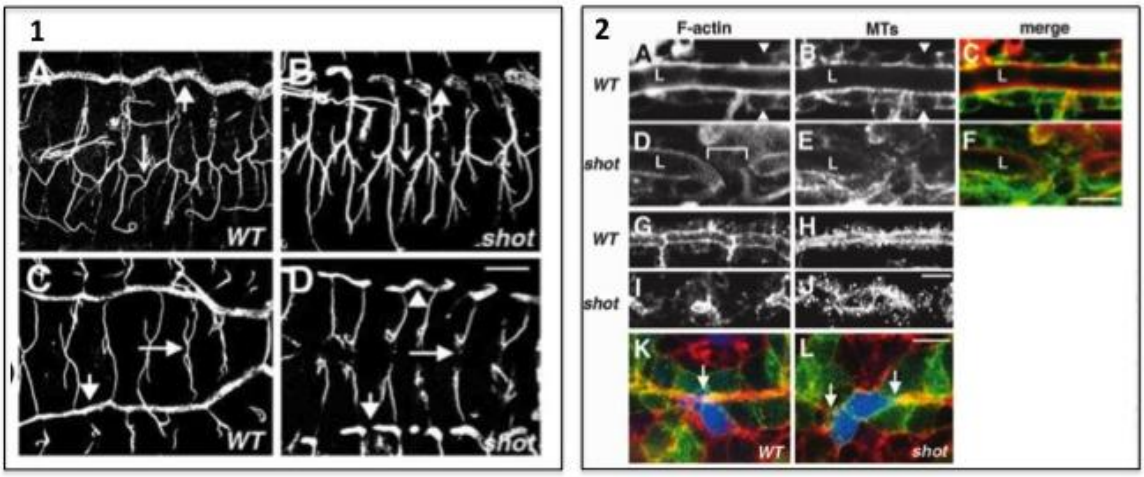

Figure 13. *shot* null allele displays defects in lumen formation at anastomosis (1) Confocal sections of st. 16 *wt* and *shot*^{3} null mutant embryos stained with mAb 2A12, which recognizes Gasp, a lumenal antigen. Anterior, left; dorsal, up. (**A**) Lateral view, *wt* and (**B**) *shot*^{3}. The lumen is discontinuous at anastomosis sites. (**C**) Dorsal view, *wt* and (**D**) *shot*^{3}. DBs have not joined their lumens at fusion. Arrows point at fusion points. **(2)** Apical cytoskeletal of tracheal cells in *wt* and *shot*^{3}. (**A-L**) confocal sections of DT tracheal cells in *wt* and *shot*^{3} mutant embryos. (A,C,G and H) St. 15, *wt*. (D,F,I and J) st. 15, *shot*^{3}. (A) F-actin (red in C) apically concentrated around a lumen. Arrowheads mark the basal surface. (B) MTs (green in C) accumulate mainly apically. (C) Merge of A and B. (D) F-actin accumulates apically around two lumens that end at an anastomosis site (bracket). (E) (F) Tubulin staining is diffuse in tracheal cells. Merge of D and E. (G) Actin-GFP is apically concentrated. (H) C-Shot L-GFP (a construct consisting in the C terminus of Shot fused with GFP), a microtubule-associated protein, localizes apically. (I) Actin-GFP concentrates apically, but tracheal tubes dead end at anastomosis sites. (J) The C-Shot L-GFP distribution in tracheal cells is disorganized. (K) St. 14, *wt*. F-actin (red) accumulates apically in tracheal cells (membranes outlined in green) and surrounds a lumen that is continuous through the fusion cells (blue). The fusion cells are compact and doughnut shaped. (L) St. 14, *shot*^{3}. F-actin (red*)* accumulates apically in tracheal cells (outlined in green) but the lumen does not extend through the fusion cells (blue). Arrows indicate apical sides of fusion cells. Figures from Lee S. et al., 2002.

Surprisingly, Shot performs its morphogenetic role at anastomosis site using its F-actin binding domain and MT binding domain in a redundant manner. In fact tracheal overexpression of the construct *UAS-shot L (A)-GFP* rescues the anastomosis defects caused by *shot* null allele in the dorsal trunk and lateral trunk. However, also tracheal expression of construct derivatives from Shot L (A) isoform that lack either the N-terminal F-actin binding domain or the C-terminal microtubule-binding site could also restore lumen formation in fusion cells. Deleting both the F-actin binding site and the MT binding site abolished rescue activity (**Fig. 14**), indicating that at least one cytoskeletal interaction domain must be present for fusion cells to form a connecting lumen. So it has been proposed that the F-actin binding domain is essential when the MT binding site is absent, and *viceversa* (Lee and Kolodziej, 2002a).

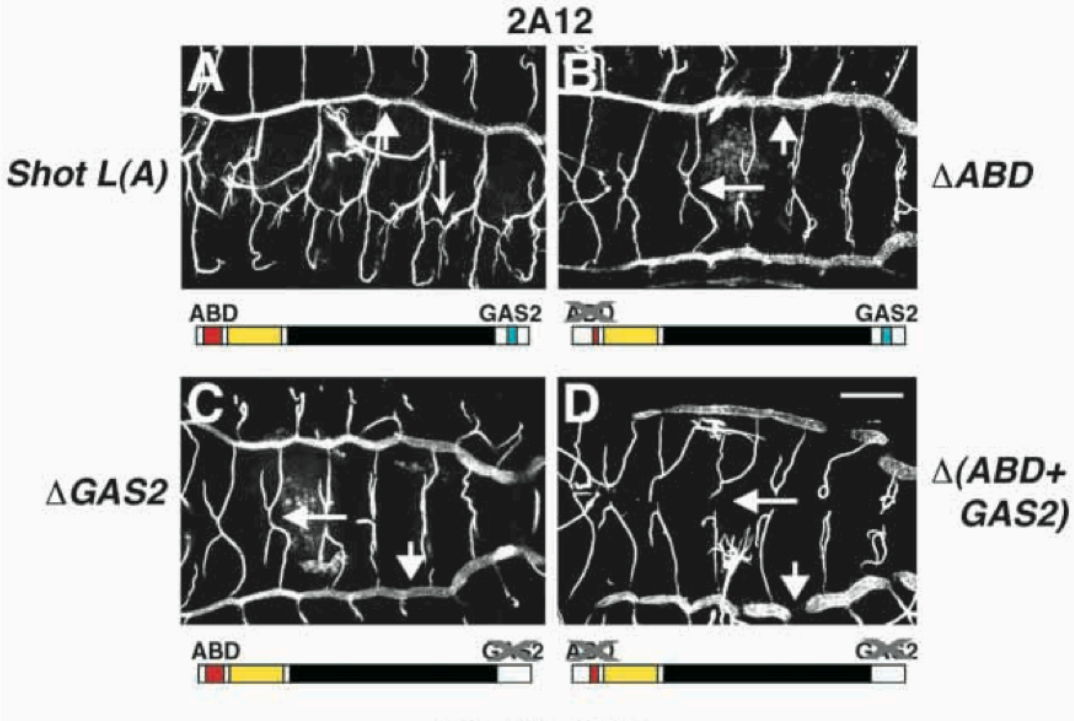

Figure 14. The F-actin- and the microtubule-binding domains of Shot proteins redundantly promote lumen formation in fusion cells. (**A-D**) Rescue activity of Shot L (A)-GFP and derivatives in stage 16 *shot*^{3} mutant embryos: N-terminal F-actin binding domain (red), central plakin-like (yellow) and spectrin repeat domains (black), and a C- terminal domain that binds microtubules via the GAS2 motif (blue). The gray X is used to indicate domains missing in Shot L(A)-GFP derivatives (schematics in B- D). (A) Lateral view. Tracheal expression of Shot L(A)-GFP restores lumen formation in fusion cells in the dorsal and lateral trunks. (B) Dorsal view. Tracheal expression of actin-binding defective Shot ΔABD restores lumen

formation in fusion cells in the dorsal trunk and at the dorsal midline. Shot L(A)-GFP derivative that lacks the microtubule binding GAS2 motif restores lumen formation in dorsal trunk and midline fusion cells. Shot L(A)-GFP that lacks both cytoskeletal interaction domains does not restore lumen formation in dorsal trunk or midline fusion cells.

The fusion branches in the dorsal midline and in the LT generate the major part of the tube with an extracellular lumen, but a minor part of the tube is seamless type, although of different nature respect to the seamless tube generated from TCs (Gervais et al., 2012). MTs in the fusion branch are organized along the lumen and MTs organization, a process in which Shot is involved, is DE- cadherin dependent and it has been proposed to facilitate vesicle coalescence to form a seamless tube (Gervais et al., 2012; Lee et al., 2003). So the defects observed in *shot*^{3} mutant reflect in part the effect of the spectraplakin in the cytoskeletal organization and in the establishment of E-Cadherin contacts, but there is also the possibility of an effect of the spectraplakin in the proper seamless tube generation, a topic analysed in this work.

1.3.7 Terminal Cells: a model for seamless tube formation

In the *Drosophila* tracheal system the main tubes are multicellular and form an extracellular lumen. However, in some branches there are cells able to form subcellular lumina. These are of two types: fusion cells and terminal cells. Fusion cells elongate shortly and undergo anastomosis to connect different branches in the network (Gervais et al., 2012). Terminal cells (TCs) are specialized cells that connect the tracheal system to the target tissues for gas exchange. They decorate the main branches and reach virtually all the tissues in the larva. 19 of the 80 tracheal cells per hemisegment develop into TCs. The TCs at the tip of the GBs and DBs are analysed in this thesis because they form subcellular lumina and they are accessible to examination (**Fig. 15G**). These cells develop embryonically from st. 14 extending their single lumenized process until the end of embryogenesis (**Fig. 15A-F)** and later on during larva stages TCs branch out profusely, resembling branched neuronal cells.

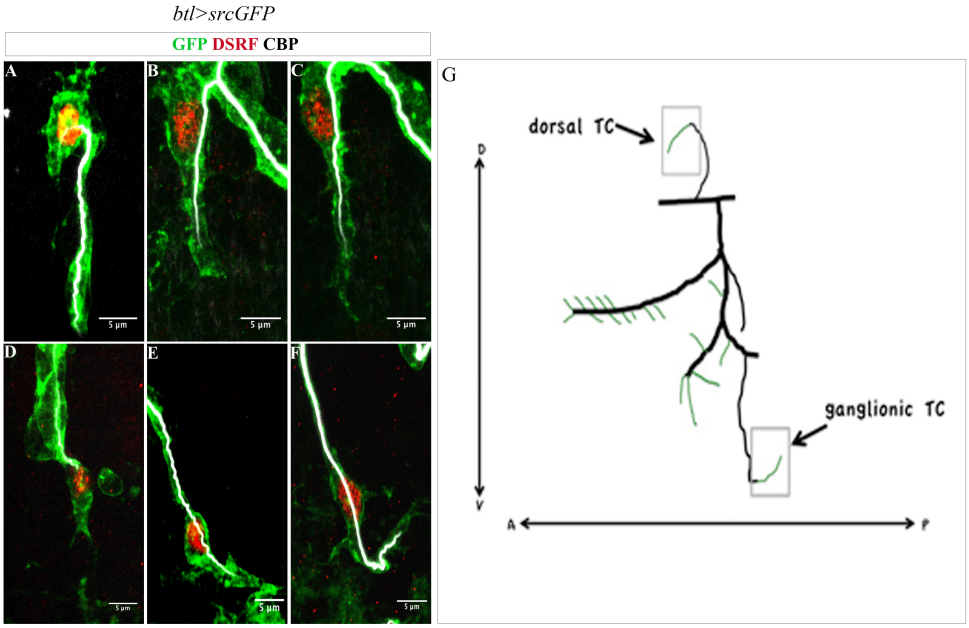

Figure 15. Terminal cells generate a seamless tube. (**A-F**) Confocal projections of dorsal (A-C) and ventral TCs (D-F) of embryos overexpressing GFP in tracheal cells (by specific tracheal driver breathless GAL4) at st. 14 (A and D), st.15 (B and E) and 16 (C and F). Anterior, leftwards; dorsal, upwards. Staining; anti-GFP recognizing all tracheal cells, CBP (chitin binding probe in white) and anti-DSRF (Drosophila serum response factor) in red to show the TC nucleus. (G) tracheal metamere at st. 16, in green the TCs.

As mentioned before, TCs can create a lumen because a patch of membrane invaginates from the intercellular junction and extends towards the inside of the cell. A lumen will form by addition of membrane vesicles inside and along the length of the cell. This will form a **seamless tube** without junctional structures. Topologically, the 'inside' of the cell is the cytoplasm between the tube membrane and the outer cell membrane, therefore the term 'subcellular' to describe these tubes (Sigurbjornsdottir et al., 2014).

1.3.8 Subcellular tube formation

Subcellular lumen formation in TCs of *Drosophila* requires the cell to establish a specific pattern of apical-basal polarity. At the initial stage, TC has a ring of apical membrane at the junction with its adjacent cell. The peripheral membrane of the TC, including the membrane at the cell tip, has basolateral properties. The initial cues that establish such polarity are still unclear. Lumen formation is possible because "tube membrane" growth inside the cell and define the outline of the lumen. This is apical membrane as indicated by the accumulation of specific apical markers like aPKC/Par6/Baz and Crb /DPatj complexes. As the lumen elongates, it also grows in diameter in a wave from the base to the tip. Following membrane formation, as for all tracheal tubes, chitin is accumulated inside the lumen (Gervais and Casanova, 2010).

Cell elongation and subcellular lumen formation are intimately associated between them (**Fig. 16**). During the first steps of cell elongation, at st. 14, TC emits short filopodia in all directions and immediately after, larger filopodia start to form, indicating the way of future elongation. Subcellular lumen appears at early st. 15 as a continuous process of expansion of new apical membrane pointing to the tip of the cell. *In vivo* analysis demonstrated that the incorporation of new apical material is not restricted to specific sites, such as the tip or the base but accumulation of vesicles carrying luminal components and recycling endosomes are localized all along all the length of the lumen. Rab11 and dRip11, proteins that are involved in the trafficking of recycled and new synthesized proteins of the apical plasma membrane, are localized near and ahead the lumen in formation. Other components involved in membrane protein transport, like the exocyst complex proteins Sec6 and Sec8 are more localized at the tip of the cell (Gervais and Casanova, 2010).

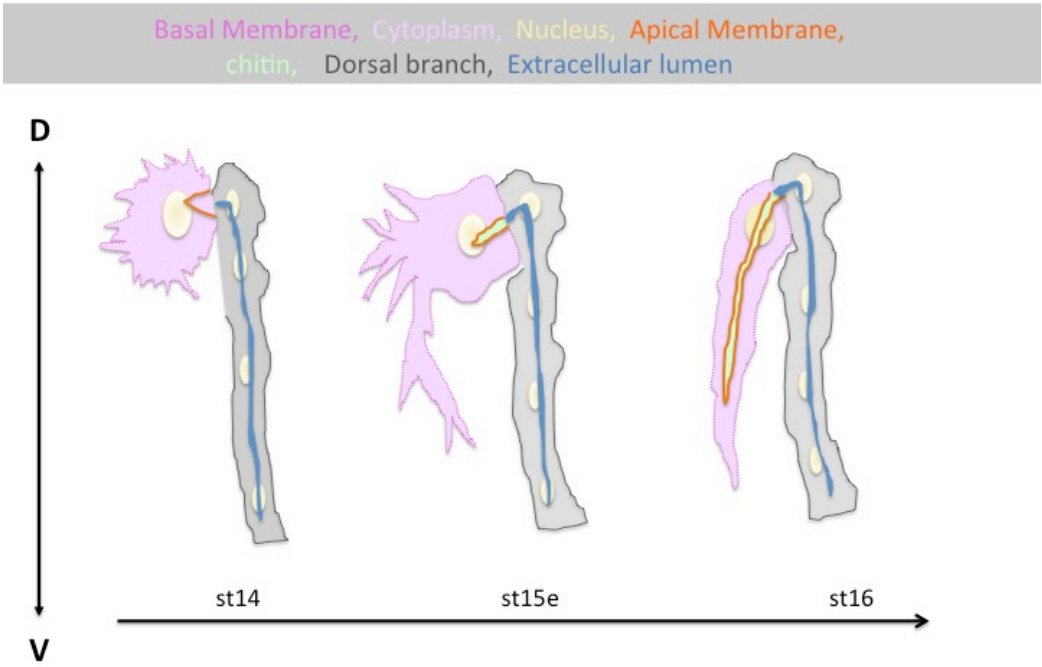

Figure 16. Subcellular lumen formation is associated with cell elongation. Representation of dorsal TCs from st. 14 to st. 16. (DB in grey, nuclei in yellow and extracellular lumen in blue). At st. 14, TC (cytoplasm in pink, nucleus in yellow, basal membrane in fuchsia and apical membrane in orange) emits short filopodia in all directions. At st. 15, long filopodia extend in direction of cell elongation and apical membrane growth in the same direction, giving rise to the outline of the subcellular lumen. At the same time the subcellular lumen is filled of chitin (in green). At st. 16 the TC is elongated and the subcellular lumen is stabilised.

The cytoskeleton organization plays a crucial role in terminal branch formation. Actin and MTs are organized in a characteristic architecture (see below) that is an essential instrumental for the correct vesicle trafficking allowing the cell elongation and subcellular lumen formation.

1.3.9 Terminal Cell differentiation

TCs have a high FGF/Btl activity that triggers the expression of several factors implicated in the correct set up for cell elongation and subcellular lumen formation.

Terminal branch formation in the embryo is controlled, during the initial phases, directly by Bnl signalling and later on, during the progression of cell elongation and sub-cellular lumen formation, by the transcription factor Pruned/Blistered, whose expression is

triggered by the same Bnl signalling. The *pruned /blistered* gene encodes the *Drosophila* homolog of mammalian serum response factor (DSRF) (Affolter et al., 1994).

The null allele *pruned* displays TCs that begin to differentiate, but cell elongation and subcellular lumen formation stop prematurely. However, high levels of Bnl can bypass the requirement of DSRF for the initiation of terminal branch formation (Gervais and Casanova, 2011). So, DSRF is dispensable for terminal branch initiation, probably because Bnl levels at this stage are high enough to promote directly the first steps of terminal branch formation, but DSRF is crucial requirement for the progression of cell elongation and lumen formation (Gervais and Casanova, 2011).

The FGF pathway as well as DSRF regulates the expression of genes involved in cytoskeleton regulation, including the gene encoding for Enabled (Ena), a VASP protein that accumulates at areas of actin remodelling and promotes filopodia formation (Gervais and Casanova, 2010).

1.3.10 Actin accumulation into the TCs

TCs require an accurate F-actin organization for their polarized elongation. From the beginning of TCs specification, F-actin is organized in different structures. Initially, a multitude of basal filopodia extends in all directions and dots of actin are diffuse inside the cell. Later on, filopodia grow toward the direction of cell elongation and dots of F-actin mature in a central core at the distal tip of the cell, resembling the growth cone of an axon (**Fig. 17**) (Oshima et al., 2006). TCs generate, during their development, at least three distinct populations of F-actin that have different functions. The **"growth-cone-like**" F-actin accumulation is involved in the correct cell elongation and subcellular lumen formation. Here, Enabled (Ena) mediates the remodelling of actin filaments and promotes the growth of filopodia. During cell elongation, Ena localizes at the base of the cell tip, where it co-localizes with F-actin and Moesin (Moe). *ena* mutants display defective terminal branch formation characterized by short and disorganized filopodia. Ena might also function in guiding lumen growth, as in *ena* mutant lumen elongate in an incorrect direction (Gervais and Casanova, 2010; Sigurbjornsdottir et al., 2014). At the outer basal membrane of the cell, **cortical actin** is essential for the stability of the TCs branches. Integrin molecules bind to the extracellular matrix through their extracellular domains and bind to adaptor molecules such as Talin through their intracellular domains to organize the basal cortical actin (Sigurbjornsdottir et al., 2014). Finally, **a dense actin**

network surrounds the luminal tube. This pool of actin is required for the delivery of apically targeted material and possibly also for structuring the tube. The interaction between this actin network and luminal membrane is mediated by complex comprising Moe and Bitesize (Btsz) that aids the incorporation of apical membrane material into the growing luminal tube (JayaNandanan et al., 2014; Oshima et al., 2006).

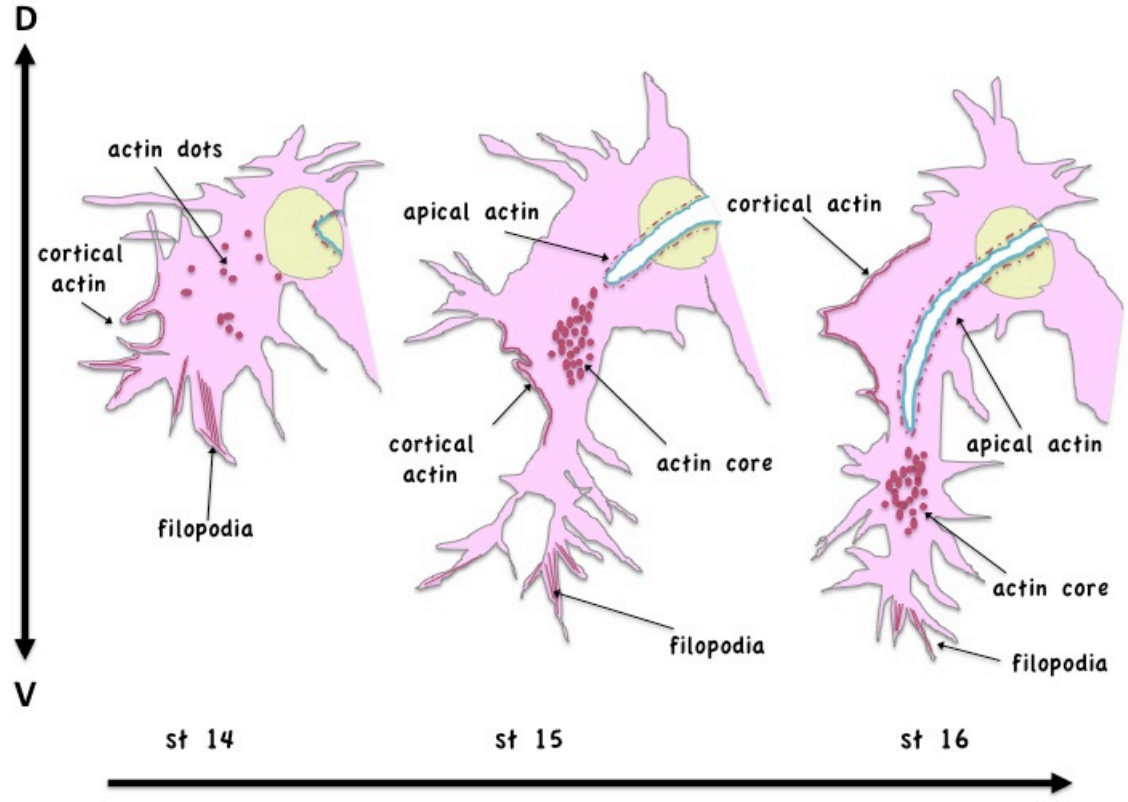

Figure 17. Actin network during TC growth. Schematic representation of dorsal TC development from st. 14 to st. 16. Basal membrane in grey, apical membrane in light blue, subcellular lumen in white, the nucleus is in yellow and the actin network in red. At st. 14 TC emits filopodia in all direction. From this stage cortical actin is detectable on the basal membrane and dots of actin are distributed into the cytoplasm. Between st. 14 and st. 15 actin dots mature in an asymmetric actin accumulation (or actin core) at the tip of the TC. At st. 15 large filopodia are mostly formed in ventral direction where the cell growth. The actin core is in front of the tip of the subcellular lumen in formation. At st. 15 and 16, at the tip of the TC, filopodia and the actin core form a structure similar to a neuronal growth cone. As the subcellular lumen growth, a dense actin network is detectable around the apical membrane.

1.3.11 TCs Microtubule network

MTs at very early stages **emanate from the junction** between the TCs and the rest of the branch, and during development point toward the tip of the cell running parallel with the subcellular lumen (**Fig. 18**). From the beginning of subcellular lumen sprouting MTs are organized along the apical membrane and accumulate next to the rich actin area at the tip of the cell. Bundles of **acetylated tubulin**, the more stable and "older" tubulin incorporated in the cell, are detected along the entire cell, strongly accumulating next to the apical surface. Alternatively, **tyrosinated tubulin**, found in newly assembled MTs, specifically accumulates at the tip and ahead of the lumen, thereby indicating that these are probably the most recently incorporated MTs (Gervais and Casanova, 2010).

TC elongation and lumen formation correlate with correct MT network stabilization. MT depolymerisation, by overexpression of Spastin in tracheal system, induces an arrest in cell elongation and subcellular lumen maturation. Also, mutants for the homolog of Lissencephaly-1 (DLis-1), a protein that participates in the MT cortical anchoring at the plasma membrane, in which the amount of MTs is reduced, displays lumen elongation defects and TCs that fail to elongate. Interestingly, in such mutant conditions TCs emanate filopodia in the correct direction and the actin network is not strongly affected (Gervais and Casanova, 2010). Conversely, in mutants affecting the actin network like *ena* mutant, MT network is affected suggesting that actin is in somehow involved in MT organization at the cell tip, as postulated for the growth cone in axons (Lowery and Van Vactor, 2009).

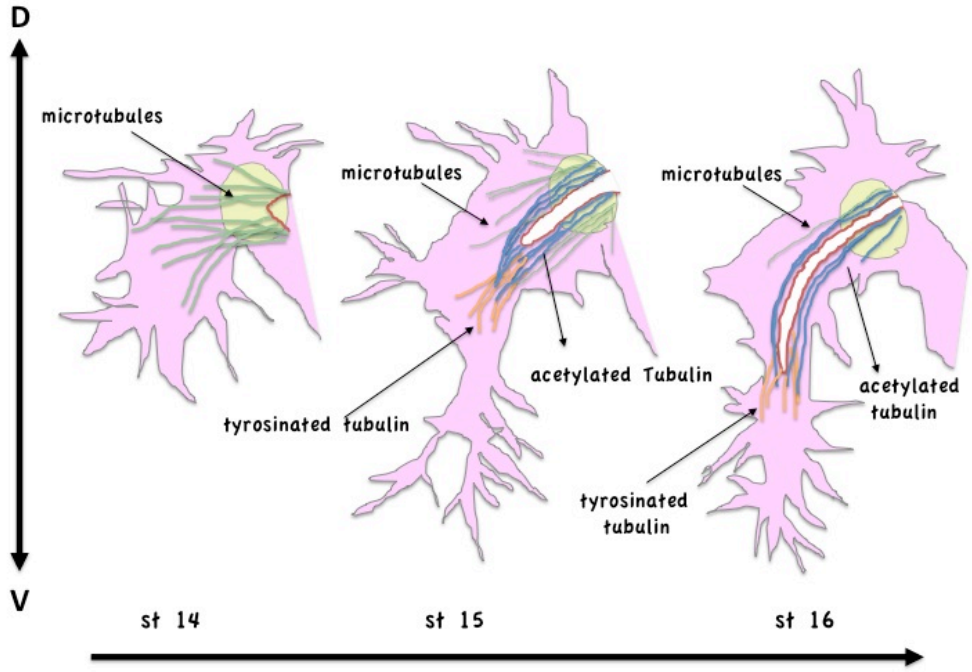

Figure 18. MT network during TC growth. Schematic representation of dorsal TC development from st. 14 to st. 16. Basal membrane in grey, apical membrane in red, subcellular lumen in white, the nucleus is in yellow, microtubules in grey, acetylated tubulin in blue and tyrosinated tubulin in orange. At st. 14 MTs extend in all direction from the junction with the DB. At st. 15 and 16 stable MTs (marked by acetylated tubulin) are detected mostly around the subcellular lumen and newly incorporated tubulin (marked by tyrosinated tubulin) is mostly accumulated at the distal part of the TC.

TCs differ from all other tracheal cells because they are programmed to elongate dramatically and give rise to a subcellular lumen, consequently they undergo different cytoskeleton rearrangement in respect to other cells forming multicellular tubes.

As described before, at early stages of TC development (st. 14) short MTs bundles emanate inside the cytoplasm from the junction with the neighbour cells but the mechanism by which this MTs are nucleated is completely unknown. It was mentioned before that acentrosomal MT networks are found in tracheal cells that build up an extra subcellular lumen, (Brodu et al., 2010) but no evidences in literature demonstrate the same organization for TCs.

It has been shown that, from when the lumen primordium appears, γ-tubulin is detected along apical surface, next to the lumen (Gervais and Casanova, 2010).

Recent work suggests that γ-tubulin has important but less well understood functions that are not simply a consequence of its function in primary microtubule nucleation. These

include roles in the regulation of plus-end microtubule dynamics. Moreover γ-tubulin complexes have been related with the function in nucleation of MTs from the sides of existing MTs (Oakley et al., 2015). Thereby, where and how the first point of MT nucleation is defined inside the TC is still an open question and will be analysed in this work.

1.3.12 Inward membrane growth model

The current accepted model introduced by Gervais and Casanova in 2010 proposes that Bnl signalling is involved in the initiation of TCs specification and activates the transcription factor DSRF. Therefore, DSRF promotes cell elongation and the growth of apical membrane inside the cell, triggering the expression of effector genes involved in the reorganization of the cytoskeleton. One of the effector genes is *ena* that participates in actin remodelling and a consequent formation of a growth cone like structure that, in turn allows specific MT organization. This cytoskeletal reorganization is instrumental in the generation of apical and basal membranes, probably by directional intracellular trafficking, thus coupling cell elongation and subcellular lumen formation.

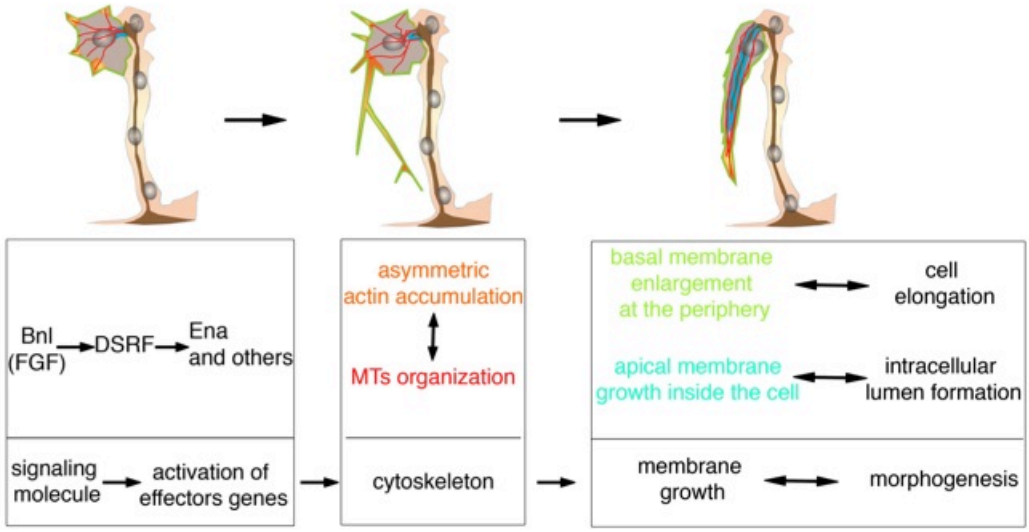

Figure 19. Inward membrane growth model. Bnl signaling activates DSRF, which in turn promotes cell elongation and intracellular lumen formation. Ena acts as an effector of this mechanism. As a result, asymmetric actin accumulation allows a specific MT organization that is instrumental in the generation of apical and basal membranes, probably by directional intracellular trafficking, thus coupling cell elongation and intracellular lumen formation. Figure from Gervais and Csanova 2010.

In order to better clarify the molecular processes involved in seamless tube formation, starting from the “Inward membrane growth model” we tried to shed light on some of the unknown aspects involved in subcellular lumen formation. How does the initiation of the subcellular lumen formation start? Where do MTs nucleate in the TC? How do MTs regulate the dynamic process of subcellular lumen formation? How are the different cytoskeletal elements connected between them? The answers to these questions will be presented in this thesis.

2 OBJECTIVES

2 OBJECTIVES

Terminal cells (TCs), specialized cells designed to connect the tracheal system to the target tissues, represent a good model for seamless tube formation. During tracheal embryonic development, terminal cells give rise to unicellular tubes, generating a cytoplasmic extension by cell elongation, and a concurrent intracellular luminal space surrounded by apical membrane. This process depends on cytoskeleton reorganization. The main aim of this work was to understand novel aspects of cytoskeletal modulation that orchestrate subcellular lumen formation. In particular we address this aim analysing mutants displaying an expansion of the subcellular lumen branching and mutants characterized by the absence of this subcellular lumen.

2.1) Mutants for *Rca1(Regulator of CycA)* were isolated from a mutagenesis screen, and previously characterized in the group of Sofia Araújo. These mutants displayed subcellular lumen bifurcations and the first goal was to clarify the effect of this mitotic protein during subcellular lumen formation, in particular:

- Analyse intracellular components involved in subcellular lumen formation in *Rca1* mutant.
- Characterize TC centrosomes in *wild-type* conditions and in *Rca1* mutants.
- Analyse subcellular lumen formation in mutants characterized by either centrosome amplification or absence of centrosomes.
- Define centrosomes as microtubule organizing center (MTOC) during subcellular lumen formation in TCs.

2.2) Spectroplakins are exceptionally long proteins characterized by the rare ability to bind single cytoskeleton elements as well as coordinating these elements between them. Because spectraplakins are crucial in cells that require an extensive and dynamic cytoskeleton, as TCs, the second goal was to investigate the role of the only spectraplakin in *Drosophila*, Short-stop (Shot) during subcellular lumen formation. In particular:

- Determine the function of Shot during subcellular lumen formation by analysing its loss of function and overexpression phenotype.
- Analyse the localization of Shot inside the TCs.
- Analyse the molecular function of Shot as a cytoskeletal mediator during subcellular lumen formation.

3 MATERIALS AND METHODS

3 MATERIALS AND METHODS

3.1 Fly strains

All *Drosophila melanogaster* strains were raised at 25°C under standard conditions. The strain y^{1} w^{188} was used as *wild type* (*wt*).

The mutant strains used in this thesis were:

$rca1^{IX}$, $rca1^{2}$, *Df(2L)6569*, $CycA^{C8LR1}$, $CycB^{2}$, Fzr^{1}, $slmb^{0295}$, $Sas\text{-}4^{2214}$, $shot^{3}$, $shot^{kakP2}$ (from Bloomington Stock Center) $Rca1^{G012}$ (Sofia Araújo). Mutant chromosomes were balanced over *CyO*, *TM3* or *TM6* marked with LacZ or GFP.

To visualize centrosomes we used *asl::YFP* and *asl::m-Kate* (C. Gonzalez).

btl::moeGFP (S. Hayashi) and *btl::moeRFP* (M. Affolter) were used to follow Moe/Actin accumulation within TCs.

The overexpression, rescue and RNAi experiments were performed using the Gal4/UAS system (Brand and Perrimon, 1993). The *btl-Gal4* (M. Affolter) and *trhGal4* (Bloomington Stock Center) were used to drive responder line expression in all tracheal system from invagination stage. *DSRF-Gal4* (from M. Calleja and G. Morata) was used to drive responder line in TCs. Responder transgenes lines used were: *UAS-Rca1* (F. Sprenger), *UAS-bazYFP* (L. Gervais), *UAS-EB1GFP* (A. Guichet), *UAS-Rca1RNAi* (VDRC), *UAS- SAKND* (M. Bettencourt-Dias), *UAS-shot L(A) GFP*, *UAS-shot L(C)-GFP*, *UAS-shot L(A)-ΔEF-GFP*, *UAS-shot-L(C)-ΔGAS2-GFP*, *UAS-shot-L(A)-ΔEF-hand-GFP*, *UAS-shot-L(A)-Δrod1-GFP*, *UAS-shot-L(A)-ΔPlakin-GFP*, $UAS\text{-}shot^{GL01286}$ *RNAi*, (All from Bloomington stock center) ,*UASshot-L(A)-ΔCtail-GFP*, *UAS-Ctail-GFP* (N. Sanchez Soriano), *UAS-tauGFP* (M. Llimargas). The tracheal expression of the membrane protein Src fused with GFP (*btl>srcGFP*) was used to visualize the outline of the TCs. Embryos expressing transgenes were collected after 18/24 h typically at 25°C or 29°C when mentioned in the text.

3.2 Embryos fixation and immunohistochemistry

Embryos, collected on agar plates overnight (O/N), were dechorionated with bleach for 2 minutes (min) and fixed for 20 min (or 10 min. for MTs staining) in 4% formaldehyde, PBS (0.1 M NaCl 10 mM phosphate buffer, pH 7.4) / Heptane 1:1. Embryos were washed with methanol twice and used immediately for immune-staining or stored at -20°C. Embryos were rinsed 3 times and washed 30 min with PBT (PBS1X with 0,1% Tween 20 from Sigma), and 30 min with PBT-BSA (PBS with 0,1% Tween 20, 0,5% Bovine Serum Albumine from Roche). Primary antibody incubation was performed in fresh PBT-BSA O/N at 4°C. Embryos were rinsed 3 times and washed 1h at room temperature in PBT and secondary antibody incubation were done in PBT-BSA at room temperature (RT) in the dark for 2h. Embryos were rinsed 3 times and washed 1h in PBT and finally mounted in Fluoromount-G (Southern biotech).

For DAB histochemistry (used to recognize 2A12/antiGasp antibody) embryos after incubation with secondary antibody (mouse IgM biotinylated antibody) were washed with PBT. In the meantime AB solution were prepared incubating for 30 min at R/T A (Avidin) - B (Biotinylated Horseradish Peroxidase H) (Vectastain-ABC KIT of Vector Laboratories) 1:200 in PBT. Embryos were incubated with A-B solution for 30 min, and then they were rinsed 3 times and washed 30 min with PBT. Embryos were incubated with the DAB solution (DAB 0,12% Nickel sulphate-Cobalt chloride, 0,3 %H_20_2) until black colour was achieved (usually 2/3 min). Then embryos were rinsed 3 times, washed 20 min with PBT and finally mounted in glycerol 70%. In all DAB staining, DSRF, and balancer GFP and LACZ were stained with secondary fluorescent antibody.

The primary antibodies used were: mouse anti Gasp 1:5, rat anti DE-cad 1:100, from Developmental Studies Hybridoma Bank (DSHB), rabbit anti apKC 1:100 (Santa Cruz Biotechnology), guinea pig anti CP3019 (V. Brodu) 1:1000, rabbit and rat anti DSRF 1:500 (both produced by N. Martín in J. Casanova Lab), anti GFP 1:500 (From Roche and Jackson), anti- β gal 1:500 (Cappel, Promega, Abcam), mouse anti α tubulin 1:100 (DM1A, Thermafisher), mouse anti acetylated tubulin 1:100 (Sigma), rabbit anti γ tubulin 1:100 (C. Gonzalez), guinea pig anti Shot 1:1000 (Katia Roper).

Cy3, Cy2 or Cy5 conjugated secondary antibody (Jackson Immuno Research) or Alexa–conjugated secondary antibody (Thermo Fischer Scientific) from Donkey and/or Gout was used 1:500 in PBT 0,5% BSA.

Two probes, to label luminal chitin were used in the same step of secondary antibody;

Fluostain 1:200 (Sigma), and chitin binding protein CBP1:500 (produced by N. Martín in J. Casanova Lab according to Luschnig Lab. protocol).

3.3 MTs disassembly and regrowth

Embryos were collected O/N at 25°C, dechorionated with bleach and incubated on ice for 6 h. To follow MT regrowth were subsequently incubated at 25°C for 2 min or 30 min. Control embryos were processed in a similar way but kept for 6h at 25°C. Embryos were then fixed and stained.

3.4 Molecular biological techniques

3.4.1 Genomic DNA extraction

Genomic DNA of *wild type* flies was isolated using "Thermo Scientific Genomic DNA purification Kit". Flies were homogenized with 180 µl of digestion buffer. The sample was treated with 20 µl Proteinase K and incubate at 56°C for 30 min. The sample was incubated 10 min with 20 µl of RNAse A solution. 200 µl of Lysis Solution was added into the tube and vortexed. The simple was washed with 400 µl of 50% ethanol.

To purify genomic DNA GenJet DNA purification kit was used. Treatment with Elution buffer 2 min at RT was used and a centrifugation 1 min 8000 rpm was performed to recover the sample. Purified genomic DNA was recovered with elution buffer and stored at -20°C.

3.4.2 Preparation of PCR template

Primers described in Table 1 were used to prepare PCR template for double stranded RNA interference (dsRNAi).

RNAi primers	Forward	Reverse
CYCA	TAATACGACTCACTATAGGGAGATTTCACGTCATGGTTCTCTT	TAATACGACTCACTATAGGGAGGCCAAGAAATCGAATGTGGT
RCA1	TAATACGACTCACTATAAGGGAGGCCTCGCTTATGGAAACCC	TAATACGACTCACTATAGGGAGTTTCAATCGCCACACAGTAG
SLIMB	TAATACGACTCACTATAGGGAGAGCACAGGCCTTCACAACCACTATG	TAATACGACTCACTATAGGGAGTTGCAGACCAGCTCGGATGATTT
SAK	TAATACGACTCACTATAGGGAGAATACGGGAGGAATTTAAGCAAGTC	TAATACGACTCACTATAGGGAGATTATAACGCGTCGGAAGCAGTCT

Table 1. List of primers used

A typical 100 µl PCR reaction was performed; 100 ng genomic DNA or cDNA, 150 ng of both forward and reverse oligonucleotides, polymerase buffer 1X dNTPs 0.2mM, 5units DNA polymerase, $MgCl_2$, H_20.

PCR reaction product was purified with the high Pure PCR Product Purification Kit (Roche). PCR purified product was eluted with DEPC-Treated H_2O.

3.4.3 dsRNA synthesis

MEGA-script T7 kit (Thermo Fisher) was used to synthesize dsRNA. 20 µl reaction was assembled with 4µl DEPC- treated H_2O, 4 µl 10x reaction buffer, 2 µl each ATP, CTP, GTP, UTP, 2 µl linearized DNA template 2 µl enzyme mix. Reaction was performed at 37°C for 4 h. Reaction product was precipitate at -20°C with 10% Sodium Acetate Solution 3M and 2.5 volumes ethanol 100%. After centrifugation at maximum speed Ethanol was removed and pellet was air dry for 15 min. RNA pellet was suspended in DEPAC-trated H_2O. RNA strands where annealed by eating at 65°C for 30 min and the slowly cooling at room temperature. Finally dsRNA was stored at -20°C.

3.5 *Drosophila* S2 Cell Culture

Drosophila S2 cell culture (Invitrogen) were maintained in complete Schneider's medium (CSM) (Schneider's medium from Sigma complemented with 10% fetal calf serum FCS from Gibco) at 28°C. For general maintenance, cells were passaged at a density of 10^7 cells/ml. The high density cells were suspended by gentile pipetting and diluted 1:10 in a new flask.

3.5.1 RNA interference in S2 cells

10^6 Cells ml $^{-1}$ in Schneider medium were used in 6-well plates. In each dish 40 mg of dsRNA and 20 ml of Transfast (Promega) where added. Cells and dsRNA were incubated for 1h at RT. After that 1ml of CSM was added in each dish and incubated at 28°C for 4 days.

3.5.2 Fixation and immunohistochemistry of S2 cells

S2 cells were rinsed 2 times with PBS for 10 min and suspended in Schneider medium. Cells where transferred to 6-well plates previously treated with concanavalin A (Sigma) 0.5 mg/ml 30 min, and were allowed to settle for 30 min at RT. Cells were washed with PBS for 10 min and fixed in PBS 4% p-formaldehyde for 15 min at RT. Cells were washed 2 times with PBS-0.3% Triton X100 0,2 BSA for 10 min.

Cells were washed and then incubated in fresh PBS-0.3% Triton X100 0,2 BSA with guinea pig anti CP309 (V. Brodu) 1:1000 at 4°C O/N.

Cells were rinsed 3 times with PBS, washed 2 times for 10 min and incubated 1 h at RT with the secondary antibody donkey anti Guinea Pig cy3 1:500 in PBS-0.3% Triton X100 0,2 BSA. Cells were washed 2 times for 10 minutes with PBS-0.3% Triton X100 and 2 times for 10 minutes with PBS. Cells were incubated with DAPI 0,04 ng/µl (Sigma) in PBT for 15 min, and washed with PBS 2 times for 10 min. Cells were finally mounted in MOWIOL (Sigma).

3.6 Microscopy

Bright field photographs were taken using a Nikon Eclipse 80i microscope with a 20X or 40X objective. A super high-pressure mercury lamp, Nikon AD1830, was used to detect fluorescent staining. Photoshop CS5 12.0 X 64 was used for measurements, adjustments

and to assemble figures. Florescence confocal images of fixed embryos where obtained with Leica TCS-SPE system using 20X and 63X (1.40-0.60 oil) objectives (Leica). Fiji (Imagej 1.47) (Shindelin et al., 2012) was used for measurements and adjustments. The images shown are, otherwise stated in the text, max-intensity projection of Z-stack section. Figures were assembled with Photoshop CS5 12.0 X 64.

3.7 Quantification and statistics

Total number of embryos, TCs and S2 cells quantified (n) are provided in text and figures. Regarding the quantification of centrosome numbers in S2 cells after RNAi experiments, data were an average of three independent experiments.

Measurement were imported and treated into the excel software 14.7.1, where graphics were generated. Error bars graphics and ± in text denote Standard Error (SE) or Standard deviation (SD). Statistical analyses were performed applying the t-test. Differences were considered significant when $p<0,05$. In graphics; *$p<0.05$, **$p<0.01$, ***$p<0.001$.

4 RESULTS

4 RESULTS

4.1 Terminal cells with 2 lumina

During embryogenesis *Drosophila* tracheal terminal cells (TCs) are able to form unicellular branches by a mechanism of cell elongation associated with the generation of a subcellular lumenal space surrounded by apical membrane. In fact, subcellular lumen formation depends on the growth of new apical membrane inside the cytoplasm of the cell, a process that requires cytoskeletal reorganization (Gervais and Casanova, 2010).

To obtain a collection of mutants useful to understand the molecular mechanisms that orchestrate TC specification, an ethyl-methane-sulfonate (EMS) screening was previously performed by the group of Sofia Araújo. This forward genetic screen generated a set of approximately 80 mutant *Drosophila melanogaster* lines with phenotypes in both the tracheal and the nervous systems. With our aim to study subcellular lumen formation in mind, we collected embryos with defects in TCs at the tip of ganglionic branches (GBs). A phenotype that was found in several mutants was the "luminal bifurcation" phenotype in which two or more subcellular lumens appeared instead of one. Many mutants displayed **luminal bifurcation** as a result of extra TCs, so more than one cell acquired a terminal cell fate and created its own intracellular lumen (Araujo and Casanova, 2011). However in the mutant *G012* the luminal bifurcation arose inside a single TC.

In this first section of results I describe some data collected by Myrto Deligiannaki before I joined the Araújo group, regarding the characterization of G012 as an allele of *Regulator of CycA 1* (*Rca1*) and its autonomous involvement during TC development. Next, I report the characterization of *CycA* subcellular branching phenotype and then I will describe the state of several intracellular components involved in subcellular lumen when it is bifurcated. I will continue with the description of centrosomes in *wt* and *Rca1* TCs. I will describe the effect of centrosome amplification and reduction in correlation with subcellular lumen formation and finally, I will give a detailed characterization, mainly done with the experimental support of Sofia Araújo, of centrosomes as microtubule organizing centers (MTOCs) into TCs.

4.1.1 *G012* displays bifurcated TCs

As described in the introduction, in *wt* embryos TCs are able to form a single subcellular lumen (**Fig. 20 A, B**). Staining of *G012* fixed embryos with the luminal marker Gasp/2A12 and with the specific TC nuclear marker DSRF antibody, revealed that such mutation induced an increase in the number of subcellular lumina. In particular, TCs were able to form a bifurcated subcellular lumen (**Fig. 20 C, D**) in 86% of embryos analysed (n=52) with a mean of 2,7 bifurcated terminal cell per embryo (quantification of embryos with at least one bifurcation), (**Fig. 21 K**, **L**).

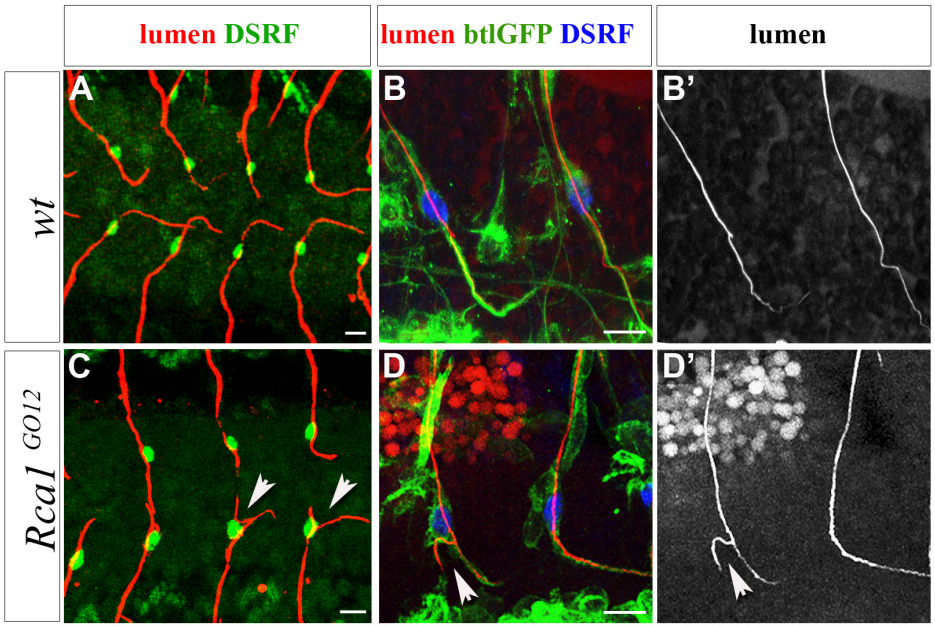

Figure 20. *G012* mutant embryos display expansion of the TCs subcellular lumen. Ventral view of GBs of *wt* (**A -B**) and *G012* (**C-D**) embryos at st. 16 stained with anti-GASP (in red in A-D in grey in B' D') DSRF (in green in A and C blue in B and C). White arrows indicate the point of extra branching. Anterior side of the embryo is on the left. Scale bars 5µm.

4.1.1.1 *G012* is a null allele of *Rca1*

The mutation was mapped and it was defined that *G012* is allelic to ***Regulator of CycA 1*** **(*Rca1*)**. In particular, *G012* was characterized as a nonsense mutation, consisting in a substitution of the tryptophan 189 with a stop codon.

Rca1 is the *Drosophila* homolog of vertebrate Emi1 and a negative regulator of Anaphase-Promoting Complex/Cyclosome (APC/C) activity at various stages of the

cell cycle (Grosskortenhaus and Sprenger, 2002; Reimann et al., 2001). APC/C is a multi-subunit E3 ubiquitin ligase that marks proteins for destruction and it is responsible for the regulation of several steps during cell division by degradation of many cell cycle proteins, like cyclins, securing and many others (Pesin and Orr-Weaver, 2008).

APC activity is restricted to mitotic stages and G1 by its activators Cdc20-Fizzy (Cdc20/Fzy) and Cdh1-Fizzy-related (Cdh1/Fzr), respectively. It has been described that Rca1 specifically inhibits the activity of APC-Cdh1/Fzr; in *Rca1* mutants, cyclins are degraded prematurely in G2 by APC-Cdh1/Fzr-dependent proteolysis, and cells fail to execute mitosis (Grosskortenhaus and Sprenger, 2002).

In order to confirm tha*t G012* was an allele of *Rca1*, trans-heterozygous combinations with other previously reported *Rca1* alleles (*Rca1I*^{X} and *Rca1*^{2} and *Df(2L)6569*) were tested. As reported in **Fig. 21C** and **K,** *G012* failed to complement other alleles and in all combinations bifurcated TCs appeared, confirming that such phenotype is caused by the absence of Rca1.

4.1.1.2 The effect of *Rca1* is autonomous in differentiated tracheal cells

Because *Rca1* have a ubiquitous expression during early embryonic development, and later on, from st 13, is expressed in several proliferating cells (Dong et al., 1997), it was analysed if the effect of *Rca1* was autonomous in tracheal cells. To do so, first a rescue of *Rca1* ^{G012} phenotype was performed overexpressing *UAS-Rca1* with the specific tracheal driver line *btlGal4*. *Rca1* over-expression in tracheal cells was sufficient to restore the normal branching pattern in 81% of embryos analysed (n = 32), suggesting that the effect of *Rca1* was autonomous in tracheal cells. To confirm it, *Rca1* was silenced in the tracheal system overexpressing an *Rca1 RNAi* line. It was observed that *Rca1* tracheal knockdown was enough to generate TC bifurcations in 47% of embryos analysed (n = 17).

These results indicated that *Rca1*, in differentiated tracheal TCs, serves to regulate subcellular branching events.

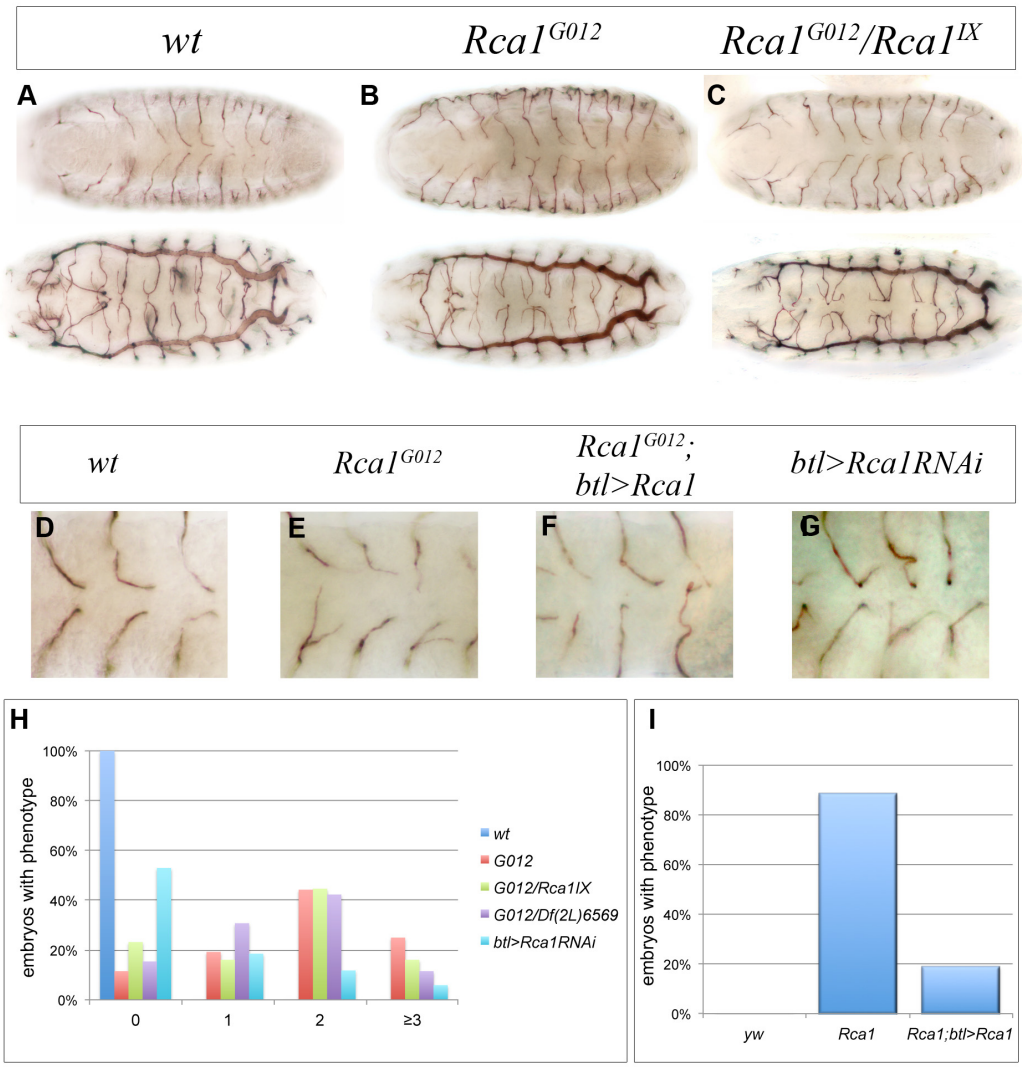

Figure 21. *G012* is allelic to *Rca1* and its effect is autonomous in tracheal system. (**A-C**) Ventral (up) and dorsal (down) view of embryos at st. 16 stained with anti Gasp to visualize the lumen; (A) *wt* (B) *Rca1* ^{G012} and (C) *Rca1* $^{G012/IX}$; **(D)** Magnified region showing GB lumina in detail of *wt*. (**E**) Same region from homozygous embryo *Rca1*^{G012} ; (**F**) *Rca1*^{G012} embryo rescued by the expression of a full length *Rca1* construct driven in tracheal cells (*btl* positive cells); (**G**) detail of an embryo where *Rca1* was down-regulated by means of *Rca1RNAi* expression in tracheal cells.

(**H**) Quantification of the number of extra sub-cellular lumen events found per embryo in each of the allelic combinations tested. The number of extra subcellular lumen events per embryo is presented in percentage of embryos displaying each of the phenotypes. *wt* n=41, *Rca1G012* n=52, *Rca1G012/Rca1IX* n=56, *Rca1G012/Df(2L)6569* n=26, *btl>Rca1RNAi* n=17. We did not differentiate between the number of extracellular lumina per terminal cell (i.e. more than one lumen per cell was quantified as a bifurcation as these represented the majority of cases).

(**I**) Percentage of embryos with extra subcellular lumen phenotypes in the wt (n=41) and *Rca1*^{G012} (n=52) compared with *Rca1* rescued embryos. The expression of a full length *Rca1* construct in tracheal cells from st. 11, rescues the terminal bifurcation phenotypes.

4.1.1.3 *Rca1* phenotype does not depend entirely on the cell cycle arrest

Rca1 is required for both mitotic and meiotic cell cycle progression, and *Rca1* mutants are characterized by lower numbers of cells than the *wt* caused by arrest in embryonic cell cycle 16 (Dong et al., 1997). We wondered if this arrest of the cell cycle was the cause of subcellular branching, thus other mutant conditions that induce a similar cell cycle arrest where analysed.

Rca1 regulates, via APC/C the degradation of several proteins between them **Cyclin B** (CycB) (Grosskortenhaus and Sprenger, 2002). CycB regulates protein kinase activity during the cell cycle and mutants for this cyclin display defects in the normal progression of the cell cycle (Grosskortenhaus and Sprenger, 2002). When we analysed *CycB*^{2} loss of function allele we observed some morphogenetic defects, probably caused by the cell-cycle phenotype, but we could not detect any subcellular branching phenotype (**Fig**. **22B** and **E**).

The cell cycle ***fizzy*** gene (*fzy*) encodes an activator of the APC/C and it is involved in the normal cell cycle-regulated proteolysis that is necessary for successful progress through mitosis (Dawson et al., 1995). We also analysed *fzy* mutant that is characterized by a cell cycle arrest similar to *Rca1* (Sigrist et al., 1995), and also in this case, we could not detect any extra subcellular lumen phenotype in the TCs (**Fig. 22D**).

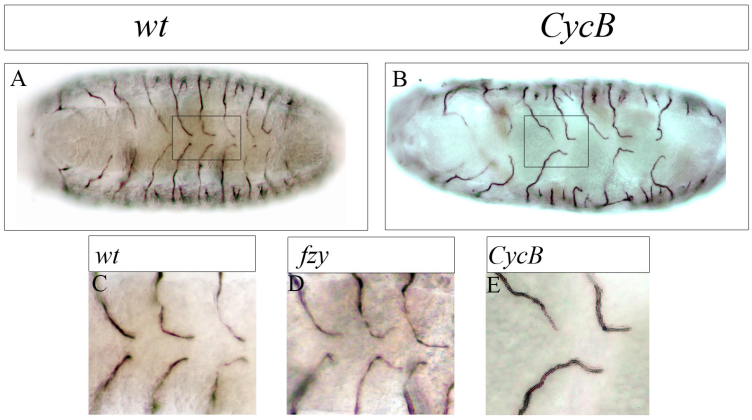

Figure 22. Cell cycle mutants do not develop subcellular lumen phenotype. Ventral view of embryos at st. 16 stained with anti Gasp antibody to visualize the lumen (**A**) *wt*, (**B**) *CycB*^{2} and (**D**) *fzy*.

(**C** and **E)** magnified region from A and B (see squares). D some tips of GBs from *fzy* embryos. Anterior side of the embryos is on the left.

4.1.1.4 *CycA* mutation induces similar subcellular branching phenotypes to *Rca1*

Rca1 positively regulates **Cyclin A** (CycA) levels, by inhibiting the APC/C activity (Dong et al., 1997; Grosskortenhaus and Sprenger, 2002). In *Rca1* mutants CycA is degraded through APC/C-dependent proteolysis. We, therefore, addressed whether the *CycA* null mutant embryos, apart from displaying cell-cycle phenotypes such as lower numbers of cells and general morphogenetic defects (Buti et al., 2014), showed a subcellular lumen phenotype related to *Rca1*. We stained fixed embryos for the amorphic allele *CycA* ^{CL8R1} (from now just *CycA*) with CBP (chitin binding protein) to visualize the lumen and DSRF to recognize the nucleus of the TCs. Surprisingly *CycA* mutant displayed TCs with extra subcellular lumina (**Fig. 23 B**). We quantified that 88% of embryos counted (n= 45) where characterized by at least one bifurcation (**Fig. 23 C**).

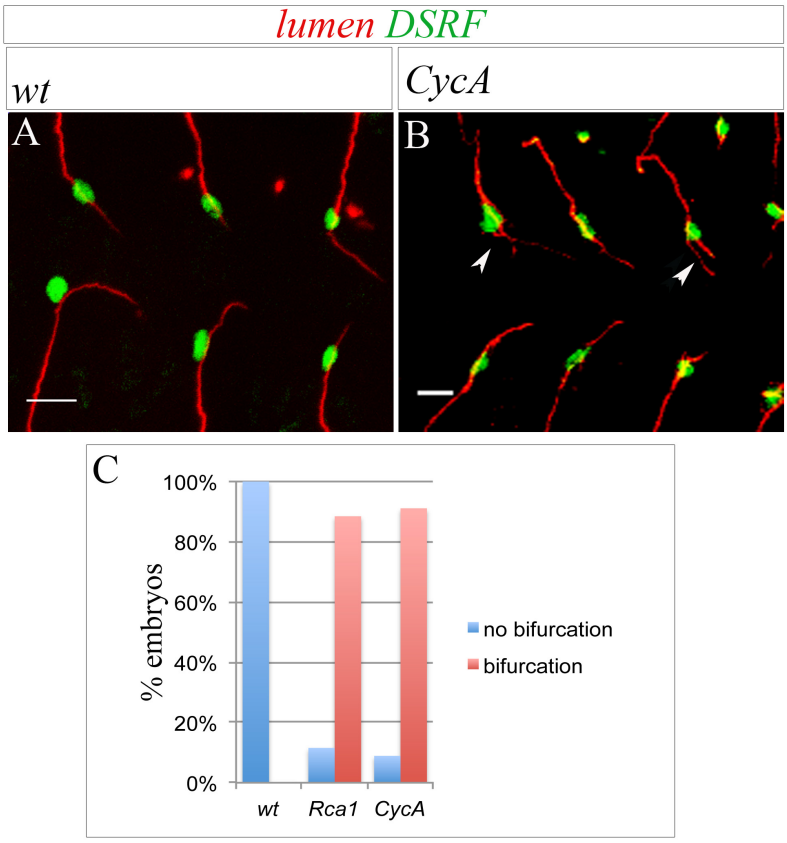

Figure 23. *CycA* mutant embryos show TC branching phenotype. Ventral view of *wt* (**A**) and *CycA*^{C8LR1} embryos at st. 16 (**B**) stained with CBP to visualize the lumen and DSRF to recognize the

nucleus of TCs. White arrows indicate extra-subcellular lumen. (Anterior side of embryos is on the left, scale bars 10 μm). (**C**) Quantification of the population of embryos with bifurcations or *wt*-like in the distinct genotypes (*wt,* n = 41, *Rca1* n=52, *CycA* n=45).

So, *Rca1* mutants were characterized by extra branching of the TC subcellular lumen and this effect was autonomous in tracheal system. There was the possibility that the phenotype observed in *Rca1* mutants depended on a constitutive degradation of CycA, since *CycA* mutants displayed the same subcellular lumen phenotype, but this effect did not depend on the cell cycle arrest and the lower cell number that affected these mutants. How did the two cell cycle proteins induce these morphogenetic defects in the TCs? It is worth mentioning that in the developing tracheal system, once placodes start invaginating at embryonic st. 11 no further cell–divisions occur. Therefore, the effect of Rca1 and CycA in the regulation of subcellular branching is most likely a **post-mitotic function/effect** of these mitotic proteins. So we continued investigating the cause of the extra subcellular branching by analysing step by step the subcellular lumen formation in *wt* and mutant condition. Since *CycA* mutant embryos displayed stronger general morphogenetic defects respect to *Rca1* mutant we decided to continue our analysis using *Rca1* mutant embryos.

4.1.2 Intracellular components in *Rca1* TCs

We followed the characterization of *Rca1* mutant phenotype analysing different intracellular components involved in subcellular lumen formation in order to understand the cause of the extra-subcellular lumen generation.

4.1.2.1 Apical membrane growth in *Rca1* is duplicated

In vivo studies of TCs at the tip of DBs in *wt* conditions, demonstrate that subcellular lumen formation depends on the growth of new apical membrane inside the TCs during its elongation (Gervais and Casanova, 2010). Therefore, apical membrane determinant **Bazooka** (Baz)/Par3 was analysed in mutant conditions. In particular, we used *bazYFP* (yellow fluorescent protein) construct, driven by a tracheal specific line (*btl-Gal4*), to visualize apical membrane in *wt* and $Rca1^{G012}$ (from now $Rca1^{G012}$ is referred just as *Rca1*).

Subcellular apical membrane formation in ganglionic TCs, as described for dorsal TCs (Gervais and Casanova, 2010), was observed as continuous process of sprouting from the surface contacting the lumen of the principal network and following the direction of cell elongation (**Fig. 24 A**). In *Rca1,* this apical membrane addition event was duplicated from the beginning of TCs development; from the apical cell-cell junction, where BazYFP is strongly accumulated, was possible to detect **a bifurcated track of apical membrane** and later-on, as the TC growth, the extension of two lumina (**Fig. 24 B**).

Also, by analysing fixed embryos of the *Rca1*; *btl>bazYFP* genotype it was possible to observe the duplication of the apical membrane (**Fig. 24 H**) and analysing the mutant, at early developmental stages of TC formation, BazYFP was detectable strongly at the cell-cell apical junction (**Fig. 24 I**). *Rca1* mutant embryos displayed an average of 5.6 TCs per embryo with **higher Baz accumulation**, in contrast to 0.6 TCs in the WT (n = 80 GB TCs) (**Fig. 24K**). Also the analysis of the apical component **atypical protein kinase C** (aPKC) at early seamless lumen growth stages in *Rca1* mutant (**Fig. 24 J**) indicated that these components accumulate apically at higher levels than in *wt* TCs (**Fig. 24 F**).

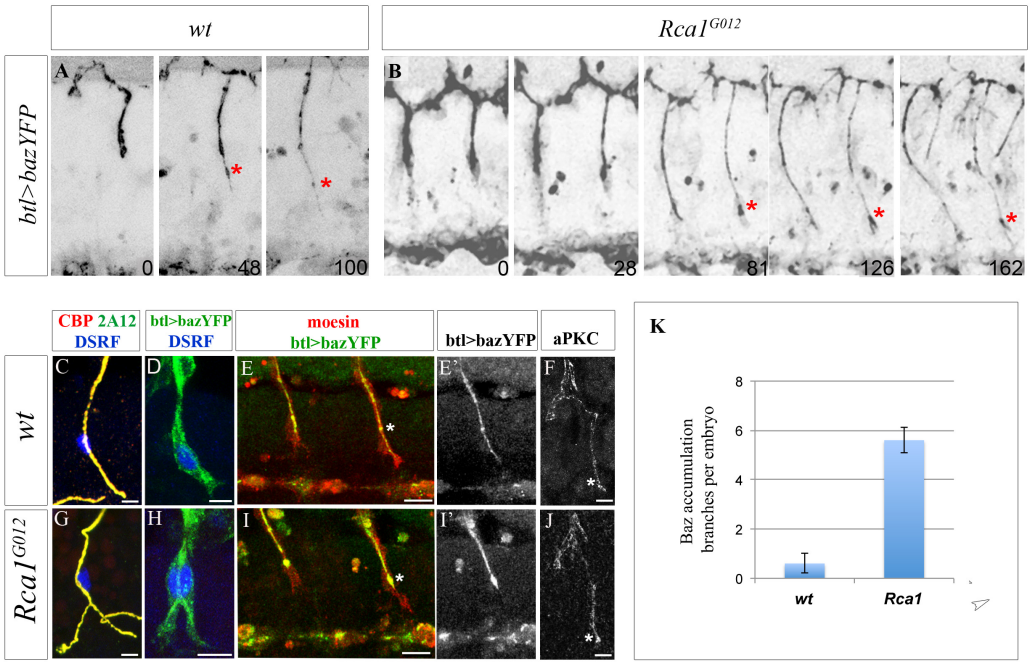

Figure 24. Apical membrane is duplicated in *Rca1* mutant. Frames from times laps experiments showing subcellular lumen extension from st 14 to st 16 in *wt* condition (**A**) and *Rca1* mutant (**B**) GBs. The growing subcellular lumen extends from the cell-cell junction between the tip and stalk cell

(indicated by a red asterisk). In the *wt,* only one subcellular lumen extends from the junction (A), whereas in the mutant, two lumina extend from this point (B). Numbers on the lower right-hand corner are minutes.

(**C–J**) Analysis of *Rca1* TC apical components in comparison with *wt*. *Rca1* TCs grow lumina that structurally resemble the *wt* in lumen components such as chitin binding protein (CBP) and Gasp/2A12 (C-G) or apical membrane markers such as Baz (D-H). In *Rca1*, at early stage of TCs development, higher amounts of Baz accumulate respect to ***wt*** (E-I asterisk) as well as aPKC (F-J asterisk). Scale bars 5 µm.

(**K**) Quantitation of Baz accumulation at the TC junction per embryo GB in wt (±SEM).

4.1.2.2 Asymmetric actin accumulation in *Rca1* is duplicated

Asymmetric Actin/Moe accumulation is involved in directing proper cell elongation and subcellular lumen formation (Gervais and Casanova, 2010; Oshima et al., 2006). In order to analyse Moe/Actin accumulation we used *btl::moe-RFP* (Red Fluorescent Protein) flies, consisting on the Moesin actin binding protein-RFP fused with the *btl* promoter. This construct allows us to visualize moesin, and therefore F-actin, in all cells expressing *btl*. In *wt* conditions and *Rca1* mutant background this construct allowed visualizing cortical membrane and the Moe/Actin accumulation at the tip of TC during cell elongation. At the tip of ganglionic TCs in *wt*, as previously described for dorsal TCs, a spot of Moe/Actin was detectable (**Fig. 25 A**). In *Rca1*, each lumen was extending in a cytoplasmatic protrusion that accumulated actin at the tip (**Fig. 25 B**).

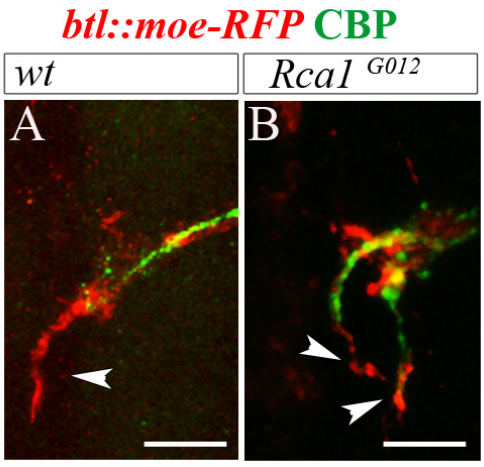

Figure 25. Asymetric actin accumulation in *Rca1.* Tip of TC from embryos *btl::moeRFP* stained with anti RFP to visualize moeRFP and CBP to visualize the lumen. Moe/Actin (in red) accumulates at the tip of the TC, and the subcellular lumina (in green) grow in the direction of this actin-rich spot (white

arrows) both in control (**A**) and *Rca1* TCs (**B**). Ventral midline of the embryo is down and the anterior side on the left. Scale bars 5 μm.

At this point we knew that luminal components, apical membrane and the Moe/Actin accumulation were duplicated in *Rca1* mutant and we asked which intracellular event could be responsible. We followed with the analysis of MT network.

4.1.3 Centrosomes during subcellular lumen formation

TCs elongation and subcellular lumen formation depend on a mechanism based on MT network organization. In fact, mutants with affected MT network display disrupted TCs (Gervais and Casanova, 2010; Sigurbjornsdottir et al., 2014). Thus, we wondered 1) whether *Rca1* and *CycA* mutants might affect the biogenesis of the MT network and 2) that the change in the MT network might be responsible for the extra subcellular lumen phenotypes.

The centrosome is the **major MT organizing center** (MTOC) of cells, and centrosomes play a crucial role in the maintenance of cell polarity and cytoplasmic architecture (Bornens, 2012). Both Rca1 and CycA modulate the activity of APC/C (Dong et al., 1997; Grosskortenhaus and Sprenger, 2002; Reimann et al., 2001) Moreover, oscillation of APC/C activity provides an additional mechanism for coupling the centrosome duplication cycle with replication (Erhardt et al., 2008; Prosser et al., 2012). We asked whether *Rca1* and *CycA* mutants showed aberrant centrosome numbers.

4.1.3.1 Centrosome number in *Rca1*

To obtain a characterization of centrosomes in TCs we used flies with an *asterless-YFP* construct (*asl::YFP*) to visualize centrioles in the embryos. This construct is expressed in all Asl-positive cells, marking all centrosomes in the embryo. As mentioned in the introduction, **Asterless** is a scaffold protein involved in the onset of centriole assembly (It is worth mentioning that a single positive Asl::YFP spot represent one pair of centrioles, or a centrosome, and this is the case also for other centriole markers used in this work). We also used *btl::moeRFP* construct to recognize the outline of all tracheal cells and therefore the TCs, and make the identification of the centrosomes belonging to TCs easier. In control TCs we detected **2 centrosomes**

localized at the apical side of the TC at embryonic stage 14 (72% n=33) (**Fig. 26 A** and **C**) and we quantified an average of 2.3 ± 0.5 centrosomes per TC (n = 33). Interestingly, we observed **an amplification of centrosome number** in *Rca1* TCs, detecting 3.8 ± 0.6 (n=42) centrosomes per TC, localized at the apical side (69%, n=42) (**Fig. 26 B** and **C**).

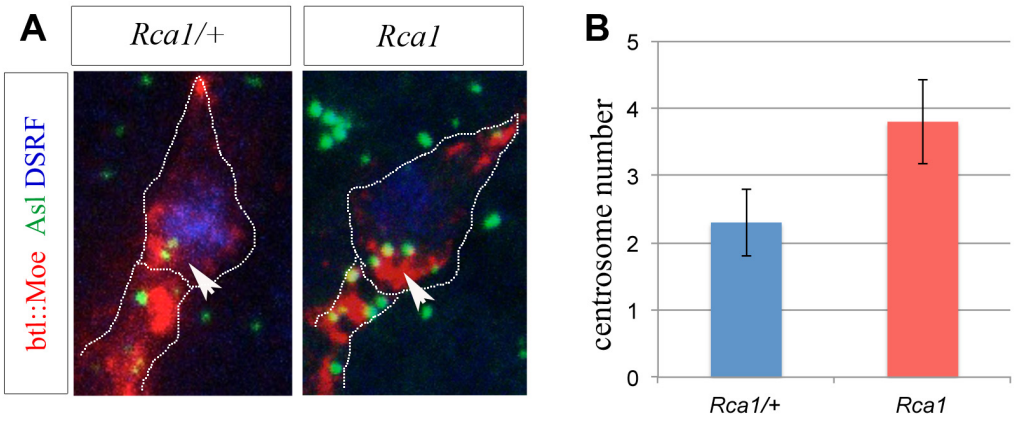

Figure 26. Supernumerary centrosomes in *Rca1* TCs. Centrioles observed in ganglionic TCs (ventral midline is up, Anterior side on the right) at the stage of initiation of luminal elongation (st. 14). (**A**) TC from *Rca1* heterozygote embryo and (**B**) from homozygote stained with GFP to mark Asl::YFP (green), RFP to mark btl::moeRFP (red), and DSRF to visualize the nucleus of the TC (blue); the white line marks the borders of the TC and the junction of the TC with the stalk cell. Note the higher numbers of centrioles in both Rca1 mutant tracheal cells and in the surrounding tissues. (**C**) Quantitation of centrioles in heterozygote (±SEM; n = 33) and mutant *Rca1* (±SEM; n = 42) TCs.

4.1.3.2 Knocking-down *Rca1* and *CycA* in S2 cells

Due to the technical difficulties of quantifying centrosome numbers in multicellular tissues and to confirm the results above, we performed RNAi knockdown of *Rca1* and *CycA* with **double-stranded RNA** (dsRNA) treatment in S2 cells culture and we quantified the numbers of centrosomes in these cells (**Fig. 27**). In this experiment, to visualize centrosomes, we used a specific antibody against the centriole component CP309/PLP. As controls, we used *β-Gal* RNAi that was expected to not induce any change in centrosome number; *slmb* RNAi and *SAK/PLK4* RNAi which were reported to increase and decrease centrosome number respectively (Bettencourt-Dias et al., 2005; Cunha-Ferreira et al., 2009; Rogers et al., 2009) (see below).

In cells depleted of *Rca1* and *CycA* (**Fig.27 D**, **E** and **F**), analogously to the down-regulation of *Slmb* (**Fig.27 B**, **F**), we detected an **increment in centrosome number** respect to the control (**Fig. 27A**).

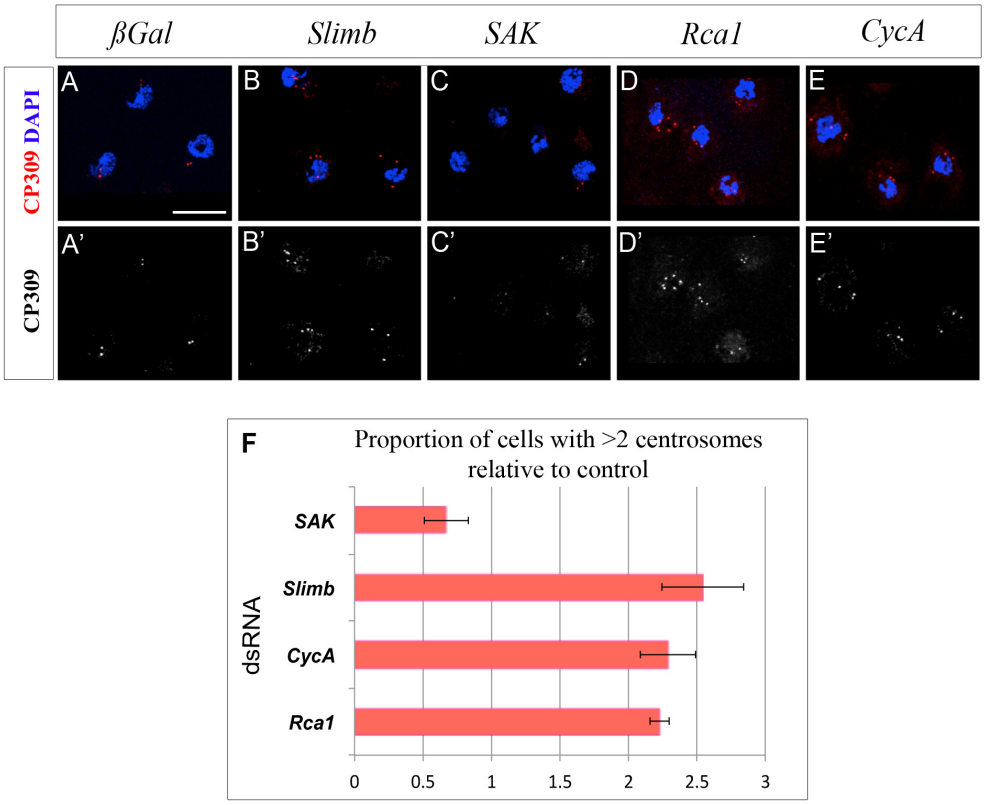

Figure 27. Centriole amplification observed after depletion of Rca1 and CycA

(**A-E**) Cells treated with dsRNA (indicated on the top) and assayed for centrosome numbers. Nuclei, stained with DAPI, are represented in blue and CP309 in red (A-D) or grey (A'-D'), Scale bar 5 µm.

(**F**) Quantitation of supernumerary centrosomes after RNAi treatment. Results were normalized relative to; RNAi β-galactosidase (β-Gal) controls (ratio is equal to 1). Data are the average of three independent RNAi experiments ± SEM (n = 200 cells in each experiment).

4.1.3.3 Analysis of subcellular lumen in "centrosome mutants"

In order to understand whether the supernumerary centrosomes in *Rca1* and *CycA* mutants might be correlated to extra subcellular branching phenotype, we analysed subcellular lumen branching in embryos bearing mutations that affect centrosome number.

The F-box protein **Slimb** (Slmb) fulfils several functions in development and cell physiology; amongst them there is a role in limiting centrosome duplication. Slmb is

directly involved in centrosome amplification through the degradation of the kinase SAK/Plk4, one of the protein kinase involved in centriole biosynthesis (Cunha-Ferreira et al., 2009; Wojcik et al., 2000). As described in the literature (Cunha-Ferreira et al., 2009) and in the previous experiment, in *slmb* loss of function conditions, there is a high proportion of cells with more than two centrosomes. When we examined TCs in $slmb^{00295}$ mutant null allele (from now just *slmb*), we found subcellular lumen extra branching phenotype in 80% of ganglionic TCs analysed (n=46), (**Fig 28 B** and **F**).

It has been described that the same effect of centrosome over-duplication is achieved when a non-degradable form of SAK, **SAK-ND**, is expressed in *Drosophila* cells (Cunha-Ferreira et al., 2009). Thereby, we overexpressed *SAK-ND* in the tracheal cells using a *btlGAL4* driver and we found that 78% of embryos displayed TCs bifurcations (n=50) (**Fig. 28 C** and **F**). Moreover, we also tested the effect of overexpression of *SAK-ND* specifically in the TCs using a *DSRFGal4* driver and also in this case we observed embryos with bifurcated TCs (**Fig. 28 E**). This data suggested that an amplification of centrosome number induced TCs to expand its subcellular lumen branching capacity.

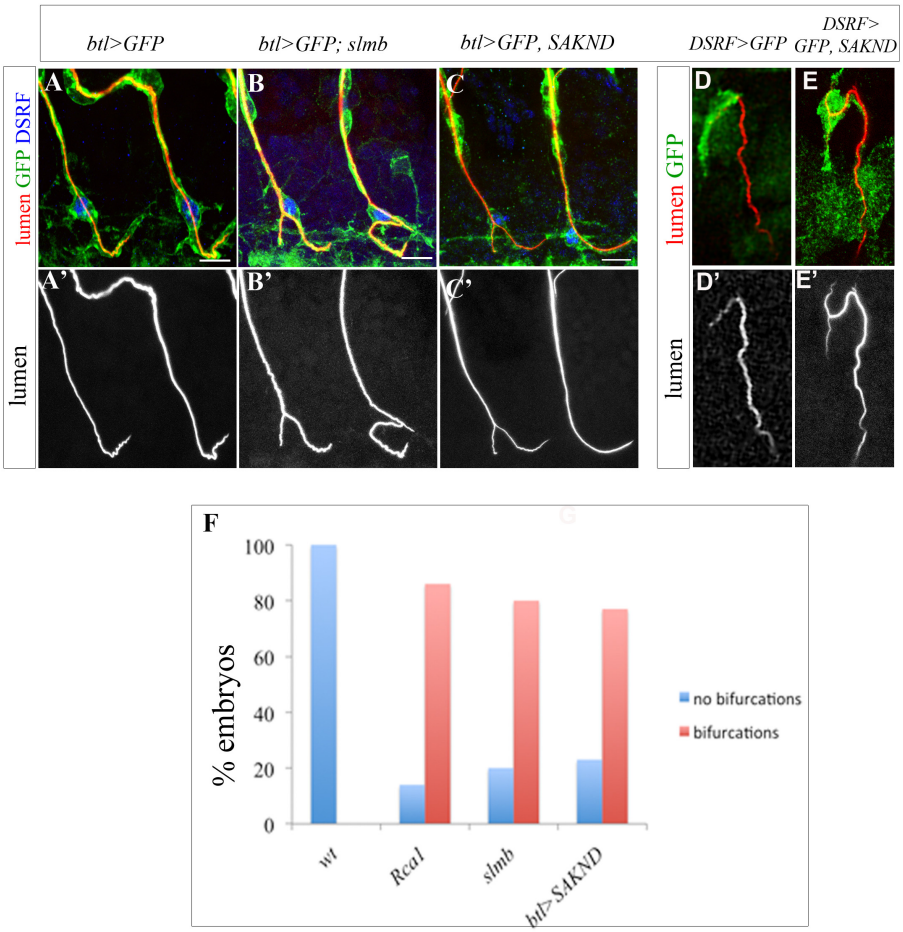

Figure 28. Mutants characterized by centrosome over-duplication display extra subcellular lumen branching. **(A–C)** Tip of tracheal GBs at embryonic st.16 stained with GFP to visualize tracheal cells (green), CBP to stain the tracheal chitinous lumen (in red in A-C and in grey in A'-C'), and DSRF to show the TC nucleus (blue). (A) *wt* TCs with a single lumen each. (B) *slmb* mutant TCs showing subcellular lumen bifurcations. (C) *btl>SAKND* tracheal cells showing one TC with a luminal bifurcation (Ventral midline is down and the anterior side of the embryo on the left. Scale bars 5µm). (**D-E**) Detail of a DB showing the TC in green due to the expression of GFP in DSRF expressing cells only. (D) control (E) TC overexpression of *SAKDN*. Lumen is in red (D-E) or in grey (D'-E'). (**F**) Quantitation of the population of embryos with bifurcations in the distinct genotypes. (wt, n = 41; $Rca1^{G012}$, n = 52; *slmb,* n = 46; *btl>SAKND*, n = 50).

If extra centrosomes lead to luminal bifurcation in tracheal TCs, then **centrosome number reduction** might impair TC subcellular lumen formation. It has been described that **Sas-4** protein is essential for centriole replication in *Drosophila* (Basto et al., 2006) and *sas-4* mutants gradually lose centrioles during embryonic development and by st. 15-16, centrioles are no longer detected in 50-80% of cells (Basto et al., 2006).

So when TCs subcellular lumen formation were examined in the *sas4* ^{s2214} loss of function allele (from now just *sas-4*) we found that the luminal phenotypes were very variable, ranging from none (*wt*-like) to very few TCs without lumen (not shown) to nearly all the embryonic GB TCs displaying no subcellular lumina (**Fig. 29B**). Due the high variability in the penetrance of the phenotypes, we quantified embryos with at least one TC **without subcellular lumen** and we counted that 88% of embryos (n=19) embryos were affected (**Fig. 29D**).

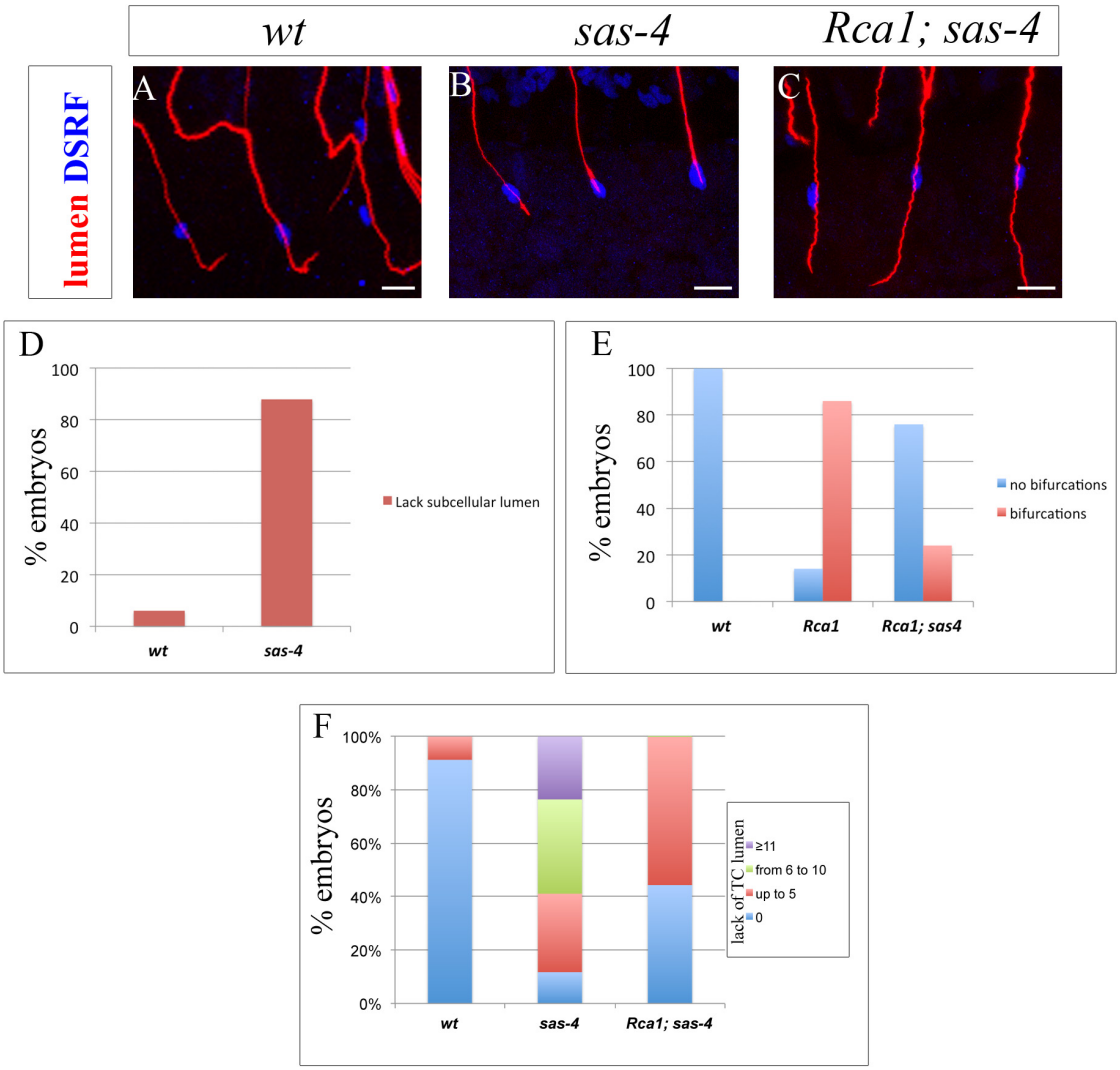

Figure 29. *sas-4* mutant lacks of subcellular lumen (**A–C**) Tips of tracheal GBs at embryonic st.16 displaying the subcellular lumen and part of the lumen of the stalk cells stained with CBP to visualize chitinous lumen (in red), and DSRF to show the TC nucleus (blue). Anterior side is on the left, ventral midline on the bottom. Scale bars 5µm. (A) *wt* (B) *sas-4* mutant displaying lack of subcellular lumen and (C) *Rca1;sas-4* double mutant in which there is rescue of the bifurcation phenotypes of *Rca1*, despite still showing guidance phenotypes.

(**D**) Quantification of *sas-4* mutant TCs phenotype of all GB TCs (n = 19 embryos). (**E**) *sas-4* mutation rescues the luminal bifurcation phenotype of *Rca1* mutant TCs. (**F**) In *Rca1; sas-4* double mutant there is a decrease of embryos with lack of TC subcellular lumen in comparison with s*as-4* mutant.

We hypothesized that if centrosome amplification was the cause of extra subcellular lumen and the lack of centrosomes was the cause of the absence of subcellular lumen we should be able to rescue the *Rca1* phenotype with a *sas-4* background. When we analysed TCs of *Rca1; sas4* embryos we noted a strong reduction of embryos with bifurcated TCs (78% n= 35) as well as observing less embryos displaying lack of subcellular lumen (more the 40% of embryos did not bearing TCs without subcellular lumen) (**Fig.29 C**, **E** and **F**).

In order to reinforce **the correlation between centrosomes and subcellular lumen formation**, we examined the number of centrosomes per TC in relation to the subcellular lumen growth in *sas-4* mutant; *sas-4; btl>srcGFP* mutant were fixed and stained with CBP to recognize the lumen, CP309 antibody to see centrioles and GFP to define the border of tracheal cells.

As described before *sas-4* mutant embryos had certain variability in the phenotype penetrance. We could correlate such variability of subcellular lumen phenotype with changeability in centrosome number. We observed that TCs of *sas-4* embryos that acquired the capacity to elongate a subcellular lumen had two 2 centrosomes (as in *wt* condition). TCs that were not able to generate a subcellular lumen were characterized by the absence of centrioles and TCs in which we detected 1 centrosome, were also not able to generate a lumen (n=29).

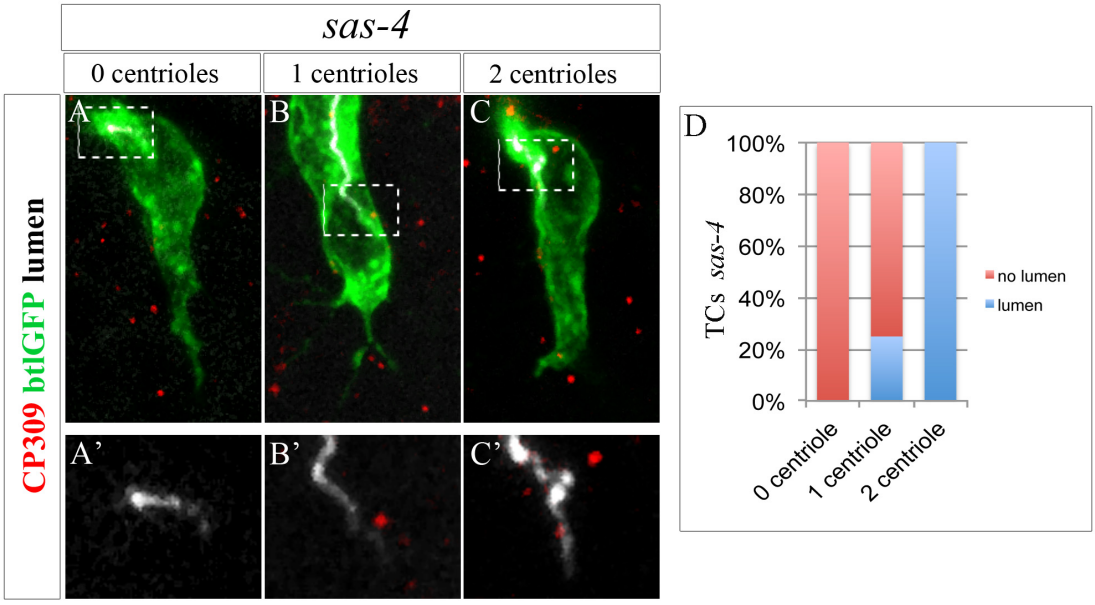

Figure 30. Correlation between centrosome number and subcellular lumen formation in *sas-4*

(**A-C**) Details of ganglionic TCs from embryos *sas-4: btl>srcGFP* stained with GFP to visualize cell membrane (in green), CBP to see the lumen (grey) and CP309 to recognize centrioles (in red). (A'-C') magnified region (see square in A-C). (A**)** TC with no centrosome; (B) TC with only one centrosome; **(**C) TC with 2 centrosomes; note how TCs have already extended in all cases and only in (C) is possible recognize a primordium of subcellular lumen. (D) Quantification of centriole number per TC in *sas-4* mutants (n=29) in correlation with lumen formation (red column represent the population of TC without lumen, blue column represent the population of TC that form lumen).

We also analysed the correlation between centrosomes and subcellular lumen formation in *Rca1; sas-4*. Also, in this case we could observe that TCs from double mutant embryos that elongated a subcellular lumen actually had 2 centrosomes (**Fig. 30 C, D**). TCs that were not able to generate a subcellular lumen were characterized by the absence of centrioles (**Fig. 30 A, D**) and TCs in which we detected one centrosome, in most of the cases, were not able to generate a lumen (n=25) (**Fig. 30 A, D**).

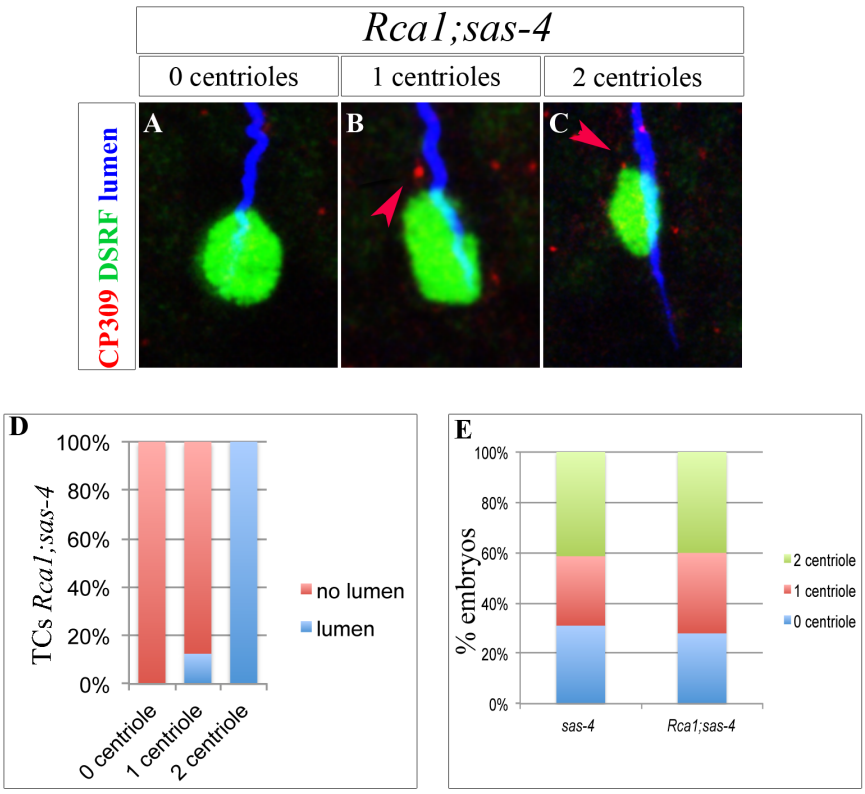

Figure 31. Correlation between centrosome number and subcellular lumen formation in *Rca1; sas-4* double mutant. (**A-C**) Details of *Rca1*^{G012}*: sas-4* ganglionic TCs at st. 15 stained with CBP to see the lumen (blue) DSRF to visualize the nucleus of the TC and CP309 to recognize centrioles (in red). (**A**) TC with no centrosome; (**B**) TC with only one centrosome; (**C**) TC with 2 centrosomes (Red arrows indicate centrosomes). (**D**) Quantitation of centriole number per TC in *Rca1;sas-4* double mutants (n=25) in correlation with lumen formation (red column population of TC without lumen, blue column population of TC that form lumen).

In *Rca1;sas4* double mutant, centrioles vary from 0 to 2 per TC, rescuing the supernumerary centrosome phenotype of *Rca1* mutant embryos. (**E**) Comparison of the number of centrioles per TC in *sas-4* mutants (n=29) and *Rca1;sas-4* double mutants (n=25). In both cases, we found that all TCs analysed that display no centrioles do not extend a subcellular lumen, whereas mutant cells with 2 centrioles extend a subcellular lumen.

4.1.3.4 Subcellular lumen branching is associated with centrosomes number

We analysed the association of centrosome number and subcellular lumen formation in *Rca1* mutant thoroughly. As described before, *Rca1* TCs were characterized by an excess of centrosomes localized apically in the cell-cell junction between TC and stalk cell (**Fig. 32 B**). The examination of lumen formation at early stages with luminal marker (CBP) in *Rca1* heterozygous embryos carrying constructs *asl::YFP* and *btl::moeRFP* confirmed that the apical pair of centrosomes in the TC were localized

near the junction between the TC and the rest of the luminal network (**Fig. 32 C**). In homozygous mutant embryos a bifurcated luminal structure arose from the supernumerary centrosomes that were also apically localized (**Fig. 32 D**).

The analysis of the association between centrosomes and subcellular lumen formation was also possible by the examination in vivo of embryos *wt* and *Rca1*, carrying constructs *asl::mKate* and *btl>bazYFP*. Also in this case in control embryos two centrosomes were detected next to the apical cell-cell junction from were the apical membrane of the TC started to grow as a continuous sprouting process (**Fig.32 E**). In *Rca1*, centrosomes were clearly duplicated, together with the events of apical membrane growth (**Fig. 32 F**).

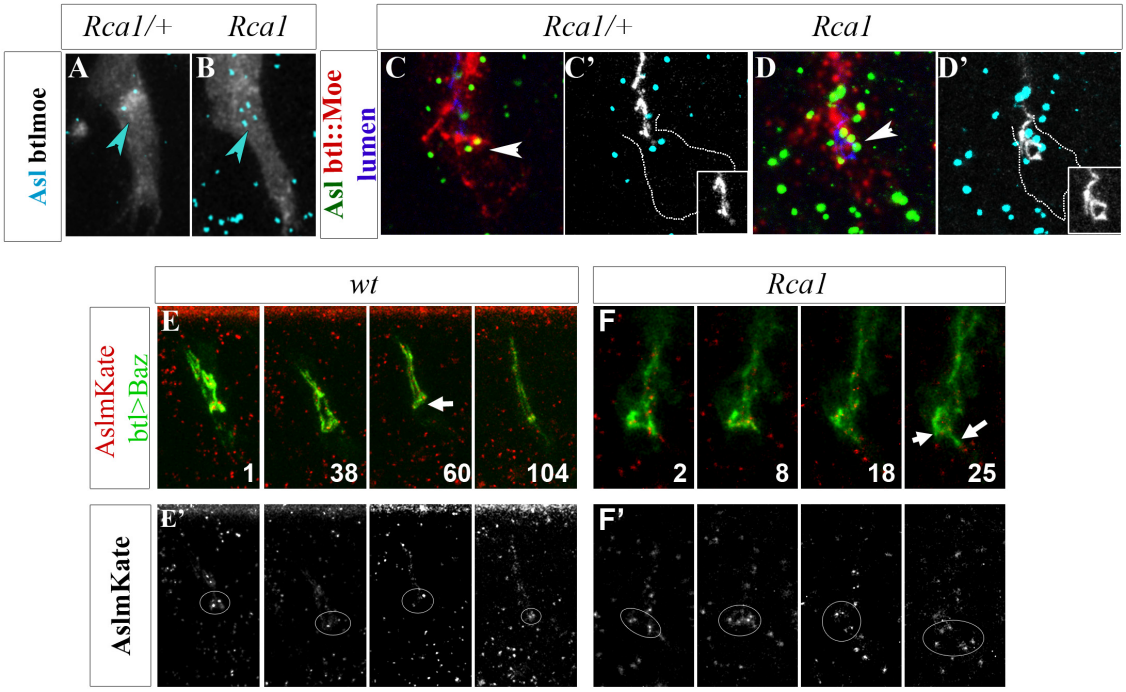

Figure 32. Centrosomes are associated with subcellular lumen. (**A-B**) Details from live frames showing the tip of GB of *Rca1* heterozygous (A) and homozygous (B) embryos carrying constructs expressing MoeRFP in all tracheal cells (*btl::moeRFP*) and *Asl::YFP* in all the embryo. (A) In *Rca1* heterozygous TC, two centrosomes next to the apical cell-cell junction are detectable. (D) *Rca1* homozygous TC with four centrosomes localized apically.

(**C-D**) TC at early stages in *Rca1* heterozygous (C) and homozygous (D) embryos carrying constructs expressing *moe::RFP* (stained red), *asl::YFP* (stained green), and stained for chitin to mark the growing lumen in blue. (C' and D') Confocal scans depicting only the lumen (in white) and centrosomes (in cyan) to show the relative positions of the centrosomes to the lumen; dotted white line marks the TC borders; insets show only the lumen. Scale bars, 5 µm.

(**E-F**) Details from live frames showing showing several stages of subcellular lumen extension in the *wt* (E) and in *Rca1* mutant (F) GBs. Embryos carry a construct that marks all centrioles in the embryo (*asl::mKate*) and another that labels Baz only in tracheal cells (*btl>bazYFP*). The growing subcellular lumen extends from the cell-cell junction between the tip and stalk cell (white arrows). In the *wt*, only one subcellular lumen extends from the junction (E), whereas in the mutant two lumina extend from this point (F). Centrosomes associate with Baz at the cell-cell junction. In (E) 2 centrosomes are associated with the TC apical junction and in (F) 4 centrosomes are associated with the TC apical junction. Numbers on the lower right hand corner are minutes. White circles mark the region where TC centrosomes localize in each frame.

4.1.4 Centrosomes are microtubule organizing centers (MTOCs) in TCs

The centrosome is the major microtubule-organizing center (MTOC) in dividing cells and many post-mitotic differentiated cells. However, in some cell types, MTOC function is reassigned from the centrosome to non-centrosomal sites (Bartolini and Gundersen, 2006; Wiese and Zheng, 2006). In particular, in tracheal multicellular tubes, MT reorganization is coupled to re-localization of the MTOC components from the centrosome to the apical luminal cell domain (Brodu et al., 2010). Since our data indicated a correlation between centrosomes and subcellular lumen, and because subcellular lumen formation depends on MTs network organization, we investigated whether TC centrosomes were active as MTOCs.

4.1.4.1 Stable MTs emanate from centrosomes

It was previously reported that MT bundles emanate from the cell-cell apical junction to the periphery of the dorsal TCs (Gervais and Casanova, 2010). During ganglionic TC extension bundles of stable microtubules were also detected around subcellular lumen as described in **Fig. 33 C-D**. In order to visualize centrosomes in TCs, as mentioned before, we used embryos carrying constructs *btl::moeRFP* to visualize the outlines of tracheal cells and *asl::YFP* to mark all centrioles in the embryo. From the beginning of TC specification, in *wt* condition 2 pairs of centrioles were detected next to the cell-cell apical junction, described as the point of MTs emanation at initial stages (**Fig. 33 A-B**). We analysed in *Rca1* heterozygote and homozygote whether such centrosomes were the initial foci from were MTs emanated. At early stages of TCs development, in the control (**Fig. 33 E**) we observed **bundles of stable MTs extending from these two pair of centrioles**. In *Rca1* TCs, also supernumerary centrosomes were observed in apical positions, where they associated with MTs (**Fig. 33 F**).

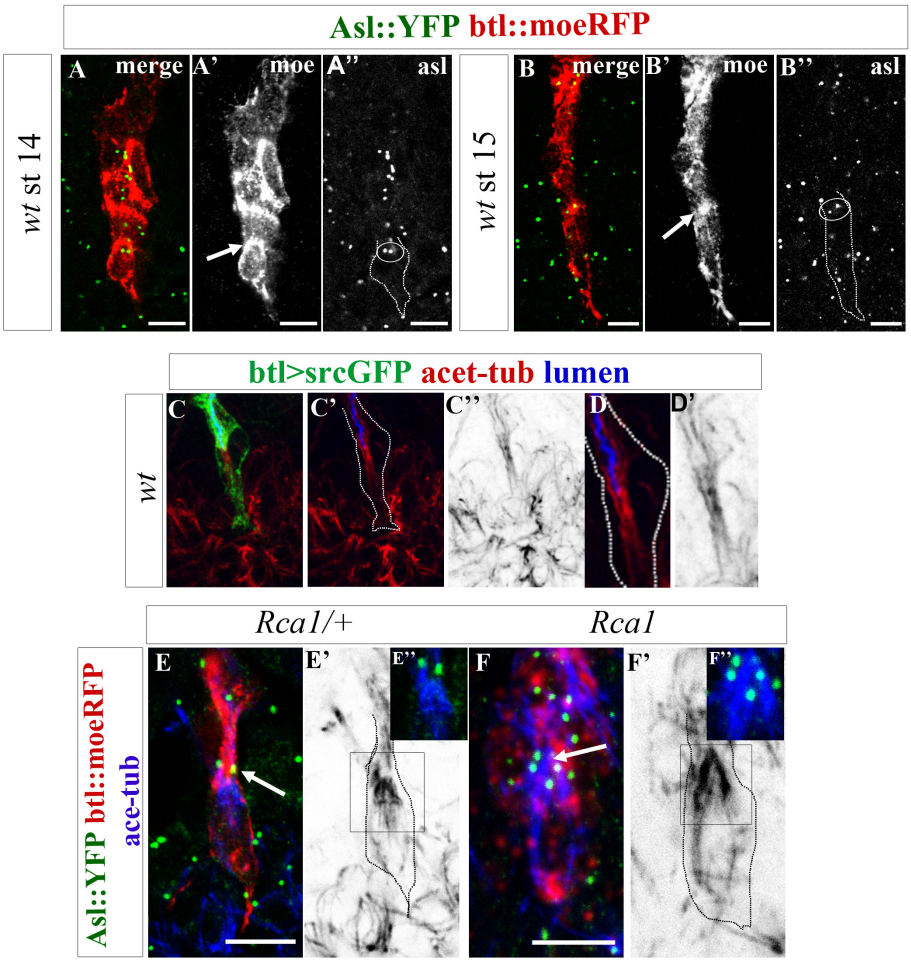

Figure 33. Stable MTs emanate from centrosomes in TCs. (**A** and **B**) Ganglionic TCs from embryos at st. 14 (A) and st. 16 (B) stained with anti-GFP to visualize YFP centrioles (green) and anti-RFP to detect btl::moeRFP and so mark tracheal cells and the junction (arrow) between the tip and stalk cells (red). The two centrosomes in the TC localize near the junction between tip cell and stalk cell (circles in A'' and B''). *AslYFP* is expressed in all cells in the embryo and not just in the tracheal cells. Images are single confocal scans or projections of only two to three scans to include the whole TC. Scale bars, 5 µm.

(**C-D**) Detail of a ganglionic TC stained with GPP (green in C) due to the expression of *btl src GFP,* with acetylated-tubulin (red in C and D and in grey in C'' and D') to mark MTs and CBP to see the lumen (blue in C and D). D is a close-up of C. the white line marks the borders of the TC.

(**E-F**) Stable MTs in *Rca1* heterozygous (E) and homozygous (F) TCs carrying constructs expressing *Moe::RFP* (stained red), *AslYFP* (stained green) and stained acetylated MTs in blue. (or in grey in E' and F'). Dotted black line in E' and F' marks the TC borders; E'' and F'' are close up of E'' and F'' that show MTs and centrosomes. Scale bars 5 µm.

4.1.4.2 TCs centrosomes recruit γ-tubulin

In order to define centrosomes as MTOC in terminal cells we searched to demonstrate that such centrosomes were active in nucleating MTs. **γ-tubulin** is the prime

component in microtubule nucleating material that catalyses the initiation of α and β tubulin polymerization. When centrosome acts as MTOC γ-tubulin is embedded within the pericentriolar material (PCM) (Luders and Stearns, 2007). So we examined, in *wt* as well as in *Rca1* mutant, for the presence of γ-tubulin at the centrosomes at early stages of TC development. We used embryos carrying *asl::YFP* and *btl::moeRFP* constructs and a specific γ-tubulin antibody. As reported in **Fig. 34 A-B** we detected γ-tubulin accumulated on centrosomes apically localized in *wt* as well as in *Rca1* mutant TCs.

4.1.4.3 MTs start to polymerize from centrosomes

In order confirm that centrosomes were MTOCs, we analysed the initial phases of MTs polymerization in TCs. To do so a cold treatment assay was used by which a **reversible depolymerisation of MTs** was induced; we depolymerized MTs at 4°C for 6hr and monitored their regrowth immediately, over 2 min and over 30 minutes at room temperature (Brodu et al., 2010). We analysed MTs in each condition, using α-tubulin antibody in embryos *asl::YFP; btl::moeRFP* in *wt* and *Rca1* mutant background. After 6 hr at 4°C, MT fibbers were depolymerized in the TCs of *wt* and *Rca1* mutants (**Fig.34 D-H**). Upon recovery for 2 min at room temperature (RT), it was possible to detect α-tubulin accumulation next to the centrosomal sites (**Fig.34 E-I**) and after 30 minutes bundles of MTs emanated from centrosomes (**Fig.34 F-J**).

Another strategy that we used to observe the first MT polymerization events was the analysis of the accumulation of the **End-Binding protein 1** (EB1) at very early stages of TC development. EB1, as described in the introduction is a key +TIPs protein involved in different aspects of MT polymerization. Time-lapse imaging experiments, using embryos *aslmKate*; *btl>EBIGFP* in *wt* condition, confirmed that MTs started to polymerize from centrosomes in TCs. In fact EB1 were recruited close to centrosomes at the initial stages of TCs development, indicating that centrosomes were the site from where MTs started to polymerize.

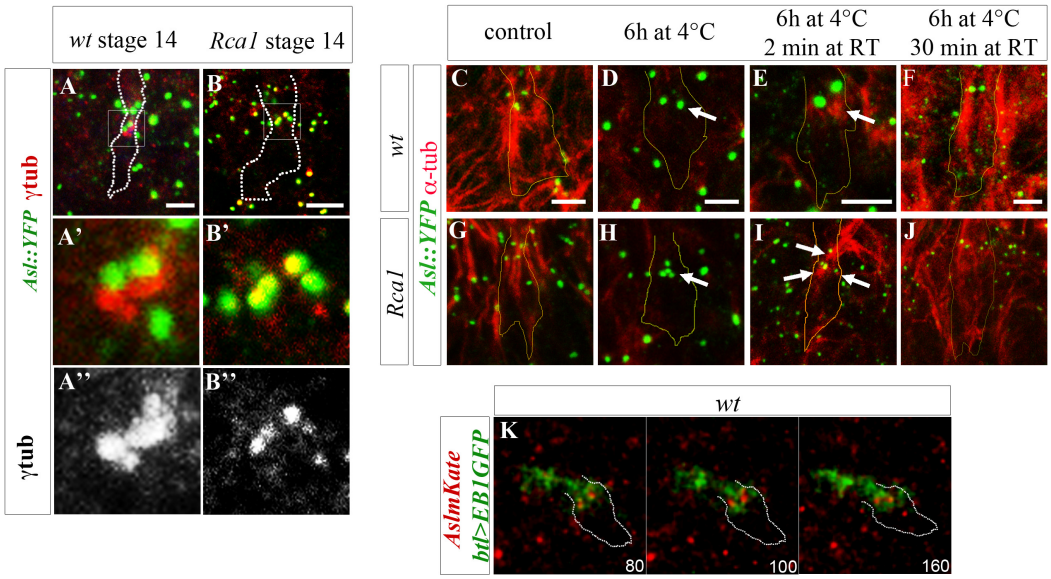

Figure 34. Centrosomes act as MTOCs in TCs. (**A** and **B**) *wt* (A) and *Rca1* (B) TCs carrying the *asl::YFP* construct and stained for GFP and γ-tub to show whether the apical TC centrosomes are active MTOCs. The white line marks the borders of the TC and part of the rest of the GB. (A' and B') show higher magnifications of (A and B) depicting how centrosomes colocalize with γ-tub. (A'' and B'') show only γ-tubulin staining in grey. Note that the centrosome outside the TC does not colocalize with γ -tubulin. Scale bars, 5 µm.

(**C–J**) MT depolymerization-repolymerization assay in *wt* (C–F) and *Rca1* (G–J) mutant embryos. After a 6-hr incubation at 4°C (D and H), MTs are depolymerized (compare C and G with D and H respectively); after 2 min at room temperature (RT), (E and I), MTs start re-growing from the centrosome pair in the *wt* and the four centrosomes in *Rca1*, near the apical junction of the TC; after 30 min at RT (F and J), MTs have fully regrown from the centrosomes. Centrioles are detected by the *asl::YFP* transgene, and MTs are detected by an α-tubulin antibody. The yellow line marks the borders of the TC. Scale bars, 2 µm.

(**K**) Frames from live imaging experiments showing initiation of subcellular lumen extension in wild-type GB. Flies carry a construct that marks all centrioles in the embryo (*AslmKate*) and another that labels EB1 only in tracheal cells (*btl>EBI1GFP*). The centrosomes at the apical junction of the TC associate with EB1. Numbers on the lower right hand corner are seconds. White line marks the TC membrane.

All together, this data confirmed that two centrosomes, apically localized in TCs were active as MTOC. The MT nucleating factor γ-tubulin colocalized with centrosomes to initiate MTs polymerization. In *Rca1* mutants, more than 2 centrosomes were able to nucleate MTs and more MT tracks were generated. This probably induces more vesicle trafficking and delivery for extra subcellular lumen formation inside the TCs.

4.2 Analysis of the spectraplakin Short-stop (Shot) during subcellular lumen formation

In order to visualize MTs in the TCs, we tested the tracheal overexpression of several constructs consisting in MT associated proteins fused with fluorophores. Amongst them we used transgenic lines overexpressing the *Drosophila* **spectraplakin Short-stop** (Shot).

As mentioned in the introduction, Shot is a **giant multifunctional protein** responsible for many aspects of cytoskeleton organization in different tissues. Shot can operate as a single cytoskeleton component as well as coordinating cytoskeletal elements between them and also interact with other cellular structures (Huelsmann and Brown, 2014).

The functional versatility of Shot is probably reflected by the **abundant generation of isoforms** and by the modulation of its domains. The full-length isoform A of Shot (Shot-A) is characterized by a NH2-terminal actin-binding domain (ABD) composed of two calponin homology domains (CH1 CH2), some central domains (like rod-like domain, plakin spectrin-like repeats and EF- hand), and C-terminal domains involved in the interaction with MTs (C-tail and GRD). This isoform A of Shot has been mainly related with the actin-microtubule crosslinking activity (Applewhite et al., 2013; Lee and Kolodziej, 2002b). Isoform C (shot-C) lacks a proper actin-binding domain and has been described to interact mainly with MTs (Bottenberg et al., 2009; Lee et al., 2000).

Due to our interest in visualizing MTs in the TCs we tested the tracheal overexpression of the Isoform C of Shot using the transgenic line *UAS-shot L(C)-GFP*; Interestingly, we found that this overexpression, not only allowed us to label MTs but also revealed that **an excess of Shot induced TCs to generate an extra-subcellular lumen**.

It had been previously reported that Shot, in the trachea, is involved in the cytoskeletal organization at the anastomosis site of the fusion cells, supporting lumen formation and that at least one cytoskeletal interaction domain of Shot must be present to form a connecting lumen (Lee and Kolodziej, 2002a). Because no information about the role

of Shot during subcellular lumen formation was available, and due to the phenotype caused by its overexpression, we decided to follow the analysis on the task of Shot during TC morphogenesis.

In this second section of results, I report the analysis of the overexpression phenotype of Shot and the involvement of its domains in generating extra subcellular lumina. Also, I will report the data about Shot endogenous localization in relation to the TC's cytoskeletal components. Later, I will describe the subcellular lumen phenotype and associated cytoskeleton defects caused by the loss of function of *shot*. And finally, I will describe some experiments designed to explore structure –function relationship of Shot in the TC.

4.2.1 *shot* overexpression induces extra subcellular lumen branching

Embryos *btl>shot-L-(C)GFP* (from this moment *shot-CGFP* or just *shot-C*) were fixed and stained with GFP to follow the **overexpression/localization of *shot-C***, CBP to visualize the lumen and DSRF antibody to mark specifically the nucleus of the TCs. Surprisingly, we found that *shot* tracheal overexpression gave rise to extra-subcellular lumina in ventral and dorsal TCs (**Fig.35**).

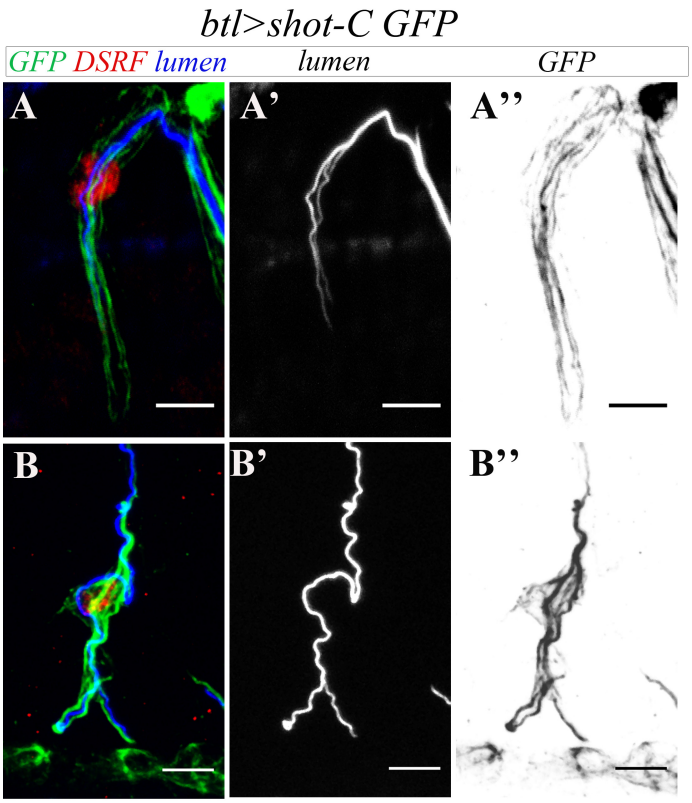

Figure 35. The overexpression of shot-C induces TC extra branching. (A) Dorsal and **(B)** ventral TCs from embryos *btl>shot-C-GFP*, showing extra-subcellular lumen phenotype. Embryos were stained with GFP to visualize Shot (in green in A-B grey in A''-B''), DSRF (in red to recognize the nucleus in TCs and CBP to detect the lumen (blue in A and B, grey in A' and B'). Anterior side of the embryo is on the left and dorsal side up. Scale bars 5µm

4.2.1.1 Overexpression of *shot -A* and *-C* give rise to the same phenotype

The tracheal overexpression of the full-length isoform *UASshot-L-(A)-GFP* (from this moment *shot-A-GFP* or just *shot-A*) was analysed and we found the same phenotype observed when overexpressing *shot-C* (**Fig.36**). The tracheal **overexpression of *shot-A*** induced phenotypes in 95% of the embryos (n=20), with TC 1.5 bifurcations *per* embryo on average (n=400). Overexpression of *shot-C* induced phenotypes in 90% of the embryos (n=20), with 2 TC bifurcations *per* embryo on average (n=400). Comparing the number of affected terminal cells (in the ganglionic and dorsal branches) of *shot-A* and *shot-C* overexpressing embryos, we could not detect any statistical difference between them (**Fig. 36G** and **H**).

Regarding GFP accumulation, in the overexpression of *shot-A* we detected the GFP diffused in the cytoplasm and partially organized in longitudinal bundles (**Fig. 36 A'' - C''** and in detail in **B'''**). This localization of GFP suggested that *shot-A* could be interacting with different cytoskeletal and subcellular structures. In contrast, in the overexpression of *shot-C* we saw GFP highly organized in longitudinal bundles (**Fig. 36 D'' - F''** and in detail in **E'''**). It has been described that the overexpression of *shot-A* and *shot-C* achieves the same expression level (Lee and Kolodziej, 2002b), so different transgene expression levels could not explain the different localization. As described before, *shot-C* harbours at its N-terminal only half of the acting binding domain present in the longest isoform *shot-A* and this half domain binds actin very weakly (Lee et al., 2000; Lee and Kolodziej, 2002b).

Therefore, if both overexpression of *shot-C* and *shot-A* were able to give rise to the extra subcellular branching, with the same penetrance, this phenotype did not depend by the CH1 actin binding domain present only in *shot-A*, So we followed our experimental line using the overexpression of *shot-C*.

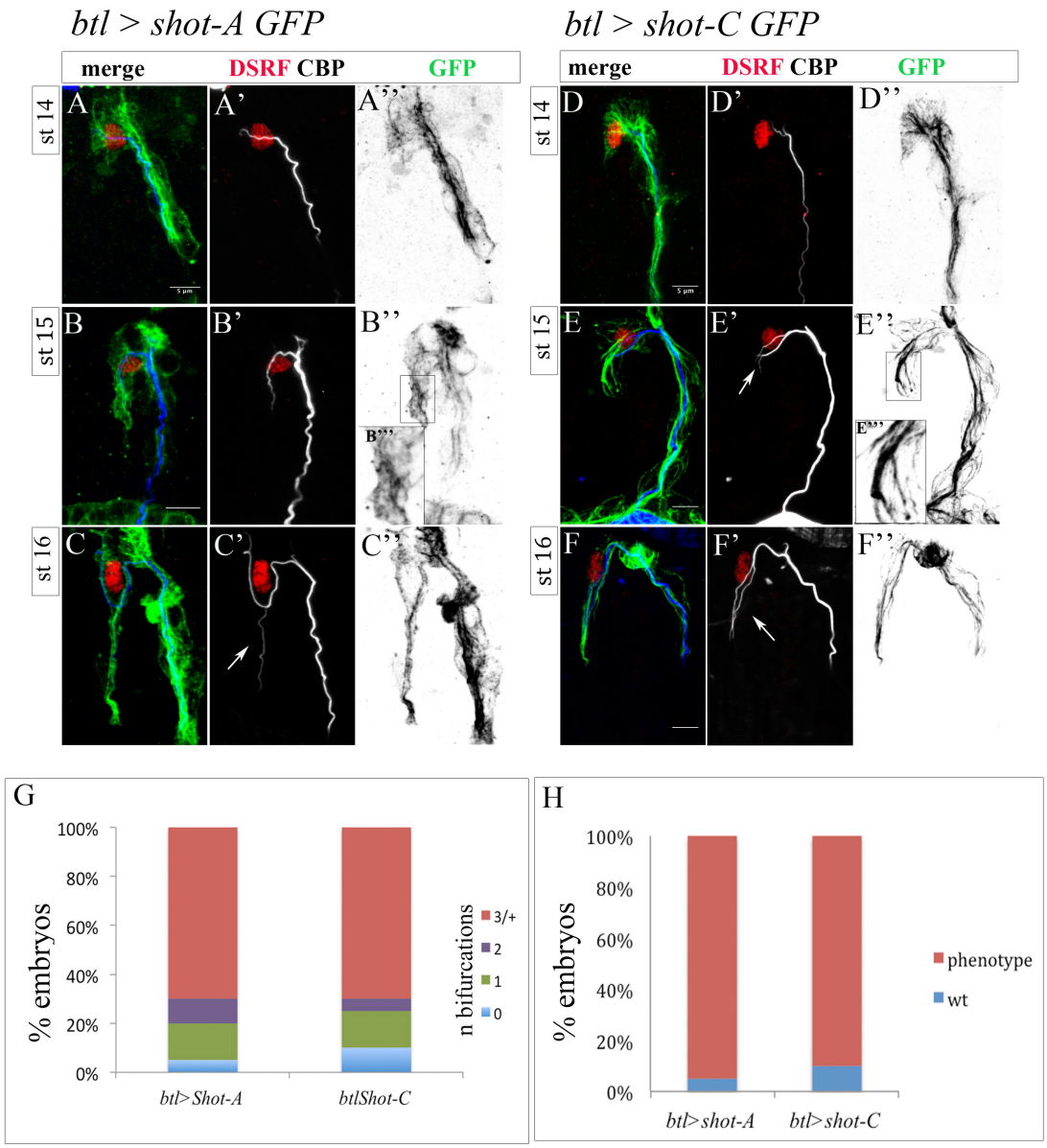

Figure 36. Over-expression of *shot* induces extra subcellular lumen: Lateral view of DBs tip from st. 14 to st. 16, of fixed embryos *btl>shot-AGFP* (**A-C**) and *btl>shot-CGFP* (**D**, **F**). Embryos were stained with GFP (green in A-D and grey A''-D'') to visualize Shot-GFP, DSRF to mark the nuclei of the TCs (in red) and CBP to stain the chitinous lumen (blue in A-D and white A'-D'). Both overexpressing conditions induced the generation of extra subcellular lumen (white arrows). Note the GFP is diffuse in the cytoplasm of the TCs of embryos overexpressing *shot-A*, and is highly organized in bands in the TCs overexpressing Shot L-C. (In detail in the magnification B''' and E'''). Anterior side of embryo is on the left and dorsal side up. Scale bars 5µm.

(G) Quantification of the bifurcation number per embryo in the tracheal overexpression of *shot-A* and *shot-C*. Embryos with 0 bifurcations are represented by the blue column; Embryos with 1 bifurcation in the green column; 2 bifurcations in the purple column; 3/more bifurcations in the red column.

(**H**) Quantification of embryos with at least one bifurcated TC at the tip of dorsal and ganglionic branches (column in red) or without phenotype (column in blue).

4.2.1.2 The overexpression phenotype of *shot-C* is dosage dependent

We generated a recombinant *btlGal4UASshotC-GFP* and examined embryos homozygous for this insertion (2 copies of the GAL4 and 2 copies of the UAS). Nicely, we observed a qualitative increase of the phenotype; in fact, we found **subcellular lumen highly ramified (Fig.37).** The same kind of phenotype was observed also when *shot-C* overexpression was performed at 29°C (temperature at which the *UAS/GAL4* system works with higher efficiency). This observation suggested that the effect of *shot* overexpression in subcellular lumen branching is dosage dependent.

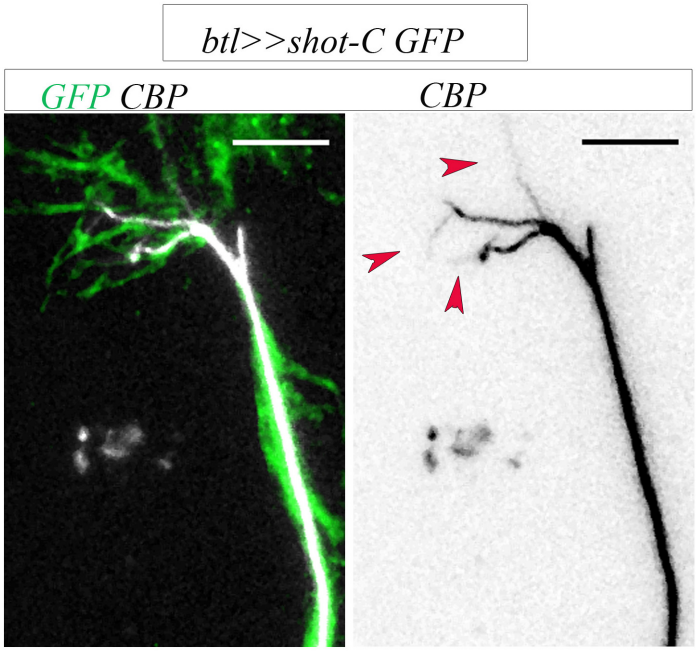

Figure 37. High overexpression of *shot-C* increases subcellular lumen branching. Example of dorsal TC of an embryo overexpressing two copies of *btlGAL4UASshot-CGFP,* stained with anti-GFP antibodies to visualize Shot and CBP to detect the lumen. Red arrows indicate extra subcellular lumen branching. Note that the extra subcellular lumina are very thin and they follow Shot positive bundles detected with GFP. Anterior side is on the left, dorsal midline is on the top. Scale bars 5µm.

4.2.1.3 Shot-C co-localizes with stable microtubules

To better characterize the localization of *shot-C* in the TCs we analysed its localization in relation to the MT bundles. In **Fig.38**, dorsal TCs from fixed embryos *btl>shot-CGFP* stained with **acetylated tubulin** antibody are shown; from st. 14 to st. 17, GFP positive bundles localized together with bundles of stable MTs, suggesting that *shot-C* interacts with this cytoskeletal component.

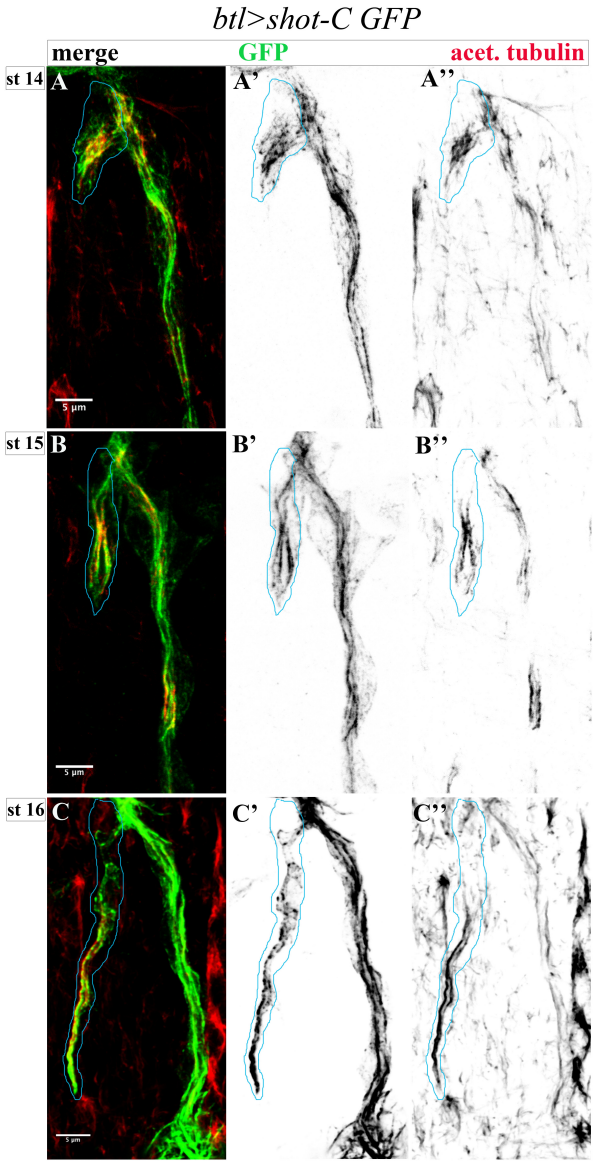

Figure 38. *shot-C* localizes with MTs. (**A-C**) Dorsal TCs of embryos, from st.14 to st.16, overexpressing in the tracheal system *shot-C-GFP*, stained with anti-GFP (in green A-C and grey A''-C'') and anti-acetylated tubulin (in red A-C and grey A'-C'). The outline of TC is plotted in blue. From

earlier stages of TCs elongation (st.14) and later on (st.15 an st.16) GFP co-localized with stable MTs (A, B and C). Anterior side of the embryos is on the left and dorsal side up, scale bars 5µm.

4.2.1.4 The overexpression of *shot-C* does not perturb the asymmetric actin accumulation in TCs

We analysed the asymmetric actin accumulation in respect to the extra subcellular lumen caused by the overexpression of *shot-C*. We used a *btl::moeRFP* fly line to visualize the border of the cell and the characteristic Moe/Actin accumulation at the tip of TC during cell elongation. We found that in 75% of the cases (n=25) the extra-branched lumen arose inside the same cytoplasmatic protrusion and only one spot of Moe/Actin was detected at the tip of the cell (**Fig. 39**). So, in this case the bifurcated lumen was not associated with a duplicated cytoplasmatic protrusion. We also observed that ***shot-C* positive bundles touched the Actin/Moe rich area** at the stage analysed (st. 15), probably contacting the MTs invading the tip of the cell during its extension.

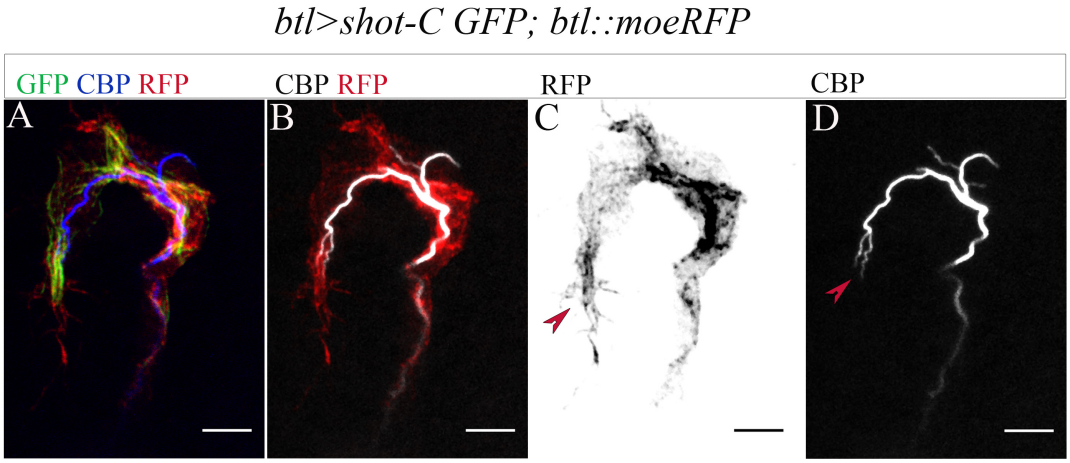

Figure 39. The extra subcellular lumen caused by the overexpression of *shot* appears inside the same cytoplasmatic protrusion. (A-D) Dorsal terminal cell and part of the DB of embryo *btl>shot-C-GFP; btl::moe RFP* stained with GFP (green in A) RFP (red in A and gray in C) and CBP (blue in A and grey in D). A single actin core is in front of the bifurcated lumen. Note that ShotC-GFP positive bundles invade the actin core. Anterior side of the embryo is on the left and dorsal side up, scale bars 5µm.

4.2.2 Is the *shot* over-expression phenotype related with *Rca1* mutant phenotype?

Since extra subcellular lumen had been observed before in a condition of centrosome amplification, we asked weather the phenotype caused by the overexpression of *shot* was, somehow, correlated with *Rca1* or with other condition affecting centrosome number.

4.2.2.1 Genetic interaction between *shot* and *Rca1*

To investigate a possible genetic interaction between *shot* and *Rca1* we compared the penetrance of the phenotype of both mutant conditions, counting defective ganglionic terminal cells (**Fig.40**). We used anti Gasp antibody to visualize the lumen and consider the degree of the penetrance of both conditions. We subdivided *Rca1* $^{-/-}$ and *btl>shot-C* embryos in groups characterized by 1, 2, "3/or more" bifurcated ganglionic terminal branches (**Fig. 40F**). In *Rca1* mutants 80% of embryos bore defective ganglionic TCs (n=40); in particular we counted that 24% of embryos had 1 bifurcation, 30% of embryos had 2 bifurcations and 28% of embryos had 3 or more bifurcations. In embryos overexpressing *shot-C* (n= 40), 57,5 % of embryos had ganglionic terminal cells affected; 25% with one bifurcation, 22,5% with two bifurcations and 10% with three or more bifurcations. In order to assess whether the means of the two conditions were statistically different we used the Student's T-test and we obtained that the two phenotypes where independent.

Then we estimated the penetrance of the phenotype of embryos over-expressing *shot* in in *Rca1*$^{+/-}$ background (n=40). In this condition, we found phenotype in 59% of the cases; 46% with 1 bifurcation, 8% with 2 bifurcations and 5% with 3 or more bifurcations. Comparing this condition with the overexpression of *shot-C* in *wt* background we could not find any statistic difference. So, a sensitized background for *Rca1* did not affect the overexpression phenotype of *shot-C*.

We also analysed embryos overexpressing *shot-C* in *Rca1*$^{-/-}$ background (n=28). Embryos bearing both mutations had a bifurcation phenotype in 96,3 % of the cases; 11,1% with 1 bifurcation 29,6% with 2 bifurcations and 55,6% with 3 or more bifurcation. The comparison between *Rca1*$^{-/-}$ *and Rca1*$^{-/-}$*, btl>shot-C* indicated that the two conditions are statistically different. So, in embryos *Rca1*$^{-/-}$ and together with the overexpression of *shot-C*, we observed an increase of embryos with 2 or 3/more bifurcation and a decrease of embryos with 0 or 1 bifurcation in respect to *Rca1*$^{-/-}$, suggesting that the effect of *Rca1* loss of function and *shot-C* overexpression are

additive. Nicely, in the double mutants we observed TCs with a highly branched subcellular lumen suggesting this **additive effect** can take place within the same TC (**Fig.40 D**), (see below).

We knew that the overexpression of *Rca1* in the tracheal system was able to rescue the $Rca1^{G012}$ phenotype. Therefore, we tried to use *UASRca1* to rescue the phenotype of the tracheal overexpression of *shot-C.* Because in this experiment we were using two targets and one driver line, (one copy of *btl-GAL4, UASshot-C* and *UasRca1*) we used as control embryos in the same conditions, (i.e. with one copy of *btl-GAL4*, and two target lines; *UASshot-C* together with *UASsrc GFP)*. Comparing these conditions, we found the same number of bifurcations per embryo. So the overexpression of *Rca1* could not rescue the effect caused by the overexpression of *shot* (**Fig. 40F**).

All together, these genetics data suggest that ***Rca1* and *shot* operate in different ways/steps** in the formation of the subcellular lumen.

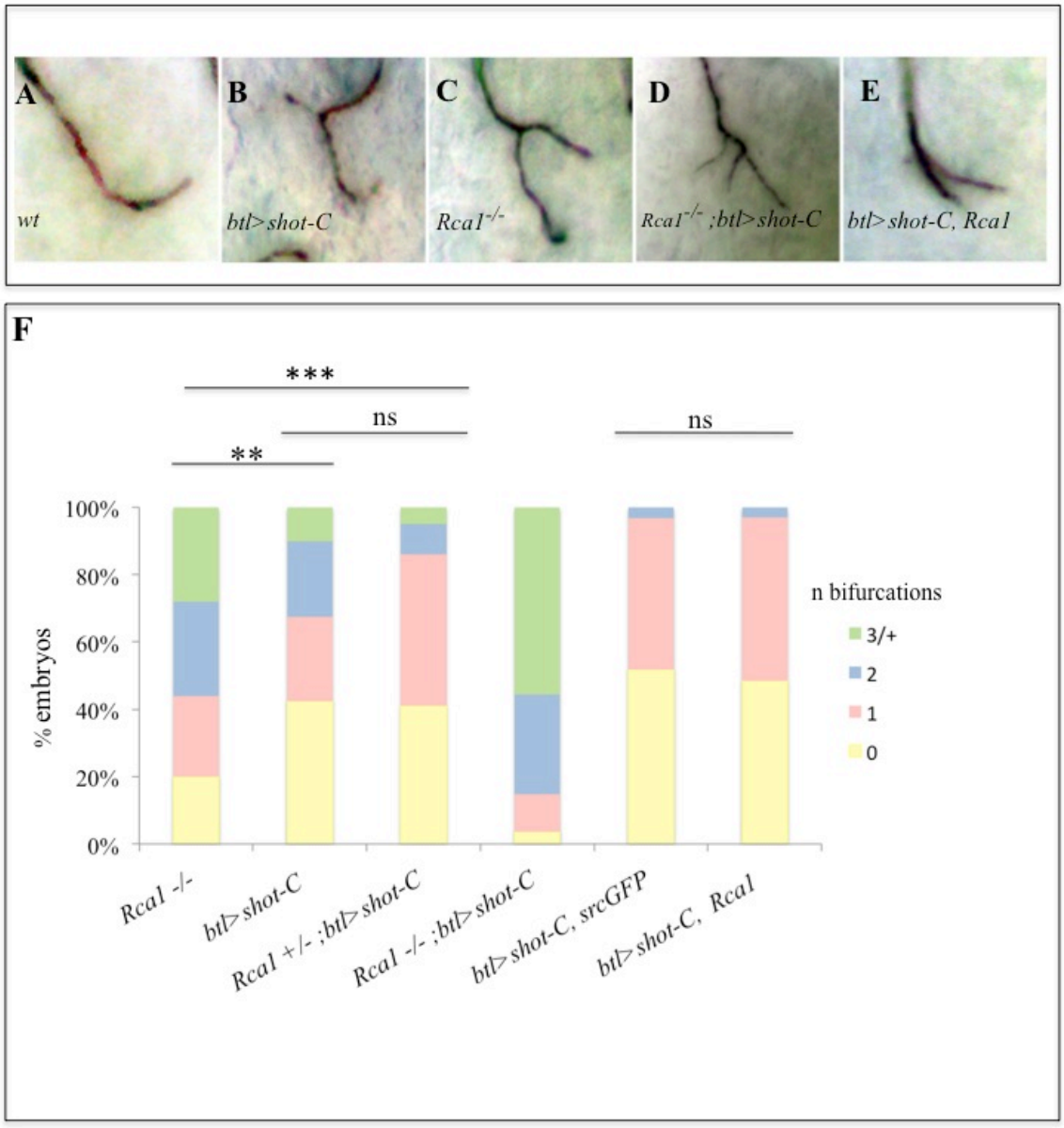

Figure 40. *Rca1* and *shot* work differentially in subcellular lumen over-branching. (**A-E)** Details of ganglionic terminal cells at st 16 from embryos stained with anti-Gasp (A) *wt* TCs with a single lumen each; (B) *btl>shot-C* showing subcellular lumen bifurcations; (C) *Rca1* showing subcellular lumen bifurcations, (D); *Rca1;btl>shot-C* showing a multi-branched subcellular lumen; (E) *btl>shot-C , Rca1 display* luminal bifurcations**.** Anterior side of the embryo is on the left ventral midline is down.
(F) Quantification of the number of bifurcations (ganglionic TCs) per embryos of the indicated genotypes. In the graft embryos whit 0 bifurcations are represented by blue columns, embryos with 1 bifurcation columns in red, 2 bifurcations columns in yellow 3/more bifurcations columns in green.

4.2.2.2 Comparative analysis of the extra-subcellular lumen morphology

In *Rca1* mutants the bifurcated subcellular lumen arose from the apical junction and continued to extend during development. Moreover, we noted that in *shot*

overexpressing embryos the extra subcellular lumen seem to arise from the pre-existing lumen, far from the apical junction.

To confirm this observation, we stained embryos *btl>shot-C* with CBP to visualize the lumen and an antibody anti-E-cadherin to better visualize the junction between the terminal cell and the stalk cell. We observed that in the 80% of the bifurcated terminal cells analysed (n=21) the bifurcation arose far from the apical junction (**Fig. 41 A**). When we analysed also the double mutant *Rca1; btl>shot-C*, both types of extra-subcellular lumen where detected and in 25% of the cases (n=12) was possible to see in the same TCs two extra subcellular lumina generated from the apical region and another one sprouting out from one lumen distally from the junction (**Fig. 41 B, B'**).

These **morphological differences** reinforced our hypothesis that *Rca1* and *shot* operate in different ways in the formation of the subcellular lumen.

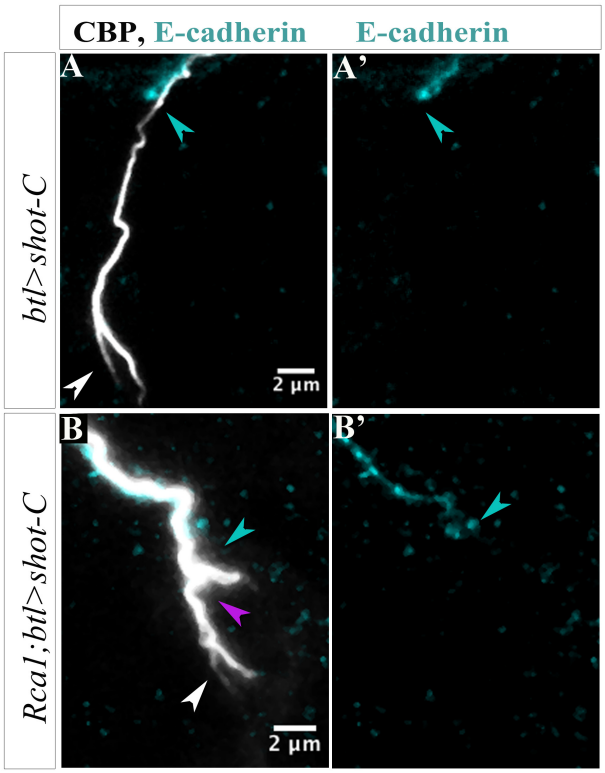

Figure 41. Extra subcellular lumen arises far away from the apical junction in *btl>shot-C* embryos. Tip of GB from embryos *btl >shot-C GFP* (**A**) and *Rca1; btl>shot-C GFP* (**B**) at st. 15, stained with CBP (in white) to visualize the lumen and E-cadherin (cyan) to recognize the apical Junction. Anterior side of the embryo is on the left and ventral midline on the bottom. Scale bar 2 µm.

The extra subcellular lumen caused by the overexpression of *shot* (white arrows) arises far from the apical junction (cyan arrows). In embryos *Rca1; btl>ShotC* it is possible to detect both luminal bifurcation: one from the apical junction (purple arrow) and another one from a pre-existing lumen.

4.2.2.3 Centrosomes number in *shot* overexpression

We wondered if Shot, independently from Rca1, was involved in centrosome amplification. We counted the number of centrosomes in the TCs of embryos *btl>shot- CGFP*. In particular, we quantified centrosomes in ganglionic TCs at stage 14, using an antibody against CP309, a specific centrosome marker. In the *control* we detected an average of 2,3 ± 0,5 (n=33) centrosomes per TC and likewise, in the tracheal overexpression of Shot we detected 2,2 ± 0,2 centrosomes (n=33 TCs) (**Fig. 42 C).** In *shot* overexpressing conditions, centrosomes (as described for *wt* and the other conditions analysed in this work) were detected at the apical side of the TCs (**Fig 42 A**). Analysing TCs at st. 15, (n=6) we could detect that the extra-subcellular lumen arose from the pre-existing subcellular lumen, distally from centrosomes (**Fig. 42 B**). These data indicate that ***shot* overexpression does not change the centrosome number** of TCs and that Shot overexpression generates extra subcellular lumen by a distinct mechanism from centrosome duplication.

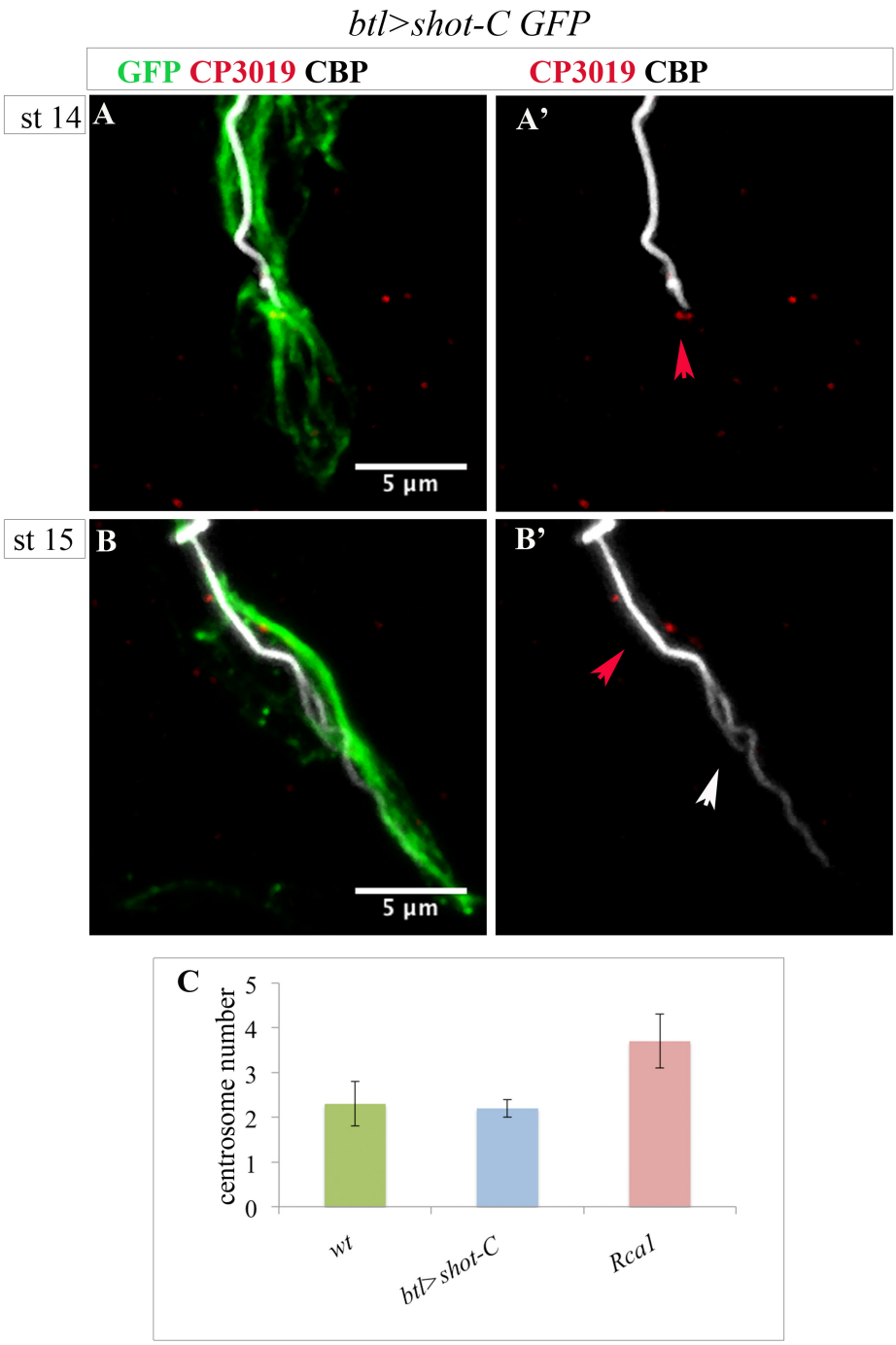

Figure 42. *shot* overexpression is not associated with centrosome amplification. TC at the tip of GB at st. 14 (**A**) and st. 15 (**B**) of embryos *btl>shot-CGFP* stained with CBP to mark lumen (white), GFP to visualize Shot (green) and CP3019 to detect centrioles (red). Red arrows indicate the couple of centrosomes apically localized and white arrow indicates the subcellular lumen bifurcated in a point far from centrosomes. Note as GFP positive bundles at early stage emanate from centrosomes. (**C**) Quantification of centrosome number in *wt and btl>shot-C* and *Rca1* embryos ± SEM.

4.2.3 Does MT over-stabilization induces extra subcellular branching?

Shot is a multifunctional protein and its wide range of molecular functions is reflected from the context specific activity of its distinct domains (Bottenberg et al., 2009). As described in the introduction, the longest isoform **Shot-A** possesses: a NH2-terminal **actin-binding domain (ABD)** composed of two calponin homology repeats CH1 and CH2; a spacer region formed by **spectrin-like repeats** that provide elasticity to the protein; the **plakin domain** that is typically involved in interaction with membrane proteins; **EF-hand** motifs involved in regulating actin association and organization. Finally at the C-terminus there are and the **GRD** and the **C-tail** involved in interaction with MTs (Hahn et al., 2016).

As described before, the overexpression of the longest isoform of Shot, Shot-L-A-GFP gave rise to extra-subcellular lumina. Equally, also the isoform Shot-L-C in which only the CH2 repeats of the ABD domain are present gave rise to phenotype. We followed the analysis of which functional domain of Shot is involved in the generation of the overexpression phenotype.

4.2.3.1 Molecular dissection of Shot function

We followed with the overexpression in the tracheal system of different constructs derived from *shot-A* and *shot-C*, but in which a specific domain was deleted. We hypothesized that if the activity of a certain domain was responsible of the phenotype observed, the overexpression of Shot deleted of such domain should not gave rise to phenotype.

We overexpressed, in the tracheal system, the following constructs; *UAS-shot-A Δ-rod1*, in which approximately 75% of the central domain of the protein, including all the spectrin repeats was deleted; *UAS-shot-A-Δ-Plakin,* in which Plakin-like domain was deleted, *UAS-shot-A-Δ-EF-hand*, in which two EF hand motifs were removed; *UAS-shot-C-Δ-GAS2* where most of the GAS2 was removed. In all these cases we observe embryos with at least one ganglionic TC forming more than one lumen (**Fig. 43**).

Next we analysed the overexpression in the tracheal system of the construct *shot-A-Δ-Ctail* **(**From now just *shot-Δ-Ctail*) which lacked the C-tail. As described in the introduction, at the molecular level the C-tail is critical for the interaction of Shot with

MTs and is involved in MT stabilization and polymerization in neuronal cells (Alves-Silva et al., 2012).

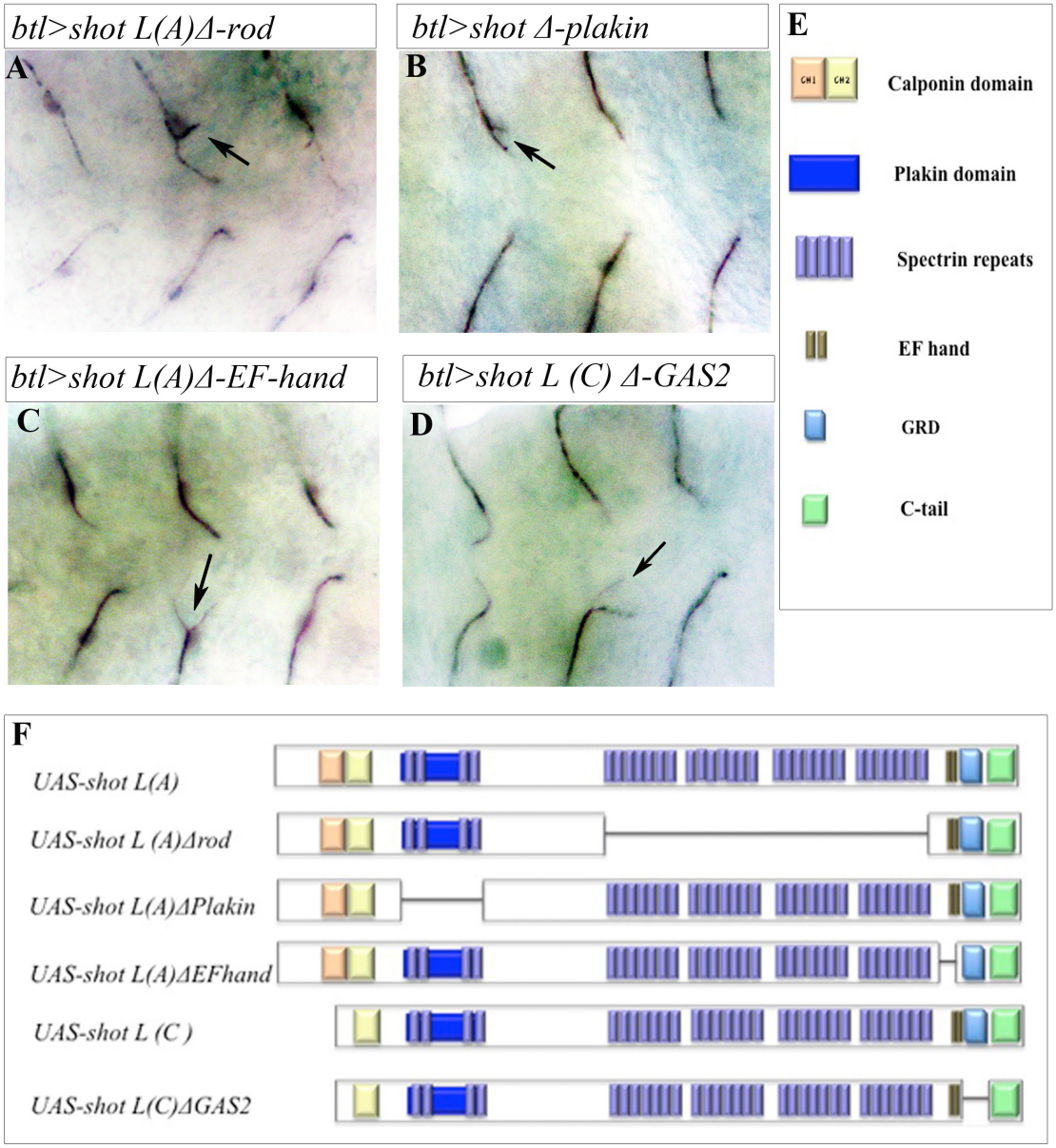

Figure 43. The overexpression of several Shot constructs gives rise to bifurcations. (A-D) Staining with anti-Gasp antibody reveals bifurcated TCs at the tips of GBs of embryos overexpressing in the tracheal system different constructs in which a specific domain of Shot was deleted (genotype is indicated on the top). Ventral view, anterior side of the embryo is on the left. **(E)** Representation of all domains of Shot (**F**) Schematic representation and genotype of the different constructs inducing TCs phenotype.

Analysing embryos overexpressing *shot-Δ-Ctail* in the trachea we noted a relevant reduction of the phenotype in respect to the overexpression of full-length isoforms, in

fact we did not detect phenotype in 93% of embryos analysed (n=40), (**Fig. 44**). So, we concluded that the C-tail is very important during extra subcellular lumen formation. Next, we overexpressed a construct consisting of the C-tail domain alone (*UAS-C-tail*) in the tracheal system. Nicely, we found that the tracheal overexpression of the *C-tail* induced terminal cell phenotype in 23% of the embryos analysed (n=40 embryos) suggesting that **the C-tail domain was directly involved in extra subcellular branching**. So, the C-tail alone is sufficient to induce terminal cells with extra subcellular lumen in spite of the lower efficiency in relation to *shot-A* or *shot-C* overexpression.

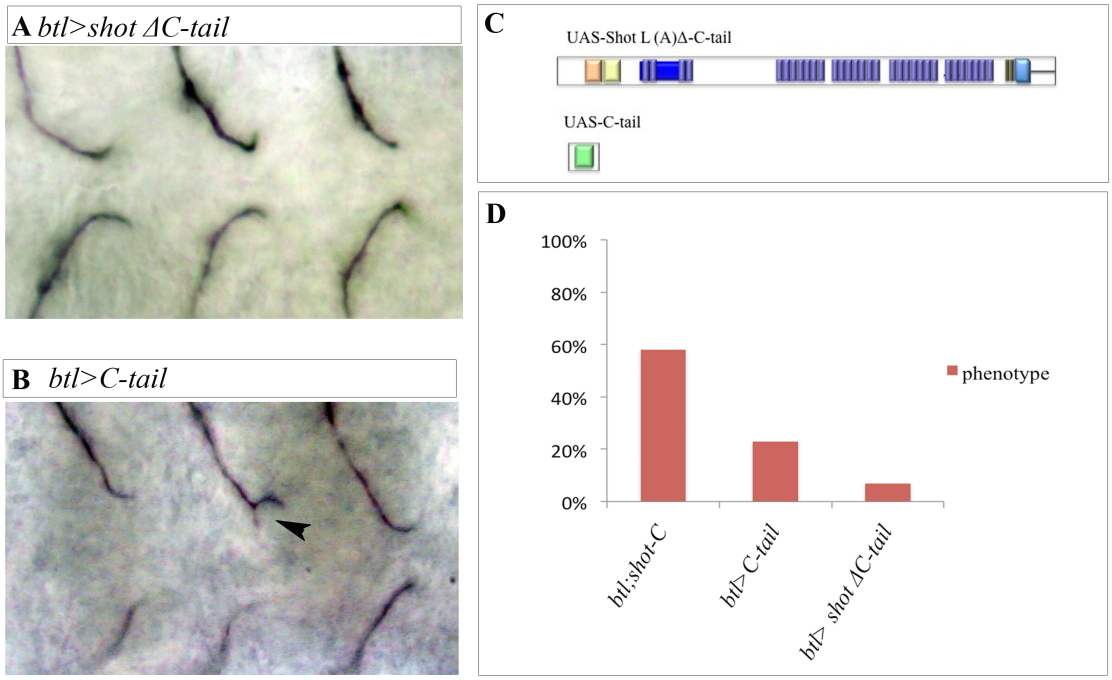

Figure 44. C tail domain is involved in extra subcellular lumen formation. (**A-B**) Tips of ganglionic terminal cells from embryos *btl>shot-ΔCtail* with a single subcellular lumen each (A) and *btl>C-tail* (B) in which one TCs is bifurcated, stained with anti-Gasp (Ventral view, anterior side of the embryo is on the left). (**C**) Schematic representation of the construct UASShotΔCtail and UASCtail. (**D**) Quantification of embryos displaying phenotype in TCs at the tip of ganglionic branches.

The data described until now shows that the tracheal overexpression of Shot induces the appearance of extra subcellular lumina at embryonic stages. This phenotype is independent from Rca1 and centrosome amplification and is mainly caused by an extra activity of the C-tail domain. In addition, these data suggests that the phenotype is induced by an over-stabilization of microtubules.

4.2.4 Shot interacts with TC's cytoskeletal components

As mentioned in the introduction, spectraplakins are crucial in cells that require extensive and dynamic cytoskeleton reorganization, e.g. epithelial, neural, and migrating cells. The loss of spectraplakin function leads to a variety of cellular defects due to disorganised cytoskeletal networks, both in terms of derangement of a specific cytoskeletal compartment and in terms of defective connection between different cytoskeletal compartments. In different tissues and in cultured S2 cells Shot can physically interact with different components of cytoskeleton (Applewhite et al., 2013; Lee et al., 2003; Sanchez-Soriano et al., 2009) Therefore, we investigated the localization of endogenous Shot respect to the TCs cytoskeleton components in *wt* condition. To do so, we used a specific anti-Shot antibody that recognizes all isoforms.

4.2.4.1 Shot co-localizes with stable MTs.

First, we examined Shot localization in relation to MTs. In particular, we used fixed embryos *btl>srcGFP* to recognize the TC membrane using a GFP antibody, fluostain to recognize the chitinous lumen, acetylated-tubulin antibody to mark stable MTs and the above mentioned Shot antibody. **Shot was strongly detected in the TC** from early stages and until the end of TC specification. At the beginning of TC specification (**Fig. 45**), when MTs emanated from the junction (**Fig. 45 A'**), Shot co-localized with the first sprouting stable MTs (**Fig. 45 A'''**). The overlap between Shot and stable MTs is strongly observed also at stage 15 (**Fig. 45 B'''**) when a track of stable MTs preceded subcellular lumen formation (**Fig.45 B'**). At st. 16, both Shot and stable MTs decorated the apical side of the TCs all around the subcellular lumen (**Fig. 45 C**).

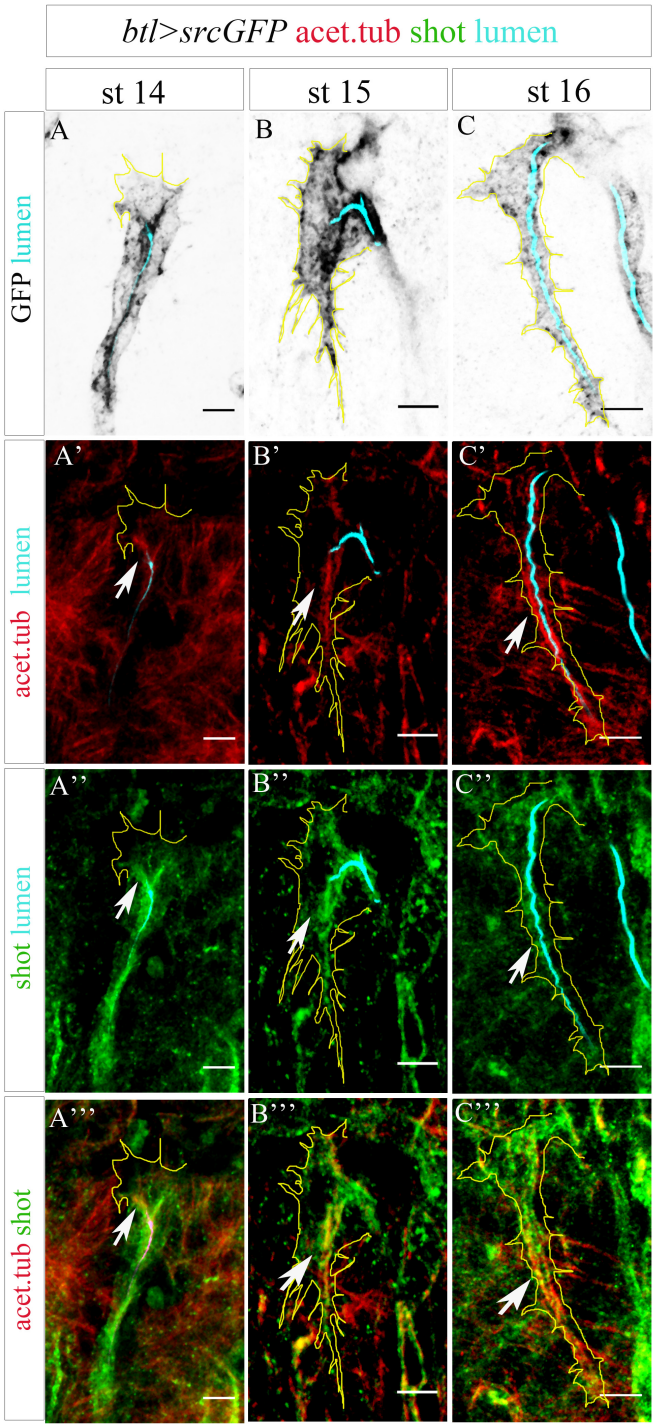

Figure 45. Shot accumulates around stable microtubules during subcellular lumen formation. (**A-C**) Dorsal TCs from fixed embryos *btl>srcGFP,* from st.14 to st. 16. GFP staining is showed in grey in panels (A-C). In all panels the outline of the TCs is drowned in yellow. Acetylated tubulin is in red (A'- C' and A'''-C''') and Shot in green (A''- C'' and A'''- C'''). The lumen was detected with Fluostain, represented in cyan (A- C'''). Acetylated tubulin and Shot (white arrows) are both mainly accumulated toward the path of growth of the subcellular lumen at earliest stages (st. 14-15) and accumulate around apical side at later stage (st. 16). Note that co-localization between acetylated tubulin and Shot is mainly detectable inside the TCs. Anterior side is on the left, dorsal midline is up. Scale bar 5μm.

Shot localization was similar to MT localization in the TC. However, we observed that the Shot antibody detected also some protein in the cytoplasm, probably due to the interaction of Shot with other cytoskeletal and/or cellular structures.

4.2.4.2 Shot and the asymmetric actin accumulation

As described before, in *wt* conditions F-actin and the actin binding protein Moesin concentrate strongly at the tip of the terminal cell participating in the correct growth and directionality of terminal cell during its morphogenesis. During elongation, MTs point to the tip of the cell, reaching the area of high Moe and F-actin accumulation (Gervais and Casanova, 2010).

A possible interaction between Shot and the high area of concentration of Moe/Actin was investigated. To visualize Moe/Actin we fixed *btl::moeRFP* embryos and we stained with anti-RFP to detect asymmetric Moe/Actin accumulation and to detect endogenous Shot we used anti-Shot antibody (**Fig. 46**). At early stages (**Fig. 46A**), when TCs started to elongate, we clearly recognized Shot co-localizing with RFP at the **tip of the terminal cell**. The overlap between Shot and RFP was maintained until the end of stage 15. It has been described that during TCs maturation stable MTs are ahead of the lumen, at the tip of the cell, invading the area of high Moe accumulation (Gervais and Casanova, 2010). Inside such area, during cell elongation, MTs and actin probably interact physically between them, for the correct growth of the cell.

Later on, at st. 16, no more Shot accumulation was detected at the Moe/Actin rich area (**Fig. 46 C**) probably because at this stage, the cell was already elongated, the lumen formed and perhaps the connection between actin and MTs was no longer necessary. To confirm this, we analysed the interaction between actin, MTs and Shot at later stages.

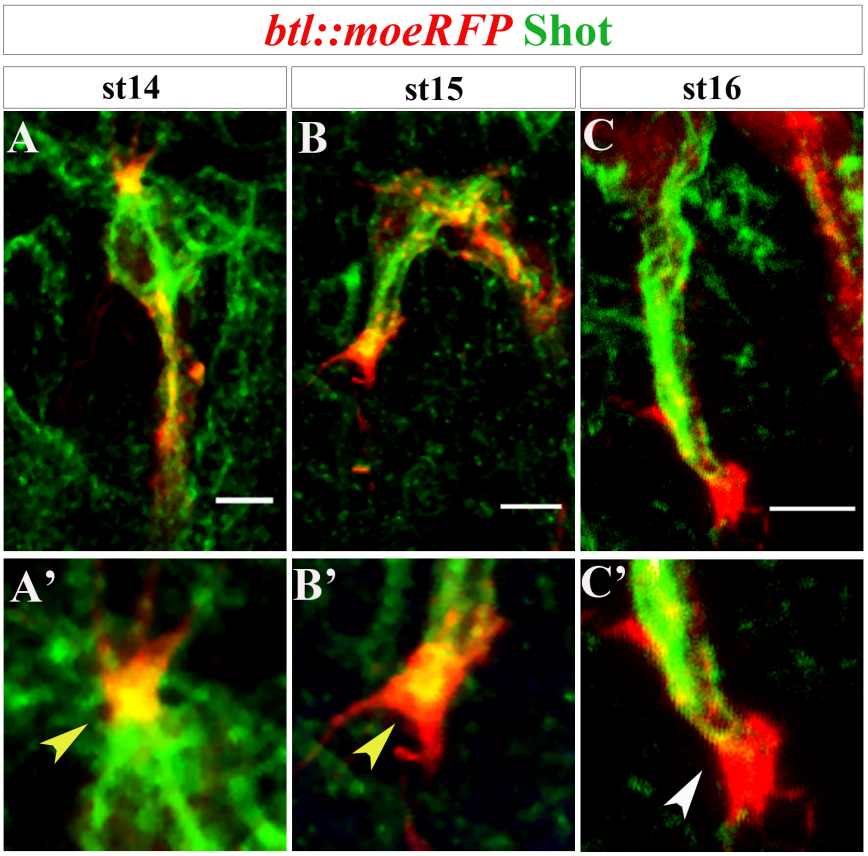

Figure 46. Shot accumulates transiently at the rich Actin/Moe area during TC development. (**A-C**) Tip of dorsal branches from stage 14 to stage 16 of embryos *btl::moeRFP* . (**A'-C'**) Magnification of the tip of the TCs. RFP is in red, Shot in green. Yellow arrows indicate co-localization points between Shot and RFP at st.14 (**A**') and st.15 (**B'**). Note that at st. 16 (C') endogenous Shot does not enter inside the rich Moe/Actin area (white arrow).

We observed that both stable MTs and Shot enriched the tip of the TC (**Fig. 47 B** and **C**), although we noted that Shot did not localize on those MTs that deeply invade the Moe/Actin area (**Fig. 47 D**). This observation could suggest that at later stages Shot is not mediating the interaction between these two cytoskeletal components anymore, but only interacting with stable MTs around the subcellular lumen area.

So, the data regarding the analysis of endogenous Shot in the TC suggests that the spectraplakin localizes with stable MTs all around the lumen and with the Moe/Actin at the tip of the TC, during the time of cell elongation and subcellular lumen formation, possibly mediating the crosstalk between the two cytoskeletal component. Later on, Shot interacts mainly with stable MTs around the subcellular lumen probably stabilizing these structures.

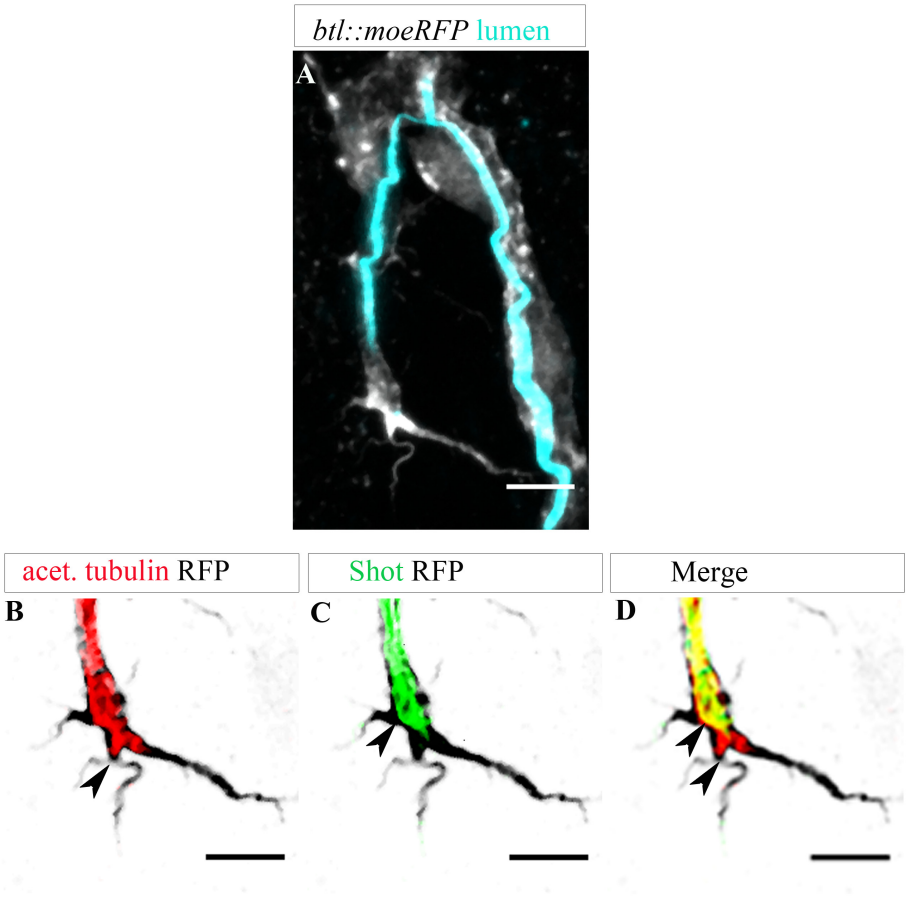

Figure 47. Shot colocalizes partially with MTs that enrich the Moe/Actin tip at later stages. (**A**) TC at the tip of dorsal branch of embryo *btl::moeRFP* at stage 16; Moe::RFP in grey, lumen in cyan. (**B-D)**; Single Z sections depicting Moe/Actin tip (in grey), stable MTs in red (B and D) and Shot in green (C and D**)**. Black arrows indicate the point of localization of stable MT and Shot within the tip of the TC. Anterior side is on the left scale bars 5 µm.

4.2.5 Shot is required for proper terminal cell formation

Previously to this work, the involvement of Shot during tracheal system development had been demonstrated, in particular when tracheal metameres connect between them to form a continuous respiratory organ (Lee and Kolodziej, 2002a). This connection is possible because specialized tracheal fusion cells join each other giving rise to an anastomosis site. To obtain a correct anastomosis process a new E-cadherin contact is established in association with a track of F-actin and MTs. The cytoskeletal organization is important in fusion cells also to generate a seamless subcellular tube, even if of different nature with respect to the seamless tube of the TC (Gervais et al.,

2012).The effect of *shot* loss of function was analysed during TC's subcellular lumen formation.

4.2.5.1 *shot* null allele displays defects in subcellular lumen formation

When we analysed the subcellular lumen at the tip of dorsal and ganglionic branches at st. 16 of $shot^3$ null allele, using anti-Gasp staining, we found phenotype ranging from misguided, shorter or not completely formed subcellular lumen (**Fig. 49 B** an **E**). Likely, the variability observed in the phenotype was caused by the maternal contribution. We quantify terminal cells that completely lost subcellular lumen formation and found that 54% of terminal cells did not elongate a proper subcellular lumen (300 ganglionic TCs and 300 dorsal TCs) (**Fig. 49 G**).

4.2.5.2 The Shot function in trachea is autonomous

shot is expressed during development in several tissues (nervous system, epidermis etc), so we corroborated that the defects observed in TCs of *shot* mutants were due to the absence of Shot in the tracheal system.

In order to clarify whether the effect of *shot* was autonomous in the tracheal system, we tested *shot*RNAi by expressing it in the trachea, in *wt* background. To decrease *shot* expression more, the RNAi experiment was performed at 29°C, temperature at which the UAS/GAL4 system works with higher efficiency and therefore more RNA interference molecules would be expressed. We founded that 40% of terminal cells analysed (n=300) at the tip of the dorsal branches (n=150) and ganglionic branches (n=150) were strongly affected in subcellular lumen formation (**Fig. 48 C**, **F** and **G**). As expected, the phenotype observed by the induction of *shot* RNAi was weaker but similar to that described in $shot^3$ null allele, so we concluded that the effect of Shot was autonomous in the tracheal system.

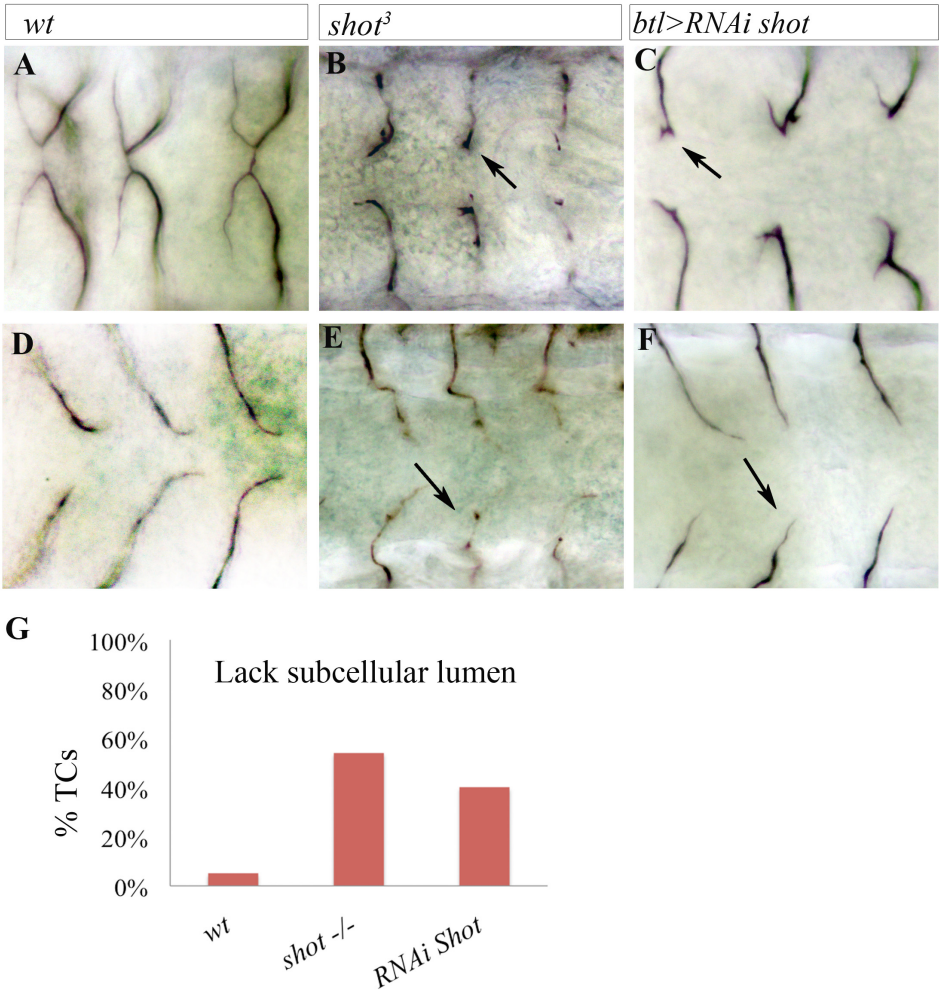

Figure 48. *shot* loss of function induces defects in subcellular lumen formation. Tips of DBs (**A-C** dorsal view) and GBs (**D-F** ventral view) of fixed embryos stained with anti-Gasp at st 16 of *wt* (A and D), *shot*^{3} (B and E) and *btl>shotRNAi* (C and F). (Ventral view, anterior side is on the left). Black arrows indicate some TCs without a proper subcellular lumen. (**G**) Quantification of embryos (genotype indicted) displaying at least one TC without subcellular lumen (*wt* n=20).

4.2.5.3 TC specification in *shot* null allele

The stronger *shot*^{3} mutant TC phenotype consisted in the total absence of subcellular lumen and in some cases the lumen was shorter respect to the *wt*. A similar phenotype was previously reported for embryos affected for the *pruned/blistered* gene that encodes the transcription factor DSRF that, as described in the introduction, regulates late formation of the TCs (Gervais and Casanova, 2011; Guillemin et al., 1996).

Because Shot is a cytoskeleton organizer, and because it has been reported that proteins involved in cytoskeleton organization could regulate cell specification including the one of TCs (Miralles et al., 2003; Pomies et al., 2007), we investigated in

shot^3 mutant a possible defect in TCs fate, using DSRF antibody. We found that DSRF is properly accumulated, also in which cases that TCs did not elongate or elongate partially the subcellular lumen (**Fig. 49**). So the phenotype observed is not caused by defects in TC fate.

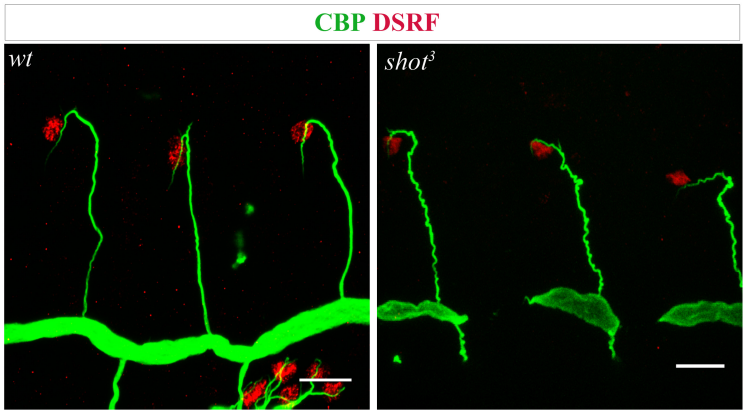

Figure 49. TC fate in not affected in *shot*^{3} mutant. DBs at st. 15 of *wt* and *shot*^{3} fixed embryos stained with CBP (green) and DSRF (red). Anterior side is on the left and dorsal midline is up, scale bars 10µm. *shot* mutant does not display defects in DSRF accumulation. Note subcellular lumen phenotype and defects at anastomosis sites in the DT.

4.2.5.4 Terminal Cell elongation in *shot* null allele

Cell elongation and subcellular lumen formation are intimately associated between them and they depend strictly on cytoskeletal organization; asymmetric actin accumulation and MT network organize vesicles trafficking to generate new apical and baso-lateral membrane (Gervais and Casanova, 2010).

It has been described that subcellular lumen formation requires proper TC elongation, and *viceversa*, a TC can not elongate properly if subcellular lumen is not properly formed (Gervais and Casanova, 2010). To better characterize the effect of Shot in the TCs, we examined the state of TC cell elongation in *shot*^{3} mutant.

We used embryos *btlGAL4UASsrcGFP* to visualize the TC membrane in control and *shot*^{3} null allele background. In the mutant, we observed different types of TC phenotype (n=25). In 52% of the TCs affected we observed that the cell partially elongated and the lumen was formed (**Fig. 50 A**) but it seemed to be shorter in respect to the control and/or with a wrong directionality. In 12% of the cases TCs were able to emanate some filopodia in ventral direction but the elongation was stopped

prematurely. In this case, a small primordium of subcellular lumen could be detected next to the nucleus (**Fig. 50 B**). 16% of terminal cells were able to generate cytoplasmatic protrusions and elongate partially but the lumen was completely absent (**Fig. 50 C**). In the most severe phenotype observed (20%) (**Fig. 50 D**), the cell was neither able to emanate filopodia nor elongate, and the subcellular lumen was absent.

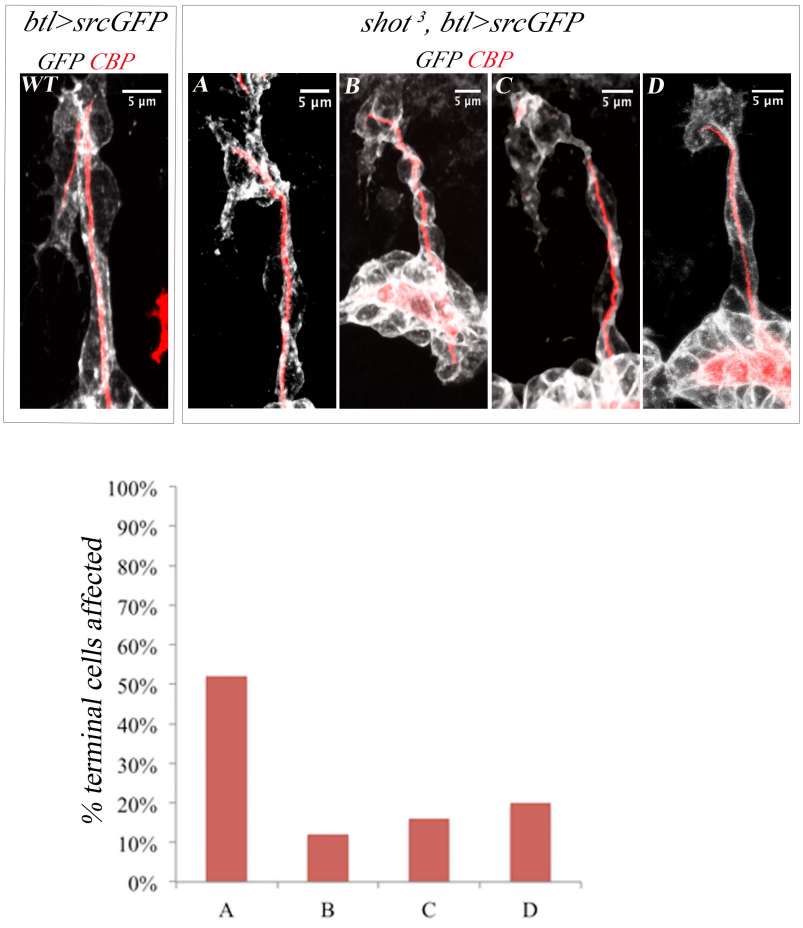

Figure 50. Different types of TC phenotype are generated in absence of Shot. Dorsal branches of *btl>srcGFP* control (*wt*) and *shot*^{3} embryos stained with GFP (grey) to visualize membrane and CBP (in red) to visualize the lumen. Anterior side is on the left and dorsal side is up. Scale bars 5µm. (**A**) TC partially elongated and the lumen was formed but with wrong directionality or **(B**) the elongation was stopped prematurely and a primordium of subcellular lumen was formed or (**C**) the cell elongates partially but the lumen was completely absent, or (**D**) the cell was not able to elongate and the lumen was absent. **(E**) Quantification of the different type of TC phenotypes reported as A-D in s*hot*^{3} (n=25)

4.2.5.5 Asymmetric actin organization in *shot* null allele

As described before, in *wt* conditions actin and Moe concentrate strongly at the tip of the TC during its development, participating in the correct growth and directionality of TCs. To visualize Moe/Actin in *shot* null allele we used *shot^{3}; btl::moeRFP* embryos and we followed Moe/Actin with RFP staining, in the control and in *shot^{3}* mutant background.

For interpreting the Moe accumulation better we used a colour scale in which the colour is linked to an intensity value (blue, green and red from low intensity to strong intensity).

At early stage 16, in control embryos, RFP was strongly detectable at the tip of the TC, in front of the tip of the lumen in 86% of terminal cell analysed (n=21). In addition, a few spots of Moe were detectable in the cytoplasm, around the subcellular lumen (**Fig.51 A**). In *shot^{3}; btl::moe RFP* we analysed the different types of phenotype ranging from cases in which the cell did not elongate at all and the subcellular lumen was not formed, to cases in which the cell, also if not properly, was able to elongate and to form the lumen. In all conditions, we found defects in Moe-RFP accumulation. In particular, we observed a reduced Moe-RFP concentration at tip of the terminal cell and an increase of scattered spots into the cytoplasm in 86% of the terminal cell analysed (n 23) (**Fig.51 B-D**).

These experiments, together with the previous analysis of the pattern expression of Shot, suggested a role of the spectraplakin in organizing/stabilizing Moe/Actin accumulation in the TC.

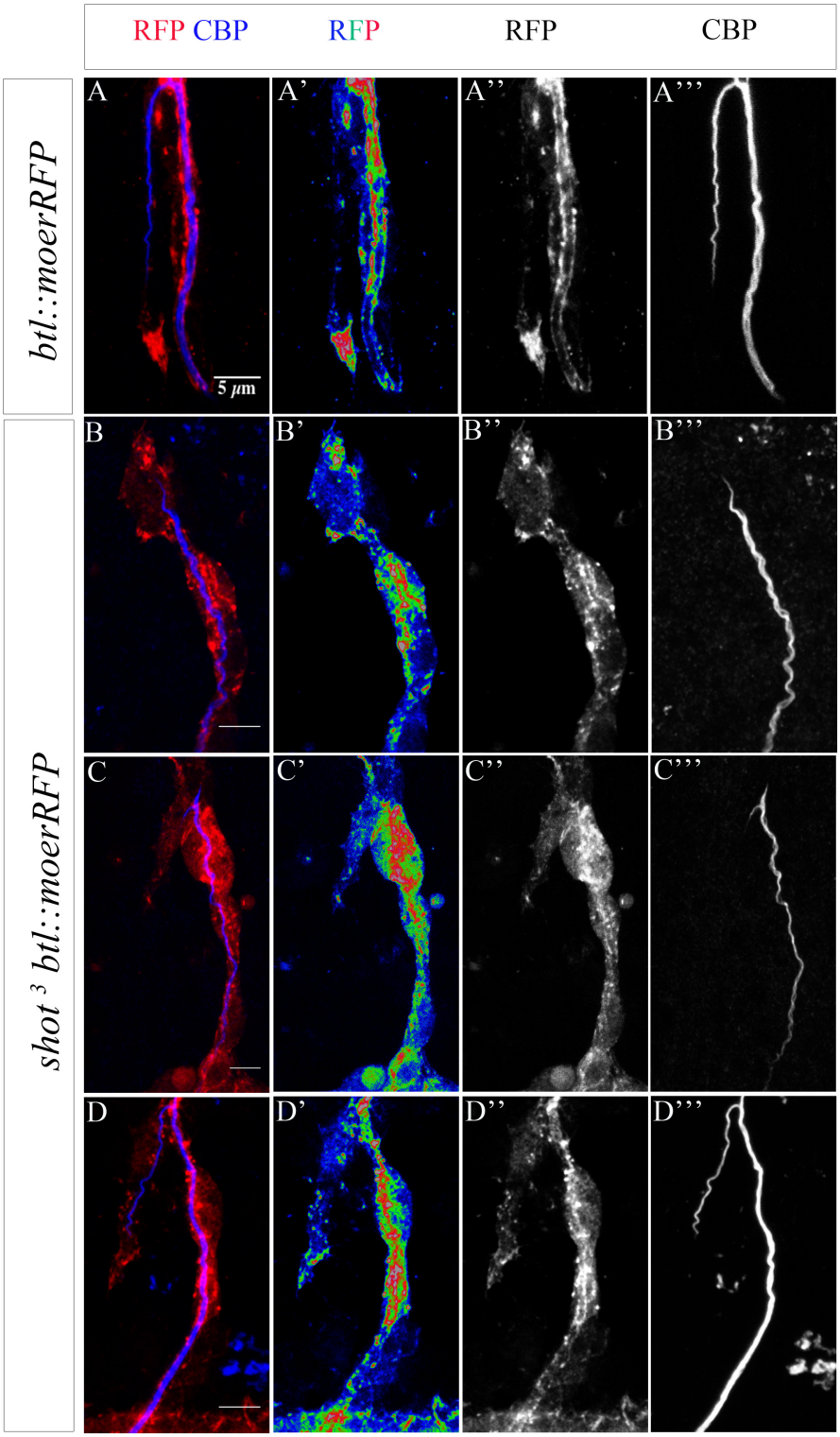

Figure 51. Asymmetric actin accumulation is affected in *shot*^{3} mutant embryos. Dorsal TC from fixed embryos *shot*^{3}/ +; *btl::moeRFP* (**A**) and *shot*^{3} ; *btl::moeRFP* (**B**,-**D**), Stained with RFP (red in A-D or in a colour scale in which blue is low, green is middle and red high intensity A'- D', or in grey

A''- D'') and CBP (blue in A'- D' or grey in A'''- D'''). In *shot* mutant Moe/Actin appears impaired accumulated. Anterior side is on the left and dorsal midline is up. Scale bars 5μm.

4.2.5.6 MTs in *shot* null allele

Shot is involved in MT dynamics in different tissues (Booth et al., 2014; Nashchekin et al., 2016; Sanchez-Soriano et al., 2009). For example, it has been described that in neuronal cells Shot is involved in polymerization as well as in stabilization (Alves-Silva et al., 2012). We analysed the bundles of MTs in $shot^3$ TCs. We used $shot^3$*;btl >srcGFP* embryos in order to visualize the outline of the TCs and acetylated tubulin antibody to recognize stable MTs into the TC. In the control, as described before, stable MTs are organized in longitudinal bundles around the subcellular lumen (**Fig. 52 A**). Also in this case, in the *shot* mutant we analysed different types of phenotype ranging from cases in which the TC partially elongate and the subcellular lumen is formed, to cases in which the TC is not proper elongated and the lumen is not formed. In all cases (n=20) of $shot^3$ TCs, we detected defects of the MT network. In particular, we observed that when the cell was not elongated, MTs bundles no longer localized in the apical region and seemed to be less then in *wt* (**Fig. 52 B**). A general disorganization (and probably a little decrease) in MT bundles in respect to the control was also observed in TCs able to partially elongate (**Fig. 52 C**).

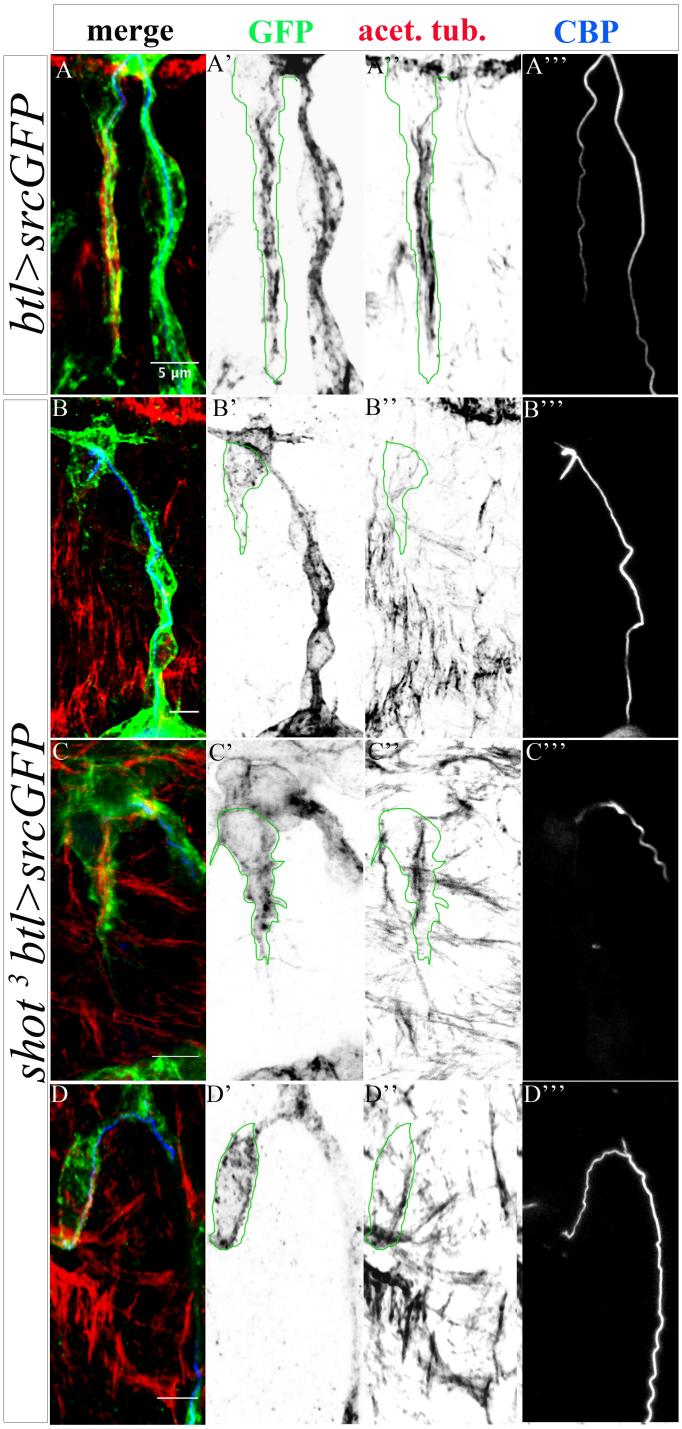

Figure 52. MT disorganization in *shot*^{3} mutant. Dorsal TC from embryo at st. 16 control (**A**) and *shot*^{3} mutants (**B-D**) stained with GFP (green in A- D and grey in A'-D'**)** acetylated tubulin (in red in A-D and in grey in A''-D'') and CBP (in blue in A-D and grey in A'''-D'''). Anterior side is on the left and dorsal midline is up. Scale bars 5µm. The border of TC is plotted in green A'-D' and A''-D''. In B the organization and the amount of stable MTs is strongly affected, in C is possible observe MT bundles disorganized along the cytoplasmatic protrusion without subcellular lumen and in D only thin track of MTs surround the subcellular lumen.

4.2.5.6 Apical membrane in *shot* ^{3}

Shot^{3} mutants display an impaired cytoskeletal organization and very probably this causes defects in vesicle trafficking and consequently in cell elongation and subcellular lumen formation.

We tried to confirm it, analysing the apical determinant Bazooka (Baz)/Par3-YFP, using *btl >BazYFP* fixed embryos. As previously reported, subcellular lumen formation in the *wt*, appeared as a continuous process of sprouting from the apical side of the TC. In these *wt* TCs, new membrane was added to the lumen of the principal network at the junction and continued in the direction of cell elongation. In *shot*^{3} fixed embryos we observed that when the lumen was formed (**Fig. 53**), BazYFP was mostly apically localized and no strong defects were apparent (n=10). When the cell was not elongated and the lumen not formed, BazYFP was not properly apically organized but scattered everywhere in the cytoplasm.

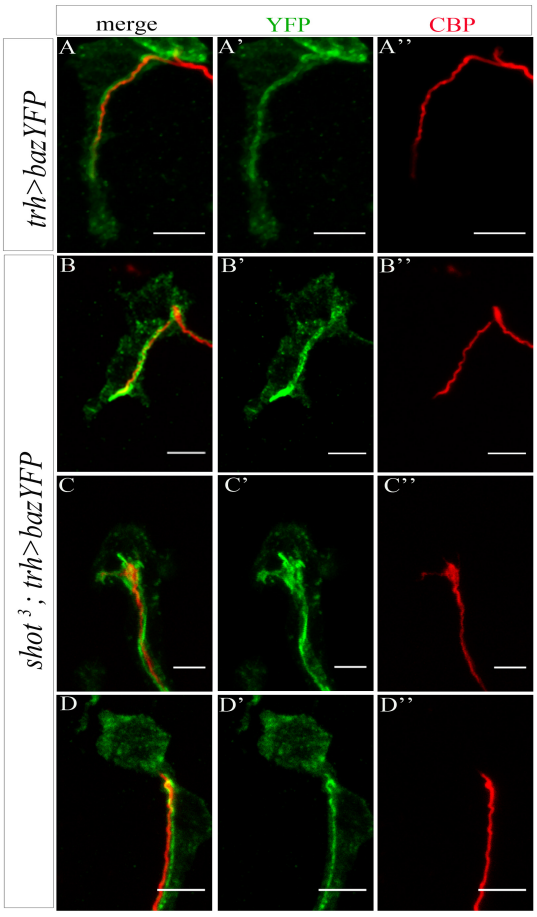

Figure 53. Apical membrane in *shot*^{3} mutant. Dorsal TCs from embryos *btl>bazYFP* control (**A**) and *Shot*^{3} mutant (**B-D**) stained with GFP to detect YFP (green in A- D and A'-D') and CBP (in red in A-D and in grey in A''-D'') Anterior side is on the left and dorsal midline is up. Scale bars 5µm.

In cases in which the cell is elongated and the lumen is formed, no strong defects in apical membrane deposition are detected. But in cases in which the cell is not elongated and the lumen not formed BazYFP is not well localized.

So, *shot*^{3} TCs are characterized by defects in actin accumulation as well as in MTs network and in turn in cell elongation and subcellular lumen formation. The phenotype of *shot* mutants resembles the loss of function of proteins involved in organization of actin as well as condition in which MTs are depolymerized or disorganized respect to the cortical actin during TC development (Gervais and Casanova, 2010). This data suggest that the spectraplakin is involved in the whole organization of the TC cytoskeletal machinery.

4.2.6 Structure function of Shot

Shot is a multifunctional protein involved in MT stabilization, organization of Actin and connection between both cytoskeletal components in different tissues. We observed that in TCs of *shot* loss of function, overall cytoskeleton organization was impaired, but we did know how Shot operated in the TCs. Is Shot affecting separately each cytoskeleton compartment? Does Shot mediate the crosstalk between Actin and MTs? Which cytoskeletal function of Shot is needed for proper subcellular lumen formation? In this last section of results we show some data providing some preliminary answers to these questions.

4.2.6.1 Use of rescue strategy

In order to clarify the molecular function of Shot during subcellular lumen formation, we tried to rescue *shot*^{3} phenotype, with different constructs.

As described, *shot*^{3} embryos had a highly variable subcellular phenotype. To simplify the quantification, we took in consideration the most severe luminal phenotype, in the mutant as well as in the rescue experiments: the absence of subcellular lumen (**Fig. 55 C-D**). As previously reported we quantified in *Shot*^{3} that 54% of TCs (at the tip of ganglionic and dorsal branches) did not form subcellular lumen (**Fig. 55 K)**.

We overexpress in the trachea of *shot*^{3} mutants the *C-tail* construct in order to address weather the Shot MTs stabilization activity could restore subcellular lumen formation.

We observed that 48% of TCs analysed at the tip of GBs and DBs (n=250) were still not able to form a subcellular lumen (**Fig. 54 E-F** and **K)**, suggesting that the overexpression of *C-tail* was not enough to rescue the null allele phenotype.

We performed a second rescue experiment, this time using the tracheal overexpression of *shot-C*. Surprising, we found that still 38% of TCs analysed (n=200), had no formed ganglionic and dorsal tip TCs (**Fig. 54 G-H** and **K)**. So, in this case we obtained only a partial rescue of the $shot^3$ phenotype.

Overexpressing *shot-A* in the trachea of $shot^3$ mutant embryos we found that only the 6% of TCs analysed (n=200) displayed TCs not well formed and in the rest of the cases we observed that subcellular lumen was formed (even if in some cases shorter or with a wrong direction) **(Fig. 54 I-J** and **K)**. Sporadically, we were able to see in all rescue experiments, some extra subcellular lumen, probably due to higher than *wt* expression of *shot* in the tracheal system. So, we considered that the overexpression of the full-length isoform A was able to rescue the stronger subcellular lumen phenotype observed in $shot^3$ embryos and had more efficiency in restoring subcellular lumen formation in comparison to isoform C or C-tail.

This data suggested that the Isoform A, and probably its activity in crosslinking Actin and MTs, is necessary for the correct subcellular lumen formation.

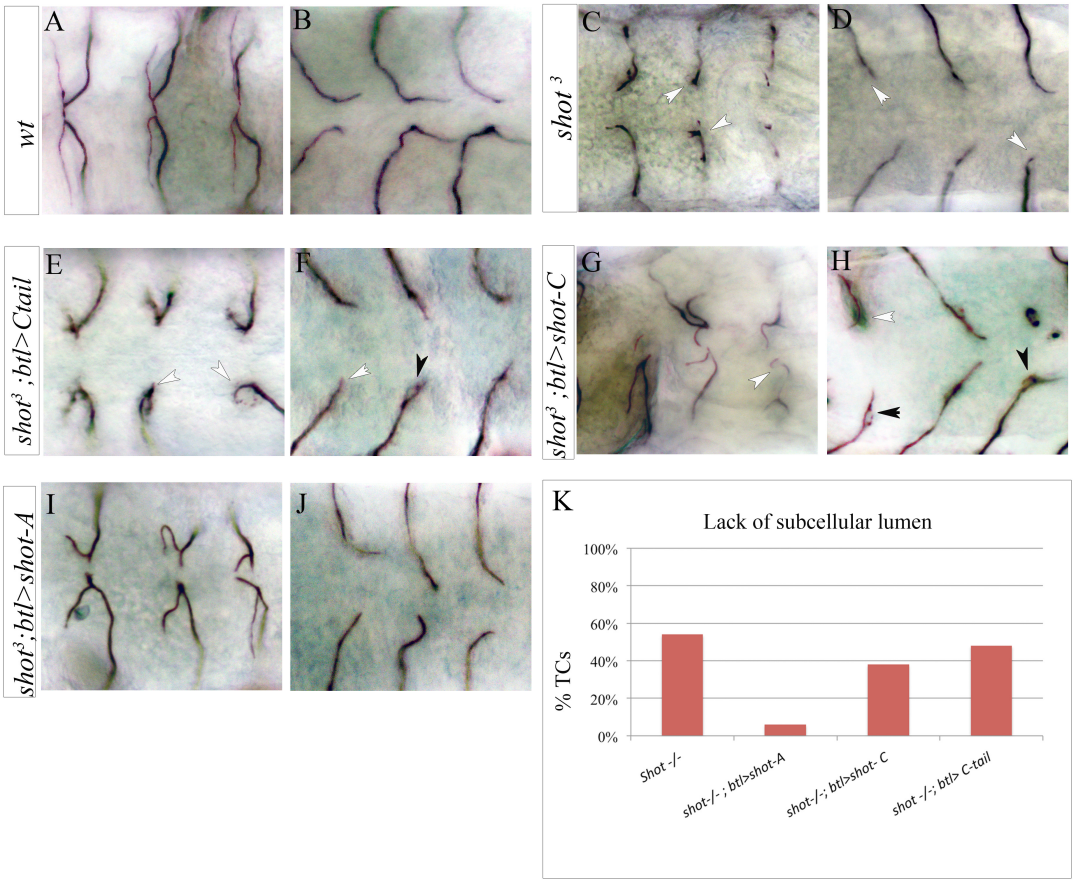

Figure 54. *shot-A* is necessary to form subcellular lumen. Tips of dorsal (**A**, **C**, **E**, **G** and **I**) and ventral (**B**, **D**, **F**, **H** and **J**) branches at st. 16 from embryos *wt* (**A**, **B**) *shot*^{3} (**C**, **D**) *shot*^{3}*; btl>Ctail* (**E**, **F**), *shot*^{3}*; btl>shot-C* (**G, H**). (**I-J**) *shot*^{3}*; btl>shot-A*. White arrows indicate the absence of TCs and black arrows indicate bifurcations. Anterior side of embryos is on the left. (*K*) Quantification of terminal cells without subcellular lumen in the mutant and in the rescues; only Shot-A properly rescues the phenotype caused by the loss of function mutation *shot*^{3}.

4.2.6.2 *shot*^{kakP2} phenotype

In order to corroborate the hypothesis that Shot-A is needed to form a proper subcellular lumen, we analysed *shot*^{kakP2} mutation. This allele carries an insertion of a transposable element into the intron between the second and the third transcriptional start site of *shot* abolishing all isoforms containing the first Calponin domain (CH1)(Bottenberg et al., 2009).

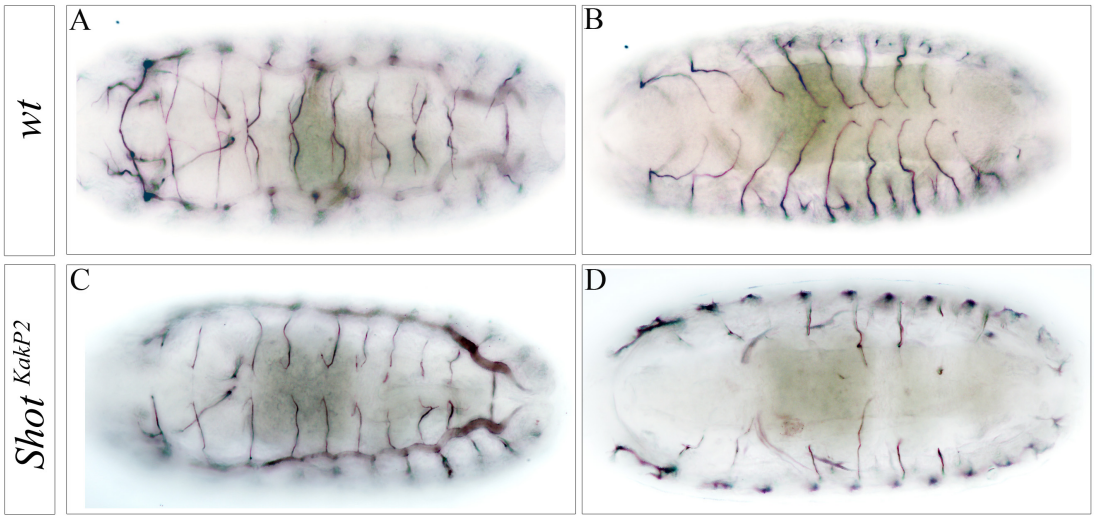

Figure 55 *shot* ^{KakP2} is characterized by lack of subcellular lumen Dorsal (**A** and **C**) and ventral (**B-D**) view of *wt* (A-B) and *Shot* ^{KakP2} embryos (C-D). *shot* ^{K03405} in which only isoforms C and D are transcribed has strong defects in TCs subcellular lumen formation.

The penetrance phenotype observed of *shot*^{kakP2} was very similar to *shot*^{3} null allele with more then 50% of TCs (n=600; 300 ganglionic and 300 dorsal TCs) that did not form a subcellular lumen (**Fig. 55**).

The data from *shot*^{kakP2} together with data from transgenic rescues with the *shot-C* construct, lacking the first CH domain, strongly suggest that Shot full length isoform A is required for *de novo* subcellular lumen formation.

4.2.7 The functions of Tau and Shot overlap during subcellular lumen formation

It has been suggested that spectraplakins might functionally overlap and compete with structural MAPs (Alves-Silva et al., 2012; Voelzmann et al., 2016). If this is the case in the TCs, also the overexpression of a MAP could induce the same phenotype as well as Shot. Tau is a major microtubule-associated protein that induces bundling and stabilization of microtubules (MTs) (Butner and Kirschner, 1991; Kadavath et al., 2015). Tau binding of MTs appears mostly in axons and different isoforms of *tau* include three or four MT-binding repeats which are highly conserved between different species and different members of the MAP family (Samsonov et al., 2004).

We overexpressed *tau* in tracheal system and we found TCs with extra subcellular lumina (**Fig. 56**). Like Shot, the effect of Tau in inducing extra subcellular lumina was dosage dependent. Overexpression of a single copy of *tau* induced at least one

bifurcation in 50% of the embryos analysed (n=23 embryos) and two copies of *tau* induced the branching phenotype in 93% of embryos (n=16).

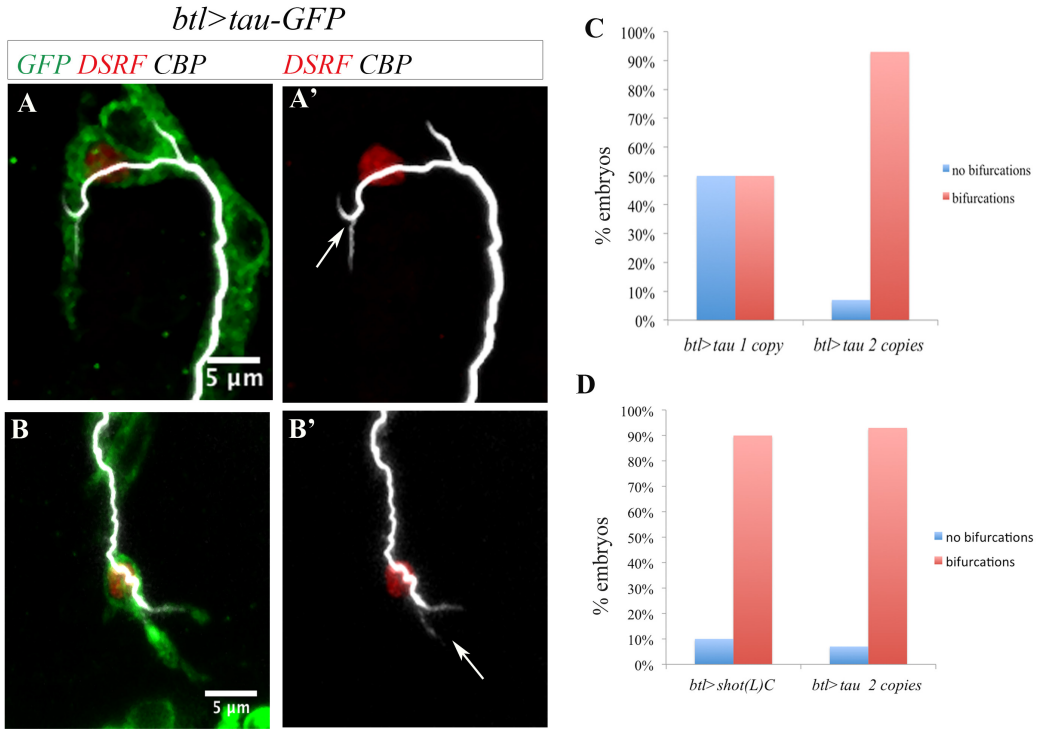

Figure 56. The overexpression of the MAP tau induces bifurcated terminal cells.

(A-B) Dorsal (A) and ganglionic (B) TC and part of the primary branch of embryos overexpressing in the tracheal system *tau-GFP*, stained with GFP (green), CBP (white) and DSRF (red), showing extra-subcellular lumen phenotype (anterior side on the left, dorsal side is up scale bar 5µm).

(**C**) Quantification of embryos overexpressing one or two copy of *btl > tau GFP* displaying at least one bifurcated terminal cell (columns in red) or not phenotype (columns blue). (**D**) Comparison between the quantification of embryos overexpressing one copy of *btl >shot-C GFP* and two copies *btl>tauGFP*.

The penetrance of the phenotype caused by the overexpression of two copies of *tau* is similar to the penetrance of the phenotype induced by one copy of *shot* suggesting that the spectraplakin has a stronger effect in respect to tau. It is possible that the overexpression phenotype of *tau*, depends on its classical activity in stabilizing MTs, reinforcing the idea that a functional overlap between spectraplakins and MAPs exists in what concerns the interaction with MTs.

Alternative functions of Tau, beyond MTs stabilization, have been described (Morris et al., 2011). Recently it has been described that Tau is involved in co-organizing the

dynamic MT and Actin networks (Elie et al., 2015), so it is possible that in absence of Shot, Tau could replace the crosstalk between two cytoskeletal components, allowing correct subcellular lumen formation. To test this hypothesis, we tried to rescue the *shot* loss of function phenotype overexpressing *tau* in the tracheal system. We found that the overexpression of one copy of *tau* was not able to restore subcellular lumen formation (**Fig. 57 E** and **F**), in fact 51% of TCs analysed (n=400) displayed lack of subcellular lumen. But by analysing the overexpression of two copies of *tau* in the tracheal system of *shot*^{3} embryos, surprisingly we found lack of subcellular lumen phenotype only in 17% of TCs (n=260) (**Fig. 57 G** and **H**). Also, in this rescue experiment we observed that some TCs bifurcated.

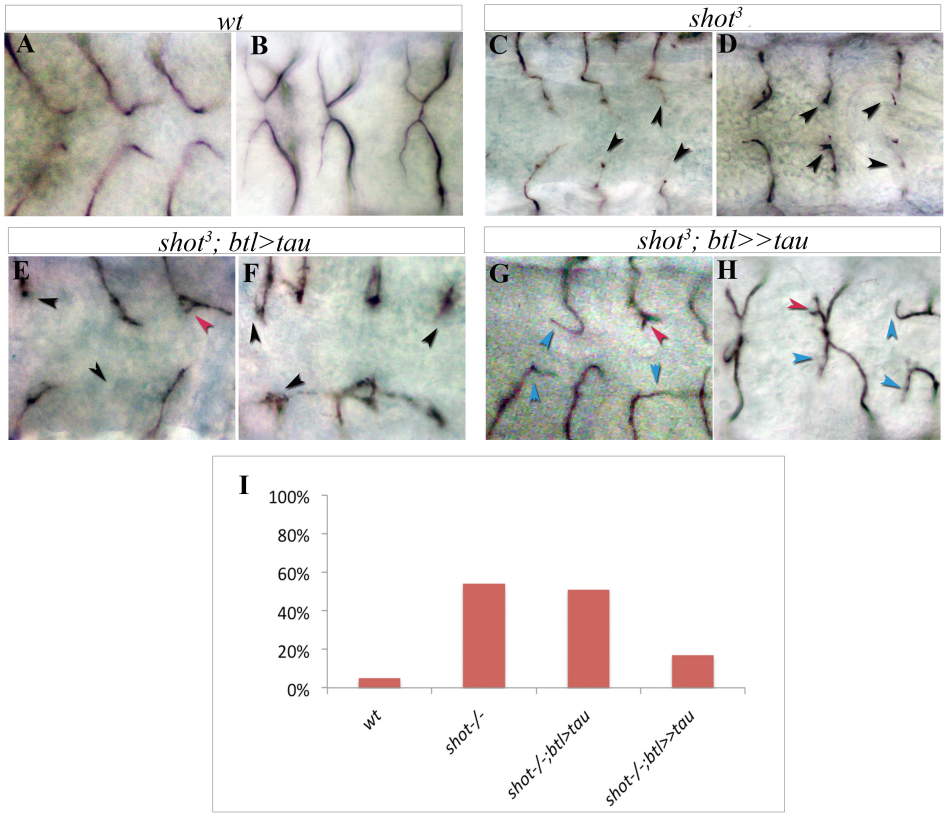

Figure 57. Tracheal MAP Tau expression in tracheal cells rescued *shot* null allele phenotype
Ventral and dorsal view of embryos *wt* (**A** and **B**) *shot*^{3}(**C** and **D**), *shot*^{3} *btl>tau* (**E** and **F**) and *shot*^{3} *btl>>tau* (**G** and **H**) stained with anti Gasp. Black arrow in (C-D) and (E-F) indicate the lack of subcellular lumen. In fact, in the overexpression of one copy of tau in *shot* mutant background many TCs still not elongate the lumen. In the case of a higher overexpression of *tau*, subcellular lumen is formed as indicated by blue arrows. In both cases, some bifurcations were detectable as indicated by red arrows.

So it is possible that an overexpression of *tau* is able to induce an hyper-stabilization of MTs, as well *shot*, but could be able to introduce a co-organization between different cytoskeletal compartments and replace the function of Shot in this context.

5 DISCUSSION

5 DISCUSSION

The aim of this study was to explore new molecular aspects involved in seamless tube formation. To this end, we have analysed mutants characterized by extra-branching or lack of subcellular lumen in the TCs of *Drosopila melanogaster.* As a consequence, we successfully obtained new insights into cytoskeletal modulation during single-cell branching. We characterized, for the first time, the role of centrosomes during subcellular lumen formation and we have described the consequences of centrosome number aberrations in these post-mitotic cells. We have also demonstrated a requirement for the long spectraplakin protein Short-stop (Shot) in the formation of the subcellular lumen. Using Shot as an entry point, have analysed the consequences of an over-stabilization of MTs and the necessity of an actin-MT crosstalk during subcellular lumen generation.

In this discussion, first I summarize and give an interpretation of the data presented about the role of the centrosomes in the TC and the consequences of changes in centrosome number. Then, I discuss the role of Shot during subcellular lumen formation in order to clarify its function in this context.

5.1. Two centrosomes into the TCs

Starting with the analysis of the interesting *Rca1* mutant phenotype we were able to demonstrate a novel role for centrosomes during subcellular lumen formation.

In *wt* conditions two centrosomes localize apically to the junction of the TC with the stalk cell. TCs are differentiated cells, but they have **1 pair of centrosomes**. This is an unusual conformation; generally 2 centrosomes characterize dividing cells and indeed in differentiated cells one solitary centrosome is present (Nigg and Stearns, 2011).

The mechanism by which TCs maintain two centrosomes after cell division is an open question; we can speculate that TCs have started endo-replication or it may be that TCs inherit one centrosome after cell division and later, during differentiation, this centrosome is duplicated. In any case, future studies and detailed experiments are necessary to clarify this issue. From our work, what we can conclude is that differentiated TCs are programmed to maintain a pair of centrosomes to allow for the

particular MT organization needed to organize the first step of subcellular lumen formation.

5.2. Centrosomes are microtubule-organizing-centres (MTOCs) in TC

We showed that centrosomes are **MTOCs** that allow the MT organization necessary to start forming the ingrowing subcellular lumen. In particular, MTs emanate from the centrosome pair and grow towards the tip of the cell. During development **two tracks of stable MTs** are assembled from the apical centrosome pair and grow along each side and ahead of the ingrowing subcellular lumen. Through these MTs tracks, vesicles can be directed to deliver membrane and the new lumen can be built (Gervais and Casanova, 2010). Moreover, the two MT tracks may have also a structural function, as discussed next, in maintaining the subcellular lumen framework.

We define centrosomes as the primary MTOC during the first steps of subcellular lumen formation because we showed that not only the MT nucleator factor **γ-tubulin** localizes on centrosomes at early stages of TC development, but also that the centrosomes are active microtubule nucleating centres. However, it was previously shown that, when the lumen is already formed, γ-tubulin also localizes around the subcellular lumen and as consequence it has been proposed that the minus end of MTs faces the apical membrane (Gervais and Casanova, 2010). So, it is also possible that during development, secondary acentrosomal points of MT nucleation are formed on the apical membrane as observed for other tracheal cells (Brodu et al., 2010). In addition, there is still the possibility that this γ-tubulin population around the apical membrane is not involved in nucleating MTs but is rather involved in other aspects of MT network, such as the organization of the plus-end dynamic, as recently described (Oakley et al., 2015).

5.3 Connection between centrosomes and apical complex components

Our data suggests that a complex formed by centrosomes and apical complex proteins is required to achieve the polarization event that triggers subcellular lumen initiation. The subcellular lumen starts in connection with the rest of the tracheal luminal network from the apical junction between TC and stalk cell, the region where centrosomes are localized (**Fig. 58**). Accordingly, previous studies have shown a close association

between Baz, aPKC, and centrosomal proteins during cytoplasmic polarization events (Chen et al., 2011; Inaba et al., 2015).

We propose that inside the TC an apical **higher order molecular structure** formed by the centrosomes, apical determinants and nascent MTs, is necessary for the organized expansion of the apical plasma membrane towards the tip of the cell.

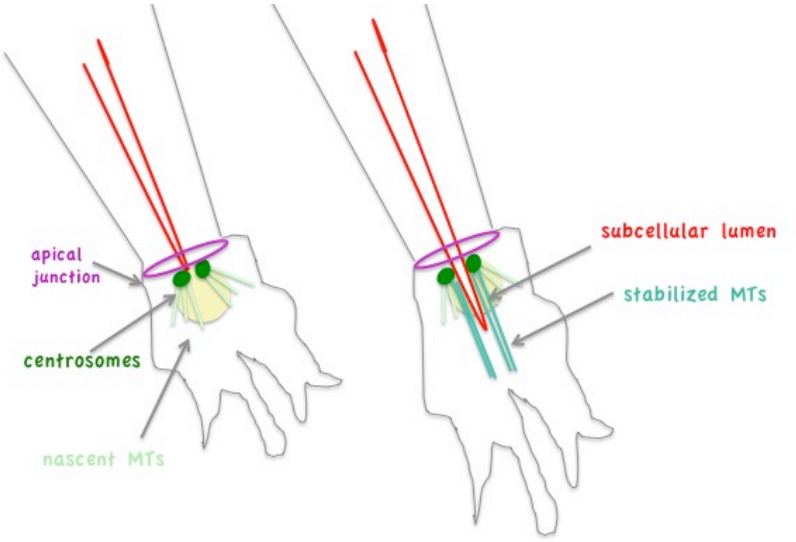

Figure 58 Graphical representation of the first phases of subcellular lumen formation. Two centrosomes, next to the cell-cell junction, are localized from where MTs arrays emanate and the apical components organize. Two nascent radial-like configurations of MT are generated and from here tracks of stable MTs are generated to direct the subcellular lumen growth.

5.4 Changing centrosome number in TCs

In *Rca1* TCs, we observed an **amplification of centrosomes** in association with higher levels of stable MTs and higher levels of apical complex proteins. So according to our model, in conditions of supernumerary centrosomes, more centrosomes can be active as MTOC and therefore the following steps are triggered: 1) more centrosome/apical complex proteins interactions are established; 2) more tracks of MTs are generated and 3) they are available as rails to direct membrane delivery. These events directly cause the immediate expansion of the apical membrane and so the extra branching phenotype. Accordingly, in *Rca1* and other mutants affected in centrosome number, the **bifurcated subcellular lumen** arises at the beginning of TC maturation, mostly from the apical junction. In *Rca1*, in the majority of the cases, we detect four centrosomes in association

with a bifurcated subcellular lumen but also other rare configurations are possible with higher number of centrosomes and/or a more branched subcellular lumen.

In association with the bifurcated lumen, we observe, in the majority of the cases, the **expansion of the cytoplasmatic protrusion** at the tip of the cell and its own asymmetric actin accumulation at the tip. Probably the initial surplus of MTs bundles and the establishment of a double intracellular polarized symmetry push the cell to split its own cytoplasm. These observations reinforce the notion that subcellular lumen formation is intimately associated with cell elongation (Gervais and Casanova, 2010) also in in cases of supernumerary lumina (**Fig. 59**).

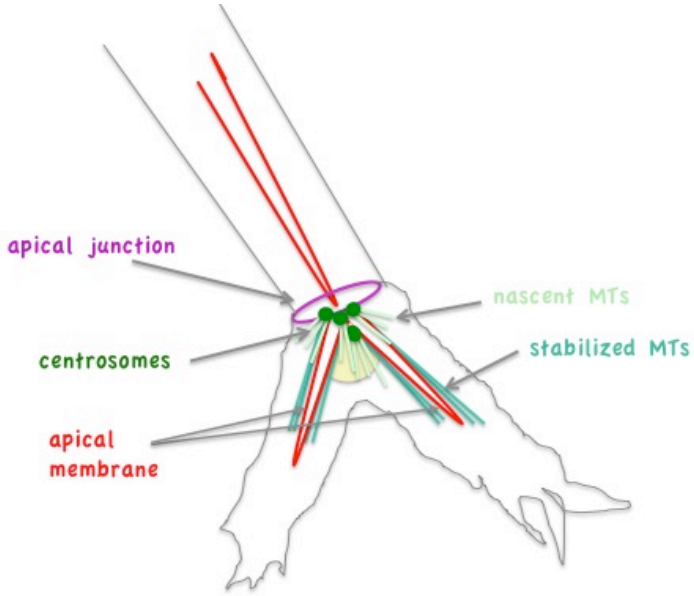

Figure 59. Centrosome amplification in TCs. Schematic representation of the consequences of centrosome amplification in the TC; four centrosomes apically localized induce an intracellular architecture that allows for the formation of a bifurcated subcellular lumen.

The correlation between centrosome amplification and TC subcellular architecture is in agreement with our observations of *sas4* and *Rca1; sas4* double mutant. **Without centrosomes**, subcellular lumen does not extend within the TC and the cell is able to elongate only partially, probably due to the scarcity of MTs directing vesicle trafficking and due to the failure interaction between apical complex proteins and centrosomes. In the double mutant, TCs lose the extra subcellular lumen branching phenotype because a balance between the effects of the two mutations restores a *wt*-like condition. Interestingly, also in cases in which only one centrosome decorates the apical region of

the TCs the subcellular lumen is not able to growth properly, reinforcing the notion that two centrosomes are necessary for the development of this type of differentiated cell.

5.5 Post-mitotic function of Rca1 and CycA

Rca1 and CycA are proteins that regulate cell cycle progression, trough the modulation of APC/C and consequently the activity of of the serine/threonine cyclin-dependent protein kinases (Cdks) (Grosskortenhaus and Sprenger, 2002). It is well known that the centrosome cycle must occur in coordination with the cell cycle otherwise normal centrosome duplication may result in abnormal centrosome amplification. This coordination is largely accomplished because cell cycle regulatory proteins, specially Cdks, also regulate the centrosome cycle (Harrison et al., 2011).

Despite stalling in embryonic mitosis 16, the centrosome amplification that we observe in *Rca1* and *CycA* tracheal terminal cells does not depend on their mitotic activity: our data point to **a post mitotic effect** of *Rca1* (and possibly of *CycA*) in centrosome amplification. The first evidence that leads to a post-mitotic function is the fact that other mutants, like *fzy* and *CycB,* displaying a similar cell cycle arrests as the one observed in *Rca1* and *CycA* mutants, do not have extra TC branching defects. Second, *Rca1* RNAi and rescue experiments were performed with *btl-GAL4*, a driver that is active from stage 11, a time of tracheal development at which cells do not divide any more (Affolter and Caussinus, 2008). Moreover, also the overexpression of *SAK* that induces supernumerary centrosomes, was performed using *btlGAL4* or *DSRFGAL4*. The latter driver is active only from stage 14, a time well away from the last tracheal cell division (Affolter and Caussinus, 2008).

However, from our data we can not extrapolate the post-mitotic pathway in which *Rca1* and *CycA* are involved in regulating centrosome number nor can we conclude a direct interaction between *Rca1* and scaffold centrosome proteins such as *Sas4*. Perhaps mechanisms involved in centrosome amplification can have an effect in the TC post-mitotically. Speculating, this could suggest a possible post-mitotic process that regulates centrosome number during the normal TC differentiation.

5.6 Centrosomes act differentially in distinct tracheal cell types

We note that centrosome amplification in all tracheal cells increases branching of only

the TCs. (It should be mentioned that extra branching phenotype was observed in all embryonic TCs but due to technical issues we focused exclusively on TCs at the tip of GBs and only in few cases at the tip of DBs).

This observation illustrates a substantial difference between the **role of centrosomes** in TCs and in other tracheal cells forming multicellular tubes, and in turn underlines the intrinsic differences between distinct cellular strategies to make a tube.

During extra-cellular lumen formation MTOC components in tracheal cells, re-localize from centrosomes to the apical membrane. Probably, the most adequate manner to arrange a multicellular tube with an extracellular lumen is to have acentrosomal MTs organized from the apical membrane (Brodu et al., 2010). In fact, apical MT anchorage is a common feature of epithelial structures in which cytoskeletal filaments orientated in non-radial but apical-basal axis might serve as a substrate for polarized movement of membrane vesicles within the cell (Meads and Schroer, 1995; Mogensen, 1999). However, in the TCs, centrosomes are programmed to be the primary MTOCs and to generate arrays of MTs with a quasi-radial conformation that is needed for **rapid and radical cytoskeletal remodelling**, and the generation of new intracellular structures. This configuration could be particularly important during periods in which fast subcellular lumen formation is required, such as rapid organ growth or angiogenesis.

5.7 Centrosome amplification and extra branching events in pathology

Several studies implicate centrosome amplification in the pathogenesis of **cancer** (D'Assoro et al., 2002). Centrosome amplification is frequently detected in a growing list of human tumours, and is a candidate "hallmark" of cancer cells. Defects in centrosome copy number give rise to genomic instability and aneuploidy and so cancer initiation and progression (Chan, 2011). Although the correlation between centrosomal aberration and pathology is well established, the consequences of centrosome amplification *in vivo* in the context of a whole organism are poorly understood. The majority of studies on this are related to cell proliferation and survival and not to the consequences of centrosome amplification in differentiated cells of specific tissues (Dzafic et al., 2015; Kulukian et al., 2015; Vitre et al., 2015). Our work reported for the first time that centrosome amplification increases branching in epithelial cells within a whole living organism.

In has been proposed that centrosome amplification also contributes to loss of tissue architecture, which has been associated with **angiogenesis in human cancers**. Using cell-culture systems, Godinho and coworkers have recently shown that centrosome amplification promotes cellular invasion, concluding that centrosome amplification can promote features of malignant transformation by altering the cytoskeleton (Godinho et al., 2014). With our work, we reported that centrosome amplification increases branching in epithelial cells within a whole living organism. This occurs during a process similar to capillary sprouting of blood vessels during angiogenesis. Therefore, our findings shed more light on the consequences of centrosome amplification in differentiated cell behaviour and further strengthen the importance of cytoskeletal regulation during subcellular lumen formation, a process involved in angiogenic sprouting.

5.8 Short-stop is involved in TC development

During this work, serendipitously, we were faced with the fact that the overexpression of the fly spectraplakin *short-stop* gives rise to extra subcellular lumen phenotype in the TCs. From this observation, we started to study the involvement of this cytoskeletal molecule in the context of the TC. Shot is a beautiful example of a **multifunctional protein** particularly important in cells that rapidly change their shape during development. In all model systems studied so far, spectraplakins are crucial in cells that require an extensive and dynamic cytoskeleton, e.g. epithelial, neural, and migrating cells (Huelsmann and Brown, 2014). As mentioned several times in this thesis, spectraplakins are able to crosslink different cytoskeletal structures but they can also bind and regulate one single cytoskeletal compartment (Alves-Silva et al., 2012; Bottenberg et al., 2009; Suozzi et al., 2012). In the TC, we consider that Shot could be active in both types of activities.

5.9 The *shot* overexpression phenotype is the result of an over stabilization of MTs in the TCs

We demonstrate that the overexpression of *shot* in the tracheal system induces extra-branching of the TCs and this effect does not depend on centrosome amplification. So,

the extra subcellular lumen branching phenotype in TCs is possibly due to a molecular mechanism, in which Shot is involved.

Studies in different tissues have suggested that spectraplakins interact with MTs using two conserved C-terminal domains, the Gas2-related domain (GRD) and the adjacent C-tail domain (C-tail). Such domains together associate along MT shafts and protect them against the MT destabilizing drug nocodazole (Alves-Silva et al., 2012; Sun et al., 2001);Lee, 2002 #253}. In different tissues, the C-tail has been reported to associate with either MT shafts (Alves-Silva et al., 2012; Sun et al., 2001) or EB1 at polymerizing MT plus ends (Applewhite et al., 2013). So, spectraplakins work as MT-stabilizing factors similar to classical MAPs and they also have roles as regulators of MT plus ends similar to +TIPs.

Our data indicate that the **C-tail domain** of Shot is involved in inducing the extra branching phenotype since the tracheal overexpression of this domain alone is able to induce extra branching and a construct in which it has been deleted has an extremely low capacity to induce extra subcellular lumen formation.

So it is possible that the over **stabilization/polymerization of MTs**, process in which C-tail is involved, is the cause of the appearance of extra subcellular lumen (**Fig. 60**). Accordingly, we have detected by the analysis of endogenous Shot or by the overexpression of isoforms containing the C-tail domain, the localization of the spectraplakin on stable microtubules fibres surrounding the ingrowing subcellular lumen.

In most cases, the extra subcellular lumen in Shot over-expression arises from the main lumen surrounded from where an excess of this spectraplakin could generate, by the over stabilization/polymerization of MTs, the formation of new tracks for vesicle trafficking.

The effect of Shot is dosage dependent, so in high overexpression conditions, the effect on the MT network organization increases and, as consequence, a highly ramified subcellular lumen is generated. Recently, it has been published that Shot recruits the minus-end protein Patronin to form noncentrosomal MTOC like structures (Nashchekin et al., 2016). These two proteins do not nucleate new MTs, (there is no involvement of γ-tubulin) but they capture and stabilize existing MT minus ends, which then allow for new MT growth. So, when the cell has nucleated sufficient MTs, it can maintain and reorganize its MT cytoskeleton by stabilizing MT minus-ends in the appropriate locations and using these, rather than the γ-tubulin ring complex, to provide the seeds

from which new MTs grow. This MT function of Shot could be suitable in the context of the TC architecture and new experiments could be designed to explore it.

Interestingly, we observed that in the majority of the cases the extra subcellular lumen induced by the overexpression of *shot* arose inside the **same cytoplasmatic protrusion**, probably because the over stabilization/polymerization of MTs happened when the initial architecture of the TCs is already established (**Fig. 60**).

Future experiments are needed to clarify the specific molecular mechanism by which Shot interacts with the MT network during seamless tube formation and a detailed analysis of the C-tail and its possible cooperation with the GRD domain could be useful to better interpret the relationship between MTs stabilization/polymerization and subcellular lumen formation.

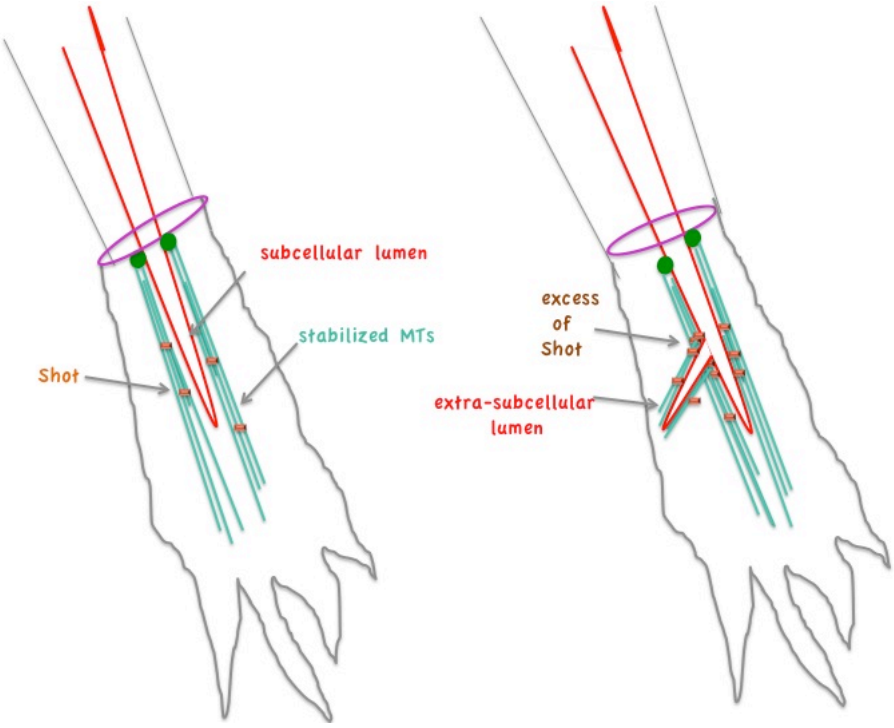

Figure 60. Shot is involved in MTs stabilization/polymerization and its overexpression induces extra subcellular lumen formation. Schematic representation of ganglionic TC in *wt* (on the left) or in the case of *shot* overexpression (on the right). Shot acts stabilizing/polymerizing MTs along the length of the ingrowing subcellular lumen and in a condition of over-stabilization/polymerization an extra subcellular lumen is formed.

5.10 The absence of Shot induces defects in TCs development.

We propose that Shot is involved in different aspects of cytoskeletal organization. By analysing endogenous Shot, we observe that the spectraplakin makes contacts not only with stable MTs around the ingrowing lumen but also with the actin at the tip of the cell. Moreover, analysing the null allele *shot*^{3} we found defects in both MTs and actin organization and, in addition, impaired cell elongation and subcellular lumen formation. In particular, through the observation of the actin binding protein Moe, we detected defects in the actin core maturation and analysing the cell membrane, we observed defects in filopodia formation. It has been previously described that in TCs of mutants affected in MT organization, the actin network is not strongly perturbed (Gervais and Casanova, 2010), so the "actin phenotype" observed in the *shot* null allele can not be related with defects observed in the MT network. This observation indicates a possible function of the spectraplakin in **organizing the actin** in the TCs. According to this hypothesis Shot and ACF7 can promote filopodia formation (Lee et al., 2007; Sanchez-Soriano et al., 2009). In particular, during axon extension of the CNS midline this function of Shot depends on the interaction of the two EF-hand domains and the positive regulator of filopodia assembly Krasavietz (Kra) So, an interesting future prospective could be to analyse the direct role of Shot, possibly through its EF-hand domain, in regulating the dynamic actin organization in the TC.

Regarding the MT network in the TCs of the *shot* null allele, we observe a general disorganization of stable MTs. This phenotype could depend on the function of Shot in 1) organizing directly the actin network or/and 2) **linking the actin with MTs**. According to these two hypothesis, the "inward membrane growth model" proposes that the establishment of a correct actin network allows for a specific MT organization and defects in actin remodelling cause defects in MT polymerization (Gervais and Casanova, 2010). Defective MT organization in the null allele *shot*^{3} could also reflect 3) a direct role of Shot in organizing this specific cytoskeletal compartment as suggested from our overexpression data. This direct or indirect role of Shot in organizing MTs is probably one of the key mechanisms regulating TC elongation and subcellular lumen formation.

5.11 Shot is involved in the cross talk between actin and MTs during TCs development.

We found that the expression of Shot-A in tracheal cells rescues *shot*^{3} subcellular lumen phenotype to 90%, whereas the expression of Shot-C only rescues the lumen phenotype to 34%. Expressing only the C-tail domain only rescues the phenotype in 17% of the TCs. These results indicate that the first calponin domain, CH1 (present only in Shot-A), is necessary for proper subcellular lumen formation. This notion was reinforced by the observation that *shot* ^{kakp2} in which only Isoform C and D are transcribed, displays the same defects in subcellular lumen formation observed in the null allele. Accordingly, it has been shown in neuronal cells that the calponin domain, present in Shot-A is necessary for the proper linkage between actin and MTs network and for the correct neuronal morphogenesis (Bottenberg et al., 2009; Sanchez-Soriano et al., 2009). In contrast, structure-function analyses in developing trachea demonstrated the first calponin domain to be dispensable, although it was required in the absence of the MT binding domains (Lee and Kolodziej, 2002a). In particular, Lee and Kolodziej suggested that in tracheal fusion cells, the binding sites for actin and MTs appear to be functionally redundant; the actin binding domain is essential when the microtubule binding site is absent, and the microtubule binding site is essential when the F-actin binding site is absent. So, according to our observations the role of Shot in TCs resembles more its function in neuronal cells than its function in tracheal fusion cells.

The geometry of the TCs can be compared, in some aspects, with neuronal ones; there is an actin- rich peripheral zone, a MT-rich central zone and the area in which MTs and F-actin prominently overlap. The peripheral actin-rich zone includes finger-like filopodia, that sense external cue and influences MT behaviours during cell extension. MTs are the essential implementers for cell extension, whereas F-actin is required for the directionality of the extension.

So, we propose that in TCs the spectraplakin Shot, like in neuronal cells could play distinct roles (**Fig. 61**). Shot with its complete N-terminal and C-terminal domains (Isoform A) could be involved in **actin-MTs crosstalk** and a process necessary for the correct cell elongation and subcellular lumen formation. Accordingly, Shot co-localizes with the area where MTs and the actin overlap between st. 14 and st. 15 when the most prominent cell elongation and subcellular lumen formation happen. Later on, Shot maintains its accumulation on stable MTs around the subcellular lumen and here the C-

tail (present in all isoforms) could be involved in **sustaining** and re-organizing **MT stabilization** and in turn maintaining the integrity of the subcellular lumen.

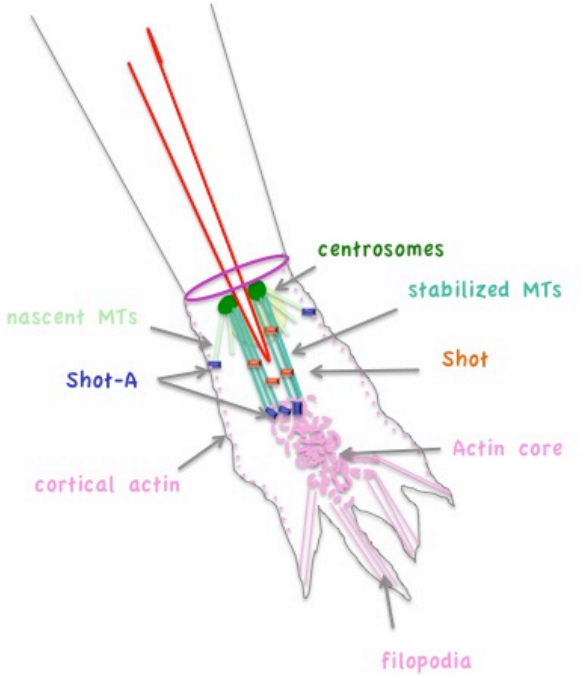

Figure 61. Involvement of Shot during TC development. Different populations of Shot act differentially during subcellular lumen formation and cell elongation. Shot can interact with the actin core at the tip of the cell and with cortical actin through its calponin domain. With its C-terminal domain it interacts with the MT network allowing the crosstalk between actin and MTs and so encouraging cell elongation and subcellular lumen formation. (Shot A). Another population of Shot is involved in maintaining the MT network and stabilizing the integrity of the subcellular luminal structure.

5.12 Does Tau function overlap with Shot in the TCs?

It has been suggested that spectraplakins might **functionally overlap** with structural MAPs. For example, the functional overlap between Shot and Tau in MT stabilization has been shown in flies (Voelzmann et al., 2016). Moreover, it has been proposed that a loss of MAP function in mammals has a relatively mild phenotype due to a functional compensation through spectroplakins (Morris et al., 2011; Riederer, 2007).

Our data from overexpression experiments suggests that also in the context of subcellular lumen formation the effect of these two proteins can overlap. When we tested the tracheal overexpression of *tau* in *wt* background, we observed extra subcellular lumen with morphology very similar to one caused by the overexpression of

Shot. In this scenario, Tau similarly to the spectraplakin could induce **an overstabilization of MTs** and in turn the generation of the phenotype. Surprisingly, the overexpression of *tau* is also able to rescue the *shot* loss of function phenotype similarly to the overexpression of Shot-A. We propose that the rescue capacity of Tau does not depend only on its classical activity in MT stabilization, since Shot-C and the C-tail over-expression are not able to restore the subcellular lumen formation. The MT binding capacity of Tau is probably just one of its functions. In fact, recently a new function of Tau in signalling and cytoskeletal organization has emerged (Morris et al., 2011). For example Elie and co-workers propose a new role for tau **in co-organizing dynamic MTs and actin network** (Elie et al., 2015). So, Tau and Shot could overlap not just on their ability to bind and stabilize MTs but also in connecting different cytoskeletal component and co-organizing them.

6 CONCLUSIONS

6 CONCLUSIONS

1) Rca1 has a post-mitotic effect/function during subcellular lumen formation and this effect is autonomous in the tracheal system.

2) The intracellular components involved in subcellular lumen formation of the TC, as the apical membrane and the asymmetric actin accumulation, are duplicated in Rca1 mutant TCs.

3) Rca1 and CycA have the same subcellular lumen branching phenotype and both are a consequence of centrosome amplification

4) Other mutant conditions characterized by centrosome amplification like *slmb* and *SAKOE*, display extra TC subcellular lumen branching.

5) In conditions of centrosome number reduction, as in *sas4* mutant, TCs lose the ability to generate a bonafide subcellular lumen.

6) In *wt* condition a pair of centrosomes are localized next to the cell-cell junction between the TC and the stalk cell. An increase in number of these centrosomes is associated with the formation of extra subcellular lumen and a decrease in the number of these centrosomes is associated with the lack of subcellular lumen.

7) MTs in TCs emanate and grow from centrosomes where γ-tubulin localizes, defining centrosomes as MTOC.

8) Shot is involved in embryonic TC development and its effect is autonomous in the tracheal system.

9) The overexpression of *shot* in the tracheal system induces extra-branching of the TCs and this effect does not depend by centrosome amplification but is probably caused by its function in stabilize/polymerize MTs.

10) The absence of *shot*, induces in the defective TCs in the overall cytoskeletal organization and consequently in cell elongation and subcellular lumen formation.

11) The complete actin-binding-domain (ABD) involved in the crosstalk between actin and MTs is needed for a proper subcellular lumen formation, but not for extra subcellular branching.

12) Shot physically interacts with stable MTs around and ahead of the subcellular lumen and with the Moe/Actin at the tip of the terminal cell, during the time of cell elongation and subcellular lumen formation, possibly mediating the crosstalk between the two cytoskeletal components. Later on, Shot interacts mainly with stable MTs around the subcellular lumen probably stabilizing this structure.

13) The overexpression of the Microtubule Associated Protein (MAP) Tau in the tracheal system induces extra subcellular lumen phenotype and, at high levels, it is able to rescue the loss of function of *shot,* suggesting a possible molecular overlap with the spectroplakin function.

14) The fact that full-length Shot is necessary to form a de novo subcellular lumen and the ABD domain is not necessary to induce later branching events, suggests that distinct Shot domains have different functions during subcellular lumen formation and branching.

.

7 BIBLIOGRAPHY

7 BIBLIOGRAPHY

Adair, T.H., and J.P. Montani. 2010. *In* Angiogenesis, San Rafael (CA).

Affolter, M., and E. Caussinus. 2008. Tracheal branching morphogenesis in Drosophila: new insights into cell behaviour and organ architecture. *Development*. 135:2055-2064.

Affolter, M., J. Montagne, U. Walldorf, J. Groppe, U. Kloter, M. LaRosa, and W.J. Gehring. 1994. The Drosophila SRF homolog is expressed in a subset of tracheal cells and maps within a genomic region required for tracheal development. *Development*. 120:743-753.

Akhmanova, A., and C.C. Hoogenraad. 2005. Microtubule plus-end-tracking proteins: mechanisms and functions. *Current opinion in cell biology*. 17:47-54.

Akhmanova, A., and C.C. Hoogenraad. 2015. Microtubule minus-end-targeting proteins. *Current biology : CB*. 25:R162-171.

Akhmanova, A., and M.O. Steinmetz. 2015. Control of microtubule organization and dynamics: two ends in the limelight. *Nature reviews. Molecular cell biology*. 16:711-726.

Alves-Silva, J., I. Hahn, O. Huber, M. Mende, A. Reissaus, and A. Prokop. 2008. Prominent actin fiber arrays in Drosophila tendon cells represent architectural elements different from stress fibers. *Molecular biology of the cell*. 19:4287-4297.

Alves-Silva, J., N. Sanchez-Soriano, R. Beaven, M. Klein, J. Parkin, T.H. Millard, H.J. Bellen, K.J. Venken, C. Ballestrem, R.A. Kammerer, and A. Prokop. 2012. Spectraplakins promote microtubule-mediated axonal growth by functioning as structural microtubule-associated proteins and EB1-dependent +TIPs (tip interacting proteins). *The Journal of neuroscience : the official journal of the Society for Neuroscience*. 32:9143-9158.

Applewhite, D.A., K.D. Grode, M.C. Duncan, and S.L. Rogers. 2013. The actin-microtubule cross-linking activity of Drosophila Short stop is regulated by intramolecular inhibition. *Molecular biology of the cell*. 24:2885-2893.

Araujo, S.J., and J. Casanova. 2011. Sequoia establishes tip-cell number in Drosophila trachea by regulating FGF levels. *Journal of cell science*. 124:2335-2340.

Bar, T., F.H. Guldner, and J.R. Wolff. 1984. "Seamless" endothelial cells of blood capillaries. *Cell and tissue research*. 235:99-106.

Bartolini, F., and G.G. Gundersen. 2006. Generation of noncentrosomal microtubule arrays. *Journal of cell science*. 119:4155-4163.

Basto, R., J. Lau, T. Vinogradova, A. Gardiol, C.G. Woods, A. Khodjakov, and J.W. Raff. 2006. Flies without centrioles. *Cell*. 125:1375-1386.

Begg, G.E., S.L. Harper, M.B. Morris, and D.W. Speicher. 2000. Initiation of spectrin dimerization involves complementary electrostatic interactions between paired triple-helical bundles. *The Journal of biological chemistry*. 275:3279-3287.

7 BIBLIOGRAPHY

Bettencourt-Dias, M., A. Rodrigues-Martins, L. Carpenter, M. Riparbelli, L. Lehmann, M.K. Gatt, N. Carmo, F. Balloux, G. Callaini, and D.M. Glover. 2005. SAK/PLK4 is required for centriole duplication and flagella development. *Current biology : CB*. 15:2199-2207.

Blachon, S., J. Gopalakrishnan, Y. Omori, A. Polyanovsky, A. Church, D. Nicastro, J. Malicki, and T. Avidor-Reiss. 2008. Drosophila asterless and vertebrate Cep152 Are orthologs essential for centriole duplication. *Genetics*. 180:2081-2094.

Blanchoin, L., R. Boujemaa-Paterski, C. Sykes, and J. Plastino. 2014. Actin dynamics, architecture, and mechanics in cell motility. *Physiological reviews*. 94:235-263.

Booth, A.J., G.B. Blanchard, R.J. Adams, and K. Roper. 2014. A dynamic microtubule cytoskeleton directs medial actomyosin function during tube formation. *Developmental cell*. 29:562-576.

Bornens, M. 2012. The centrosome in cells and organisms. *Science*. 335:422-426.

Bottenberg, W., N. Sanchez-Soriano, J. Alves-Silva, I. Hahn, M. Mende, and A. Prokop. 2009. Context-specific requirements of functional domains of the Spectraplakin Short stop in vivo. *Mechanisms of development*. 126:489-502.

Brand, A.H., and N. Perrimon. 1993. Targeted gene expression as a means of altering cell fates and generating dominant phenotypes. *Development*. 118:401-415.

Bratman, S.V., and F. Chang. 2008. Mechanisms for maintaining microtubule bundles. *Trends in cell biology*. 18:580-586.

Brinkley, B.R. 1985. Microtubule organizing centers. *Annual review of cell biology*. 1:145-172.

Broadie, K., S. Baumgartner, and A. Prokop. 2011. Extracellular matrix and its receptors in Drosophila neural development. *Developmental neurobiology*. 71:1102-1130.

Brodu, V., A.D. Baffet, P.M. Le Droguen, J. Casanova, and A. Guichet. 2010. A developmentally regulated two-step process generates a noncentrosomal microtubule network in Drosophila tracheal cells. *Developmental cell*. 18:790-801.

Buechner, M. 2002. Tubes and the single C. elegans excretory cell. *Trends in cell biology*. 12:479-484.

Buti, E., D. Mesquita, and S.J. Araujo. 2014. Hedgehog is a positive regulator of FGF signalling during embryonic tracheal cell migration. *PloS one*. 9:e92682.

Butner, K.A., and M.W. Kirschner. 1991. Tau protein binds to microtubules through a flexible array of distributed weak sites. *The Journal of cell biology*. 115:717-730.

Castle, W.E. 1906. Inbreeding, Cross-Breeding and Sterility in Drosophila. *Science*. 23:153.

Caussinus, E., J. Colombelli, and M. Affolter. 2008. Tip-cell migration controls stalk-cell intercalation during Drosophila tracheal tube elongation. *Current biology : CB*. 18:1727-1734.

Chan, J.Y. 2011. A clinical overview of centrosome amplification in human cancers. *International journal of biological sciences*. 7:1122-1144.

7 BIBLIOGRAPHY

Chen, G., A.K. Rogers, G.P. League, and S.C. Nam. 2011. Genetic interaction of centrosomin and bazooka in apical domain regulation in Drosophila photoreceptor. *PloS one*. 6:e16127.

Chung, S., C. Chavez, and D.J. Andrew. 2011. Trachealess (Trh) regulates all tracheal genes during Drosophila embryogenesis. *Developmental biology*. 360:160-172.

Cooper, G.M. 2000. The Cell - A Molecular Approach 2nd Edition. Sunderland (MA): Sinauer Associates.

Cunha-Ferreira, I., A. Rodrigues-Martins, I. Bento, M. Riparbelli, W. Zhang, E. Laue, G. Callaini, D.M. Glover, and M. Bettencourt-Dias. 2009. The SCF/Slimb ubiquitin ligase limits centrosome amplification through degradation of SAK/PLK4. *Current biology : CB*. 19:43-49.

D'Assoro, A.B., W.L. Lingle, and J.L. Salisbury. 2002. Centrosome amplification and the development of cancer. *Oncogene*. 21:6146-6153.

Davis, G.E., S.M. Black, and K.J. Bayless. 2000. Capillary morphogenesis during human endothelial cell invasion of three-dimensional collagen matrices. *In vitro cellular & developmental biology. Animal*. 36:513-519.

Dawson, I.A., S. Roth, and S. Artavanis-Tsakonas. 1995. The Drosophila cell cycle gene fizzy is required for normal degradation of cyclins A and B during mitosis and has homology to the CDC20 gene of Saccharomyces cerevisiae. *The Journal of cell biology*. 129:725-737.

Dehmelt, L., and S. Halpain. 2005. The MAP2/Tau family of microtubule-associated proteins. *Genome biology*. 6:204.

Dong, X., K.H. Zavitz, B.J. Thomas, M. Lin, S. Campbell, and S.L. Zipursky. 1997. Control of G1 in the developing Drosophila eye: rca1 regulates Cyclin A. *Genes & development*. 11:94-105.

Dzafic, E., P.J. Strzyz, M. Wilsch-Brauninger, and C. Norden. 2015. Centriole Amplification in Zebrafish Affects Proliferation and Survival but Not Differentiation of Neural Progenitor Cells. *Cell reports*. 13:168-182.

Elie, A., E. Prezel, C. Guerin, E. Denarier, S. Ramirez-Rios, L. Serre, A. Andrieux, A. Fourest-Lieuvin, L. Blanchoin, and I. Arnal. 2015. Tau co-organizes dynamic microtubule and actin networks. *Scientific reports*. 5:9964.

Erhardt, S., B.G. Mellone, C.M. Betts, W. Zhang, G.H. Karpen, and A.F. Straight. 2008. Genome-wide analysis reveals a cell cycle-dependent mechanism controlling centromere propagation. *The Journal of cell biology*. 183:805-818.

Fletcher, D.A., and R.D. Mullins. 2010. Cell mechanics and the cytoskeleton. *Nature*. 463:485-492.

Fuss, B., F. Josten, M. Feix, and M. Hoch. 2004. Cell movements controlled by the Notch signalling cascade during foregut development in Drosophila. *Development*. 131:1587-1595.

Galjart, N. 2010. Plus-end-tracking proteins and their interactions at microtubule ends. *Current biology : CB*. 20:R528-537.

Gao, F.B., J.E. Brenman, L.Y. Jan, and Y.N. Jan. 1999. Genes regulating dendritic outgrowth, branching, and routing in Drosophila. *Genes & development*. 13:2549-2561.

Gervais, L., and J. Casanova. 2010. In vivo coupling of cell elongation and lumen formation in a single cell. *Current biology : CB*. 20:359-366.

Gervais, L., and J. Casanova. 2011. The Drosophila homologue of SRF acts as a boosting mechanism to sustain FGF-induced terminal branching in the tracheal system. *Development*. 138:1269-1274.

Gervais, L., G. Lebreton, and J. Casanova. 2012. The making of a fusion branch in the Drosophila trachea. *Developmental biology*. 362:187-193.

Godinho, S.A., R. Picone, M. Burute, R. Dagher, Y. Su, C.T. Leung, K. Polyak, J.S. Brugge, M. Thery, and D. Pellman. 2014. Oncogene-like induction of cellular invasion from centrosome amplification. *Nature*. 510:167-171.

Goshima, G., and R.D. Vale. 2003. The roles of microtubule-based motor proteins in mitosis: comprehensive RNAi analysis in the Drosophila S2 cell line. *The Journal of cell biology*. 162:1003-1016.

Grosskortenhaus, R., and F. Sprenger. 2002. Rca1 inhibits APC-Cdh1(Fzr) and is required to prevent cyclin degradation in G2. *Developmental cell*. 2:29-40.

Guillemin, K., J. Groppe, K. Ducker, R. Treisman, E. Hafen, M. Affolter, and M.A. Krasnow. 1996. The pruned gene encodes the Drosophila serum response factor and regulates cytoplasmic outgrowth during terminal branching of the tracheal system. *Development*. 122:1353-1362.

Hahn, I., M. Ronshaugen, N. Sanchez-Soriano, and A. Prokop. 2016. Functional and Genetic Analysis of Spectraplakins in Drosophila. *Methods in enzymology*. 569:373-405.

Hammond, J.W., D. Cai, and K.J. Verhey. 2008. Tubulin modifications and their cellular functions. *Current opinion in cell biology*. 20:71-76.

Harrison, M.K., A.M. Adon, and H.I. Saavedra. 2011. The G1 phase Cdks regulate the centrosome cycle and mediate oncogene-dependent centrosome amplification. *Cell division*. 6:2.

Huelsmann, S., and N.H. Brown. 2014. Spectraplakins. *Current biology : CB*. 24:R307-308.

Inaba, M., Z.G. Venkei, and Y.M. Yamashita. 2015. The polarity protein Baz forms a platform for the centrosome orientation during asymmetric stem cell division in the Drosophila male germline. *eLife*. 4.

Iruela-Arispe, M.L., and G.J. Beitel. 2013. Tubulogenesis. *Development*. 140:2851-2855.

JayaNandanan, N., R. Mathew, and M. Leptin. 2014. Guidance of subcellular tubulogenesis by actin under the control of a synaptotagmin-like protein and Moesin. *Nature communications*. 5:3036.

Jefferson, J.J., C.L. Leung, and R.K. Liem. 2004. Plakins: goliaths that link cell junctions and the cytoskeleton. *Nature reviews. Molecular cell biology*. 5:542-553.

Kadavath, H., R.V. Hofele, J. Biernat, S. Kumar, K. Tepper, H. Urlaub, E. Mandelkow, and M. Zweckstetter. 2015. Tau stabilizes microtubules by binding at the interface between tubulin heterodimers. *Proceedings of the National Academy of Sciences of the United States of America*. 112:7501-7506.

Kamei, M., W.B. Saunders, K.J. Bayless, L. Dye, G.E. Davis, and B.M. Weinstein. 2006. Endothelial tubes assemble from intracellular vacuoles in vivo. *Nature*. 442:453-456.

Kapitein, L.C., and C.C. Hoogenraad. 2015. Building the Neuronal Microtubule Cytoskeleton. *Neuron*. 87:492-506.

Karakesisoglou, I., Y. Yang, and E. Fuchs. 2000. An epidermal plakin that integrates actin and microtubule networks at cellular junctions. *The Journal of cell biology*. 149:195-208.

Kerman, B.E., A.M. Cheshire, and D.J. Andrew. 2006. From fate to function: the Drosophila trachea and salivary gland as models for tubulogenesis. *Differentiation; research in biological diversity*. 74:326-348.

Khanal, I., A. Elbediwy, C. Diaz de la Loza Mdel, G.C. Fletcher, and B.J. Thompson. 2016. Shot and Patronin polarise microtubules to direct membrane traffic and biogenesis of microvilli in epithelia. *Journal of cell science*. 129:2651-2659.

Kulukian, A., A.J. Holland, B. Vitre, S. Naik, D.W. Cleveland, and E. Fuchs. 2015. Epidermal development, growth control, and homeostasis in the face of centrosome amplification. *Proceedings of the National Academy of Sciences of the United States of America*. 112:E6311-6320.

Lacey, K.R., P.K. Jackson, and T. Stearns. 1999. Cyclin-dependent kinase control of centrosome duplication. *Proceedings of the National Academy of Sciences of the United States of America*. 96:2817-2822.

Lampugnani, M.G., A. Zanetti, F. Breviario, G. Balconi, F. Orsenigo, M. Corada, R. Spagnuolo, M. Betson, V. Braga, and E. Dejana. 2002. VE-cadherin regulates endothelial actin activating Rac and increasing membrane association of Tiam. *Molecular biology of the cell*. 13:1175-1189.

Le Droguen, P.M., S. Claret, A. Guichet, and V. Brodu. 2015. Microtubule-dependent apical restriction of recycling endosomes sustains adherens junctions during morphogenesis of the Drosophila tracheal system. *Development*. 142:363-374.

Lebrand, C., E.W. Dent, G.A. Strasser, L.M. Lanier, M. Krause, T.M. Svitkina, G.G. Borisy, and F.B. Gertler. 2004. Critical role of Ena/VASP proteins for filopodia formation in neurons and in function downstream of netrin-1. *Neuron*. 42:37-49.

Lee, M., S. Lee, A.D. Zadeh, and P.A. Kolodziej. 2003. Distinct sites in E-cadherin regulate different steps in Drosophila tracheal tube fusion. *Development*. 130:5989-5999.

Lee, S., K.L. Harris, P.M. Whitington, and P.A. Kolodziej. 2000. short stop is allelic to kakapo, and encodes rod-like cytoskeletal-associated proteins required for axon extension. *The Journal of neuroscience : the official journal of the Society for Neuroscience*. 20:1096-1108.

Lee, S., and P.A. Kolodziej. 2002a. The plakin Short Stop and the RhoA GTPase are required for E-cadherin-dependent apical surface remodeling during tracheal tube fusion. *Development*. 129:1509-1520.

Lee, S., and P.A. Kolodziej. 2002b. Short Stop provides an essential link between F-actin and microtubules during axon extension. *Development*. 129:1195-1204.

Lee, S., M. Nahm, M. Lee, M. Kwon, E. Kim, A.D. Zadeh, H. Cao, H.J. Kim, Z.H. Lee, S.B. Oh, J. Yim, P.A. Kolodziej, and S. Lee. 2007. The F-actin-microtubule crosslinker Shot is a platform for Krasavietz-mediated translational regulation of midline axon repulsion. *Development*. 134:1767-1777.

Lee, T., A. Lee, and L. Luo. 1999. Development of the Drosophila mushroom bodies: sequential generation of three distinct types of neurons from a neuroblast. *Development*. 126:4065-4076.

Leidel, S., and P. Gonczy. 2003. SAS-4 is essential for centrosome duplication in C elegans and is recruited to daughter centrioles once per cell cycle. *Developmental cell*. 4:431-439.

Leijnse, N., L.B. Oddershede, and P.M. Bendix. 2015. An updated look at actin dynamics in filopodia. *Cytoskeleton*. 72:71-79.

Leung, C.L., D. Sun, M. Zheng, D.R. Knowles, and R.K. Liem. 1999. Microtubule actin cross-linking factor (MACF): a hybrid of dystonin and dystrophin that can interact with the actin and microtubule cytoskeletons. *The Journal of cell biology*. 147:1275-1286.

Lin, T.C., A. Neuner, and E. Schiebel. 2015. Targeting of gamma-tubulin complexes to microtubule organizing centers: conservation and divergence. *Trends in cell biology*. 25:296-307.

Lohr, R., T. Godenschwege, E. Buchner, and A. Prokop. 2002. Compartmentalization of central neurons in Drosophila: a new strategy of mosaic analysis reveals localization of presynaptic sites to specific segments of neurites. *The Journal of neuroscience : the official journal of the Society for Neuroscience*. 22:10357-10367.

Lowery, L.A., and D. Van Vactor. 2009. The trip of the tip: understanding the growth cone machinery. *Nature reviews. Molecular cell biology*. 10:332-343.

Lubarsky, B., and M.A. Krasnow. 2003. Tube morphogenesis: making and shaping biological tubes. *Cell*. 112:19-28.

Luders, J., and T. Stearns. 2007. Microtubule-organizing centres: a re-evaluation. *Nature reviews. Molecular cell biology*. 8:161-167.

Manning, G., and M.A. Krasnow. 1993. Development of the Drosophila tracheal system. 609-685.

Meads, T., and T.A. Schroer. 1995. Polarity and nucleation of microtubules in polarized epithelial cells. *Cell motility and the cytoskeleton*. 32:273-288.

Miralles, F., G. Posern, A.I. Zaromytidou, and R. Treisman. 2003. Actin dynamics control SRF activity by regulation of its coactivator MAL. *Cell*. 113:329-342.

Mogensen, M.M. 1999. Microtubule release and capture in epithelial cells. *Biology of the cell*. 91:331-341.

Morris, M., S. Maeda, K. Vossel, and L. Mucke. 2011. The many faces of tau. *Neuron*. 70:410-426.

Mui, U.N., C.M. Lubczyk, and S.C. Nam. 2011. Role of spectraplakin in Drosophila photoreceptor morphogenesis. *PloS one*. 6:e25965.

Nashchekin, D., A.R. Fernandes, and D. St Johnston. 2016. Patronin/Shot Cortical Foci Assemble the Noncentrosomal Microtubule Array that Specifies the Drosophila Anterior-Posterior Axis. *Developmental cell*. 38:61-72.

Nelson, F.K., P.S. Albert, and D.L. Riddle. 1983. Fine structure of the Caenorhabditis elegans secretory-excretory system. *Journal of ultrastructure research*. 82:156-171.

Nigg, E.A., and T. Stearns. 2011. The centrosome cycle: Centriole biogenesis, duplication and inherent asymmetries. *Nature cell biology*. 13:1154-1160.

Oakley, B.R., V. Paolillo, and Y. Zheng. 2015. gamma-Tubulin complexes in microtubule nucleation and beyond. *Molecular biology of the cell*. 26:2957-2962.

Okenve-Ramos, P., and M. Llimargas. 2014a. Fascin links Btl/FGFR signalling to the actin cytoskeleton during Drosophila tracheal morphogenesis. *Development*. 141:929-939.

Okenve-Ramos, P., and M. Llimargas. 2014b. Fascin, may the Forked be with you. *Fly*. 8:157-164.

Oshima, K., M. Takeda, E. Kuranaga, R. Ueda, T. Aigaki, M. Miura, and S. Hayashi. 2006. IKK epsilon regulates F actin assembly and interacts with Drosophila IAP1 in cellular morphogenesis. *Current biology : CB*. 16:1531-1537.

Peel, N., N.R. Stevens, R. Basto, and J.W. Raff. 2007. Overexpressing centriole-replication proteins in vivo induces centriole overduplication and de novo formation. *Current biology : CB*. 17:834-843.

Pesin, J.A., and T.L. Orr-Weaver. 2008. Regulation of APC/C activators in mitosis and meiosis. *Annual review of cell and developmental biology*. 24:475-499.

Pomies, P., M. Pashmforoush, C. Vegezzi, K.R. Chien, C. Auffray, and M.C. Beckerle. 2007. The cytoskeleton-associated PDZ-LIM protein, ALP, acts on serum response factor activity to regulate muscle differentiation. *Molecular biology of the cell*. 18:1723-1733.

Prokop, A., R. Beaven, Y. Qu, and N. Sanchez-Soriano. 2013. Using fly genetics to dissect the cytoskeletal machinery of neurons during axonal growth and maintenance. *Journal of cell science*. 126:2331-2341.

Prokop, A., S. Bray, E. Harrison, and G.M. Technau. 1998a. Homeotic regulation of segment-specific differences in neuroblast numbers and proliferation in the Drosophila central nervous system. *Mechanisms of development*. 74:99-110.

Prokop, A., M.D. Martin-Bermudo, M. Bate, and N.H. Brown. 1998b. Absence of PS integrins or laminin A affects extracellular adhesion, but not intracellular assembly, of hemiadherens and neuromuscular junctions in Drosophila embryos. *Developmental biology*. 196:58-76.

Prosser, S.L., M.D. Samant, J.E. Baxter, C.G. Morrison, and A.M. Fry. 2012. Oscillation of APC/C activity during cell cycle arrest promotes centrosome amplification. *Journal of cell science*. 125:5353-5368.

Reimann, J.D., E. Freed, J.Y. Hsu, E.R. Kramer, J.M. Peters, and P.K. Jackson. 2001. Emi1 is a mitotic regulator that interacts with Cdc20 and inhibits the anaphase promoting complex. *Cell*. 105:645-655.

Riederer, B.M. 2007. Microtubule-associated protein 1B, a growth-associated and phosphorylated scaffold protein. *Brain research bulletin*. 71:541-558.

Rogers, G.C., N.M. Rusan, D.M. Roberts, M. Peifer, and S.L. Rogers. 2009. The SCF Slimb ubiquitin ligase regulates Plk4/Sak levels to block centriole reduplication. *The Journal of cell biology*. 184:225-239.

Roper, K., S.L. Gregory, and N.H. Brown. 2002. The 'spectraplakins': cytoskeletal giants with characteristics of both spectrin and plakin families. *Journal of cell science*. 115:4215-4225.

Samakovlis, C., G. Manning, P. Steneberg, N. Hacohen, R. Cantera, and M.A. Krasnow. 1996. Genetic control of epithelial tube fusion during Drosophila tracheal development. *Development*. 122:3531-3536.

Samsonov, A., J.Z. Yu, M. Rasenick, and S.V. Popov. 2004. Tau interaction with microtubules in vivo. *Journal of cell science*. 117:6129-6141.

Sanchez-Soriano, N., M. Travis, F. Dajas-Bailador, C. Goncalves-Pimentel, A.J. Whitmarsh, and A. Prokop. 2009. Mouse ACF7 and drosophila short stop modulate filopodia formation and microtubule organisation during neuronal growth. *Journal of cell science*. 122:2534-2542.

Sigrist, S., H. Jacobs, R. Stratmann, and C.F. Lehner. 1995. Exit from mitosis is regulated by Drosophila fizzy and the sequential destruction of cyclins A, B and B3. *The EMBO journal*. 14:4827-4838.

Sigurbjornsdottir, S., R. Mathew, and M. Leptin. 2014. Molecular mechanisms of de novo lumen formation. *Nature reviews. Molecular cell biology*. 15:665-676.

Subramanian, A., A. Prokop, M. Yamamoto, K. Sugimura, T. Uemura, J. Betschinger, J.A. Knoblich, and T. Volk. 2003. Shortstop recruits EB1/APC1 and promotes microtubule assembly at the muscle-tendon junction. *Current biology : CB*. 13:1086-1095.

Subramanian, R., and T.M. Kapoor. 2012. Building complexity: insights into self-organized assembly of microtubule-based architectures. *Developmental cell*. 23:874-885.

Sun, D., C.L. Leung, and R.K. Liem. 2001. Characterization of the microtubule binding domain of microtubule actin crosslinking factor (MACF): identification of a novel group of microtubule associated proteins. *Journal of cell science*. 114:161-172.

Sundaram, M.V., and J.D. Cohen. 2016. Time to make the doughnuts: Building and shaping seamless tubes. *Seminars in cell & developmental biology*.

Suozzi, K.C., X. Wu, and E. Fuchs. 2012. Spectraplakins: master orchestrators of cytoskeletal dynamics. *The Journal of cell biology*. 197:465-475.

Sutherland, D., C. Samakovlis, and M.A. Krasnow. 1996. branchless encodes a Drosophila FGF homolog that controls tracheal cell migration and the pattern of branching. *Cell*. 87:1091-1101.

Vactor, D.V., H. Sink, D. Fambrough, R. Tsoo, and C.S. Goodman. 1993. Genes that control neuromuscular specificity in Drosophila. *Cell*. 73:1137-1153.

Vitre, B., A.J. Holland, A. Kulukian, O. Shoshani, M. Hirai, Y. Wang, M. Maldonado, T. Cho, J. Boubaker, D.A. Swing, L. Tessarollo, S.M. Evans, E. Fuchs, and

D.W. Cleveland. 2015. Chronic centrosome amplification without tumorigenesis. *Proceedings of the National Academy of Sciences of the United States of America*. 112:E6321-6330.

Voelzmann, A., P. Okenve-Ramos, Y. Qu, M. Chojnowska-Monga, M. Del Cano-Espinel, A. Prokop, and N. Sanchez-Soriano. 2016. Tau and spectraplakins promote synapse formation and maintenance through Jun kinase and neuronal trafficking. *eLife*. 5.

Wickstead, B., and K. Gull. 2011. The evolution of the cytoskeleton. *The Journal of cell biology*. 194:513-525.

Wiese, C., and Y. Zheng. 2006. Microtubule nucleation: gamma-tubulin and beyond. *Journal of cell science*. 119:4143-4153.

Wilk, R., I. Weizman, and B.Z. Shilo. 1996. trachealess encodes a bHLH-PAS protein that is an inducer of tracheal cell fates in Drosophila. *Genes & development*. 10:93-102.

Wilson, W.R., and M.P. Hay. 2011. Targeting hypoxia in cancer therapy. *Nature reviews. Cancer*. 11:393-410.

Wojcik, E.J., D.M. Glover, and T.S. Hays. 2000. The SCF ubiquitin ligase protein slimb regulates centrosome duplication in Drosophila. *Current biology : CB*. 10:1131-1134.

Wolf, C., N. Gerlach, and R. Schuh. 2002. Drosophila tracheal system formation involves FGF-dependent cell extensions contacting bridge-cells. *EMBO reports*. 3:563-568.

Yang, Y., J. Dowling, Q.C. Yu, P. Kouklis, D.W. Cleveland, and E. Fuchs. 1996. An essential cytoskeletal linker protein connecting actin microfilaments to intermediate filaments. *Cell*. 86:655-665.

8 APPENDICES

8 APPENDICES

8.1 list of abreviations

Ab	antibody
ABP	Actin Binding Protein
Acet	Acetylated
APC/C	Anaphase-Promoting Complex/Cyclosome
aPKC	atypical Protein kinase C
asl	*asterless*
baz	*bazooka*
bnl	*branchless*
btl	*breathless*
CDK	Cyclin Dependent Kinase
CycA	*Cyclin A*
CycB	*Cyclin B*
DB	Dorsal branch
dsRNAi	double stranded RNA interference
DSRF	*Drosophila Serum Response Factor*
DT	Dorsal Trunk
ena	*enabled*
F actin	Filamentous actin
FGF	Fibroblast Growth Factor
FGFR	Fibroblast Growth Factor Receptor
Fig.	Figure
fzy	*fizzy*
GASP	*Gene Analogous to Small Peritrophins*
GB	Ganglionic Branch
GFP	Green Fluorescent Protein
GRD	Gas2-*related* domain

IF	Intermediated Filaments
LT	Lateral trunk
MAP	Microtubule Associated Protein
MF	Micro Filaments
Moe	Moesin
MT	Microtubules
MTOC	Microtubule organizing center
PCM	Pericentriolar material
PTM	Post transcriptional modification
Rca1	*Regulator of CycA1*
RFP	Red Florescent Protein
SAK	Serine/threonine-protein kinase
SAKND	*SAK* non degradable
sas-4	*spindle assembly abnormal protein 4*
SEM	standard error of the mean
shot	*short stop*
shot-C	*shot(L)C/ shot(L)CGFP*
shot-A	*shot(L)A/ shot(L)AGFP*
slmb	*Slimb*
spas	*spastin*
st	stage
S2 cells	Schneider 2 cells
TC	Terminal cells
trh	*trachealess*
VASP	Vasodilator Stimulated Phosphoprotein
wt	*wild-type*
YFP	Yellow Florescent Protein
β-gal	beta-galactosidase
+TIP	Microtubule *plus-end tracking proteins*

8.2 Summary

The embryonic tracheal system of *Drosophila melanogaster* consists of a network of interconnected epithelial tubes of different size and architecture characterized by different cellular mechanisms of tube formation. The main branches of the *Drosophila* tracheal system have an extracellular lumen because their cells fold to form a tube. However, terminal cells (TCs), specialized cells designed to connect the tracheal system to target tissues, form unicellular branches by generating of a subcellular lumen. This topology of unicellular tubes is a good model to clarify the mechanisms that orchestrate single-cell branching, a process parallel to capillary sprouting in blood vessels. During tracheal embryonic development, TCs produce seamless tubes, generating a cytoplasmic extension, by cell elongation, and a concurrent intracellular luminal space surrounded by an apical membrane. Cell elongation and subcellular lumen formation are very much dependent on cytoskeleton reorganization.

The main aim of this thesis was to understand new aspects of cytoskeletal modulation that orchestrate subcellular lumen formation. In particular, we have addressed this aim analysing mutants displaying an increase in subcellular lumen branching and mutants characterized by the absence of the subcellular lumen.

We found that mutations in *Regulator of Cyclin A (Rca1)* and *Cyclin A (CycA)* affect subcellular branching, causing TCs to form more than one subcellular lumen. The effect of *Rca1* is post-mitotic in the tracheal system, and depends on an amplification of centrosome number. Other mutant conditions, characterized by the increase of centrosome number, such as *Slimb* (*slmb*) and the overexpression of *SAK* also show excess of subcellular lumen branching. Furthermore, we showed that *de novo* lumen formation is impaired in mutant embryos with low centrosome numbers such as *sas4* and is restored in the double mutant *Rca1; sas4*.

The data presented here define a requirement for the centrosome as a microtubule organizing center (MTOC) for the initiation of subcellular lumen formation. We propose that in *wt* condition two centrosomes are needed to arrange the specific intracellular TC organization necessary to generate a subcellular lumen, and that an excess of centrosome numbers allows for an increase in single- cell branching.

We also analysed the involvement of the spectraplakin Short-stop (Shot) in the cytoskeletal organization of the TCs. Shot is a multifunctional protein involved in many aspects of cytoskeletal organization in different tissues, which can operate as a single

cytoskeleton component as well as coordinating cytoskeletal elements between them. This functional versatility of Shot is probably reflected by the abundant generation of isoforms and by the modulation of its numerous domains.

We found that the overexpression of *shot* in the tracheal system induces extra-branching of the subcellular lumen and this effect depends mainly on the C-tail domain at the C-terminus and its involvement in the stabilization/polimerization of MTs. On the other hand, by examining loss of function alleles, analysing its structural function and visualizing Shot accumulation, we suggest that Shot is not just involved in MT organization in the TC but it also acts as a crosslinker between MTs and the actin network. The first calponin domain (CH1) of the acting binding domain (ABD) at the N-terminal is involved in this cross-linking activity.

Finally, we provide some data indicating a functional overlap between the spectraplakin and the microtubule associated protein (MAP) Tau during subcellular lumen formation.

8.3 Resumen en castellano

Las células terminales (TCs) de la tráquea del embrión de *Drosophila melanogaster* son capaces de generar un lumen subcelular y son utilizadas como modelo para la formación de tubos unicelulares de tipo "*seamless*". La generación de dicho lumen depende estrictamente de una especifica organización del citoesqueleto que permite la formación de una nueva membrana apical en el interior de la TC. El objetivo del trabajo aquí presentado ha sido lo de aclarar nuevos aspectos de la modulación del citoesqueleto en el contexto de la formación del lumen sub-celular.

Los mutantes de *Regulator of Cyclin A* (*Rca1*) y *CycA* (*Cyclin A*) están caracterizados por TC con mas de un lumen subcelular. El efecto de *Rca1* es post-mitótico y esta causado por un aumento del numero de centrosomas. Reportamos, atraves el estudio de *Rca1* y otros mutantes afectados en el numero de centrosomas, una estricta asociación entre centrosomas y formación del lumen sub-celular.

Nuestros datos revelan, por primer vez, la función de los centrosomas como centros de organización de microtubulos (MTOC) en la TC y que un exceso de centrosomas puede causar un aumento en la capacidad de ramificación del lumen.

En este trabajo también hemos analizado la función de la spectraplakina Short-stop (Shot). A través de experimentos de sobre-expresión y falta de función de *shot*, integrados con estudios estructura-función y de localización de sus productos proteicos hemos concluido que la spectraplakina actúa el la TC acudiendo a diferentes grados de organización citosqueletrica; en nuestro modelo Shot es capaz de promover la estabilización/polymerizacion de microtubulos, y un exceso de esta función puede causar extra ramificación en la TC. Por otro lado, Shot esta implicado en la correcta conexión entre la red de microtubulos y la actina y su falta influye negativamente la formación del lumen sub-celular. También reportamos datos preliminares que indican una superposición funcional entre Shot y la proteína asociada a microtulos (MAP) Tau durante el desarrollo del la TC.

8.4 Papers published

The following published paper is attached:

Centrosome Amplification Increases Single-Cell Branching in Post-Mitotic Cells.
Delia Ricolo, Myrto Deligiannaki, Jordi Casanova, Sofia Araúo.
Current Biology 26 (20), 2805-2813..

Report

Current Biology

Centrosome Amplification Increases Single-Cell Branching in Post-mitotic Cells

Graphical Abstract

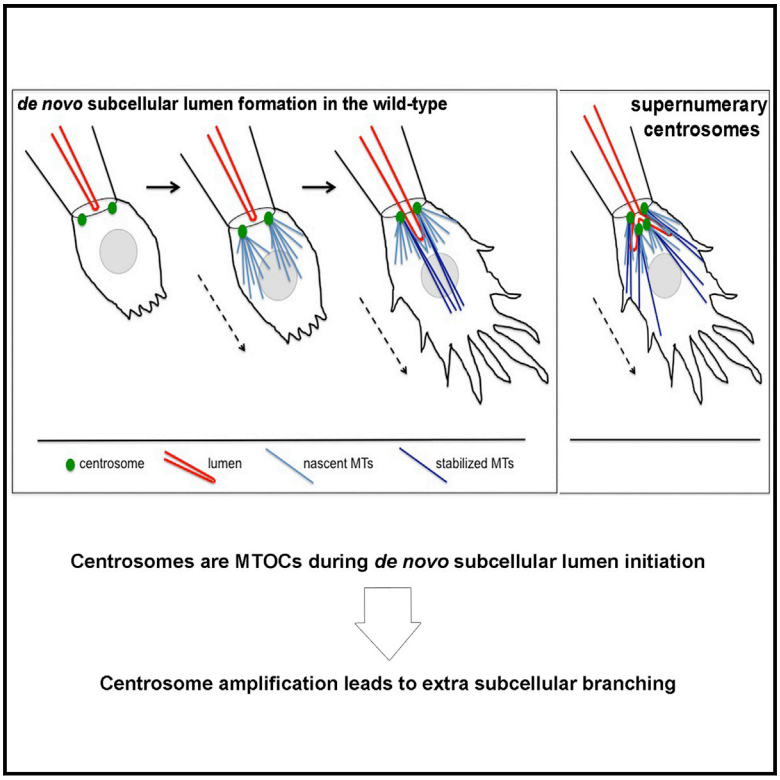

Authors

Delia Ricolo, Myrto Deligiannaki, Jordi Casanova, Sofia J. Araújo

Correspondence

sarbmc@ibmb.csic.es

In Brief

Centrosome function in differentiated cells is not well understood. Ricolo et al. show that post-mitotic tracheal cells with supernumerary centrosomes grow extra subcellular lumina and that de novo lumen formation is impaired in cells with less centrioles. Cellular analysis reveals that centrosomes are MTOCs during subcellular lumen formation.

Highlights

- *Rca1* mutant cells have supernumerary centrosomes
- Centrosome amplification leads to extra subcellular branching
- De novo lumen formation is impaired in cells with less centrioles
- Centrosomes are MTOCs during subcellular lumen initiation

Ricolo et al., 2016, Current Biology *26*, 2805–2813
October 24, 2016
http://dx.doi.org/10.1016/j.cub.2016.08.020

Current Biology
Report

Centrosome Amplification Increases Single-Cell Branching in Post-mitotic Cells

Delia Ricolo,[1,2] Myrto Deligiannaki,[1,3] Jordi Casanova,[1,2] and Sofia J. Araújo[1,2,4,*]
[1]Institut de Biologia Molecular de Barcelona (IBMB-CSIC), Parc Cientific de Barcelona, Carrer de Baldiri Reixac 10, 08028 Barcelona, Spain
[2]Institute for Research in Biomedicine (IRB Barcelona), The Barcelona Institute of Science and Technology, Carrer de Baldiri Reixac 10, 08028 Barcelona, Spain
[3]Present address: Gene Center, Department of Biochemistry, Center of Protein Science CIPSM, Ludwig-Maximilians University, Feodor-Lynen- Straße 25, Munich 81377, Germany
[4]Lead Contact
*Correspondence: sarbmc@ibmb.csic.es
http://dx.doi.org/10.1016/j.cub.2016.08.020

SUMMARY

Centrosome amplification is a hallmark of cancer, although we are still far from understanding how this process affects tumorigenesis [1, 2]. Besides the contribution of supernumerary centrosomes to mitotic defects, their biological effects in the post-mitotic cell are not well known. Here, we exploit the effects of centrosome amplification in post-mitotic cells during single-cell branching. We show that *Drosophila* tracheal cells with extra centrosomes branch more than wild-type cells. We found that mutations in *Rca1* and *CycA* affect subcellular branching, causing tracheal tip cells to form more than one subcellular lumen. We show that *Rca1* and *CycA* post-mitotic cells have supernumerary centrosomes and that other mutant conditions that increase centrosome number also show excess of subcellular lumen branching. Furthermore, we show that de novo lumen formation is impaired in mutant embryos with fewer centrioles. The data presented here define a requirement for the centrosome as a microtubule-organizing center (MTOC) for the initiation of subcellular lumen formation. We propose that centrosomes are necessary to drive subcellular lumen formation. In addition, centrosome amplification increases single-cell branching, a process parallel to capillary sprouting in blood vessels [3]. These results shed new light on how centrosomes can contribute to pathology independently of mitotic defects.

RESULTS

Regulator of cyclin A1 Is Required for the Modulation of Subcellular Branching

In *Drosophila*, tracheal terminal cells (TCs) are formed during embryogenesis, and they branch extensively during larval stages. During embryonic development, they form unicellular branches by generating a cytoplasmic extension and a concurrent lumen in the cytoplasm (Figures 1A and 1B). This so-called intracellular or subcellular lumen [3, 4] arises by de novo growth of an apical membrane toward the inside of the cell, a process that depends on cytoplasmic extension, asymmetric actin accumulation, microtubule (MT) network organization, and vesicle trafficking guided by the cytoskeleton [5–7]. However, the detailed molecular mechanisms by which a seamless lumen forms and multiple subcellular branches are generated inside a single cell are still not well understood. With this purpose, we started by searching for TC lumen bifurcations within a collection of tracheal developmental mutants generated in an ethyl methanesulfonate (EMS) screen. While many of the mutants displayed luminal bifurcations as a result of extra TCs [8], we identified one complementation group (alleles G012 and GA134) where bifurcations arose inside the TCs (Figures 1C and 1D). Mutants belonging to this group failed to complement previously reported *Regulator of cyclin A1* (*Rca1*^{IX} and *Rca1*^{2}) alleles [9, 10]. These mutant alleles and all transheterozygous combinations also showed the same subcellular branching phenotype (Figures 1E and 1F; Figures S1C, S1F, and S1L). *Rca1* is the *Drosophila* homolog of vertebrate Emi1 and a regulator of anaphase-promoting complex/cyclosome (APC/C) activity at various stages of the cell cycle [9, 11]. It shows high and ubiquitous expression during early embryonic development, this high expression becoming restricted to proliferating cells after stage 13 [12]. Rca1 is required for both mitotic and meiotic cell-cycle progression, and *Rca1* mutants are arrested in the G2 phase of embryonic cell-cycle 16, with lower numbers of cells than the wild-type (WT) [12] (see also modENCODE, the Model Organism Encyclopedia of DNA Elements [13]). However, this arrest is not the cause of *Rca1* mutant subcellular branching phenotypes, since other mutant conditions that induce the same cell-cycle arrest, such as *fzy* mutants [14], do not show TC bifurcations (Figure S1H). *Rca1* expression in tracheal cells was sufficient to restore the normal branching pattern autonomously (81%, n = 32; Figures S1J and S1M). Furthermore, *Rca1* knockdown in tracheal cells was enough to generate TC bifurcations (in 47% of embryos, n = 17; Figures 1E and 1F; Figures S1K and S1L). These results indicate that Rca1 in differentiated tracheal TCs serves to regulate subcellular branching events.

Rca1 Mutations Expand the Subcellular Branching Machinery

From early developmental stages, *Rca1* subcellular TC lumen formation followed the reported normal progression (Figures

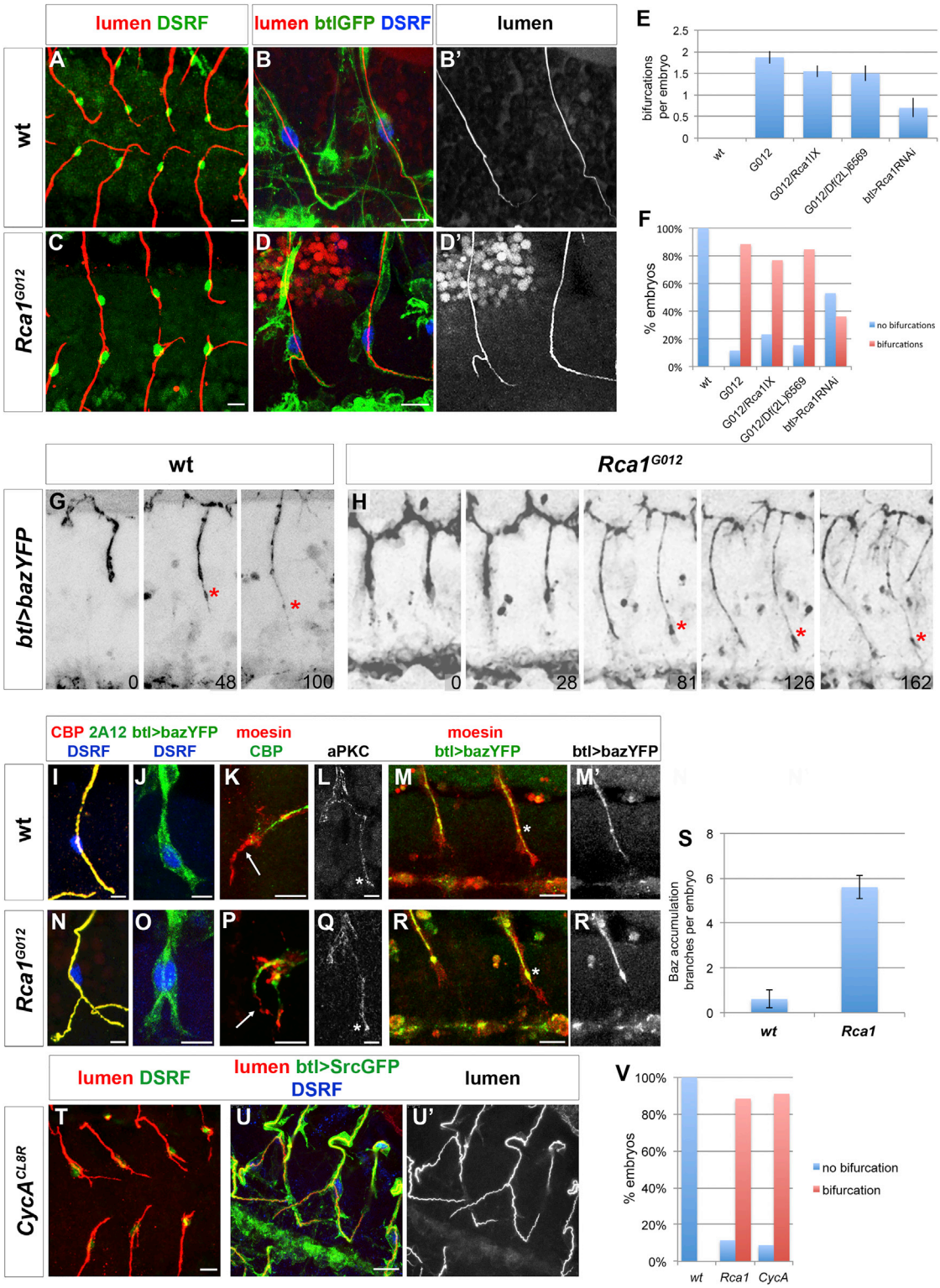

Figure 1. *Rca1* Mutant Embryos Show Tracheal TC Branching Phenotypes

(A–D) Tip of tracheal GBs at embryonic stage 16, displaying the tip and stalk cells and their lumina and stained for lumen (with chitin binding probe [CBP] in red) and breathless (btl)GFP in (B and D) to visualize tracheal cells (green) and Drosophilia serum response factor (DSRF) to show the TC nucleus (green in A and C and blue in B and D). (A and B) WT TCs with a single lumen each. (C and D) *Rca1* mutant TCs showing subcellular lumen bifurcations. Scale bars, 5 μm.

(E) Quantitation of the number of luminal bifurcations per embryo (±SEM) in various allelic combinations of *Rca1* and when *Rca1* is downregulated in tracheal cells by RNAi.

(legend continued on next page)

1G and 1H) [5]. However, it was also apparent early on that these events were duplicated within the cytoplasm (Figure 1H; Movie S1) an observation corroborated by further characterization, using various cell markers. *Rca1* mutant TCs that showed excess subcellular branching extended cytoplasmic protrusions and grew a new apical membrane and subcellular chitin lumen accordingly (Figures 1H–1J, 1N, and 1O).

To visualize the dynamics of subcellular apical membrane formation in living embryos, we used a Bazooka (Baz)/Par3-YFP (yellow fluorescent protein) construct driven by a trachea-specific line. As previously reported for dorsal branch (DB) TCs [5], subcellular lumen formation in the WT ganglionic branch (GB) TCs appeared as a continuous process of sprouting from the apical side of the TC (Figure 1G; Movies S1 and S2). In these WT TCs, new membrane was added to the lumen of the principal network at the junction and continued in the direction of cell elongation (Figure 1G; Movie S1). In *Rca1* mutant TCs, this membrane addition started as a double lumen from the apical junction and continued to extend as two lumina as the TC extended (Figure 1H; Movie S1). Each of the extending cytoplasmatic protrusions accumulated actin asymetrically at the tip, as detected by moesin, an F-actin-binding protein (Figures 1K and 1P). Interestingly, detailed analysis of *Rca1* mutant TCs for constituents of the atypical protein kinase C (aPKC)/Par6/Baz at early seamless lumen growth stages indicated that these components accumulate apically at higher levels than in WT TCs (Figures 1L, 1M, and 1Q–1S).

CycA Mutations Induce Similar Subcellular Branching Phenotypes to *Rca1*

Rca1 positively regulates cyclin A (CycA) levels by inhibiting APC/C activity [9, 12]. In *Rca1* mutants, CycA is degraded through APC/C-dependent proteolysis. We therefore addressed whether the *CycA* null mutant phenotype showed the same subcellular branching phenotypes as *Rca1*. Like *Rca1*, *CycA* mutant TCs displayed luminal bifurcations (Figures 1T–1V). However, they also have cell-cycle phenotypes, lower numbers of tracheal cells [15, 16], and morphogenetic defects [17]. Cyclin B (CycB) was also found to be degraded prematurely in *Rca1* mutants [9]; however, while *CycB* mutants have cell-cycle defects, they did not show subcellular branching phenotypes (Figures S1N–S1P). As previously concluded from the analysis of *fzy* mutants, the CycB results are consistent with the subcellular branching phenotypes present in *Rca1* and *CycA* mutants not being directly attributable to the mitotic arrest in embryonic cell cycles.

Rca1 and *CycA* Mutant Cells Have Supernumerary Centrosomes

What could the function of two so-called mitotic proteins in differentiation be? It is worth mentioning that, in the developing tracheal system, once placodes start invagination, no further cell division occurs. Therefore, the effect of Rca1 and CycA in the regulation of subcellular branching is, most likely, a post-mitotic function/effect of these mitotic proteins.

Subcellular lumen formation depends on a mechanism based on MT network organization [3, 5]. Therefore, we wondered whether (1) *Rca1* and *CycA* mutations affect the MT network and whether (2) changes in the MT network might be responsible for the extra subcellular lumen phenotypes.

Both Rca1 and CycA modulate the activity of APC/C [9, 11, 18–20]. Moreover, oscillation of APC/C activity provides an additional mechanism for coupling the centrosome duplication cycle with replication [18]. The centrosome is the major MT organizing center (MTOC) of cells, and centrosomes play a crucial role in the maintenance of cell polarity and cytoplasmic architecture [21]. Therefore, we asked whether *Rca1* and *CycA* mutants showed aberrant centrosome numbers.

We first quantified centrosome numbers in WT and *Rca1* mutant TCs. We detected an average of 2.3 ± 0.5 centrosomes per TC in the WT (n = 33) and 3.8 ± 0.6 centrosomes per TC in *Rca1* mutants (n = 42) (Figures 2A and 2B). In WT and *Rca1* TCs, centrosomes localized at the apical side of the TC at embryonic stage 14 (72% in WT, n = 33; and 69% in *Rca1*, n = 42) (Figures 4A and 4B). Centrosome number was variable between cells in the same mutant embryo.

Due to the technical difficulties of quantifying centrosome numbers in multicellular tissues and to confirm the results above, we quantified the numbers of centrosomes in *Rca1* and *CycA* mutant cells in culture. To do so, we performed RNAi of both *Rca1* and *CycA* in S2 cells. An increment in centrosome number was detected after either *Rca1* or *CycA* downregulation (Figures 2C and 2D). As controls, we used *slmb* and *SAK/PLK4*, which have been reported to increase and decrease centrosome number, respectively [22–24]. RNAi of *slimb* in the same conditions resulted in a similar increase in the proportion of cells with more than two centrioles, and RNAi of SAK/PLK4 led to a reduction in the number of cells with more than two centrioles (Figures 2C and 2D).

(F) Quantitation of the population of embryos that show luminal bifurcations in various allelic combinations of *Rca1* and when *Rca1* is downregulated in tracheal cells by RNAi. WT, n = 41; $Rca1^{G012}$, n = 52; $Rca1^{G012}/Rca1^{IX}$, n = 56; $Rca1^{G012}/Df(2L)ED6569$, n = 26; *btl>Rca1RNAi*, n = 17. See also Figure S1.

(G and H) Frames from Movie S1, WT (G) and *Rca1* (H) showing several stages of subcellular lumen extension in the WT (G) and *Rca1* mutant (H) GBs. The growing subcellular lumen extends from the cell-cell junction between the tip and stalk cell (indicated by a red asterisk). In the WT, only one subcellular lumen extends from the junction (G), whereas in the mutant, two lumina extend from this point (H). Numbers on the lower right-hand corner are minutes.

(I–R) Analysis of *Rca1* TC characteristics in comparison with WT TCs. (I, J, O, and P) *Rca1* TCs grow lumina that structurally resemble the WT in lumen components such as chitin and Gasp/2A12 (N) or apical membrane markers such as Baz (O). (K and P) Actin accumulates at the tip of the TC, and the subcellular lumina grow in the direction of this actin-rich spot (arrows) both in WT (K) and *Rca1* TCs (P). (L, M, Q, and R) *Rca1* TCs accumulate higher amounts of apical components such as aPKC (Q, asterisk) and Baz (R, asterisk). Scale bars, represent 5 μm.

(S) Quantitation of Baz accumulation at the TC junction per embryo GB in WT (±SEM, n = 5 embryos) and *Rca1* (±SEM, n = 5 embryos). *Rca1* mutant embryos display an average of 5.6 TCs per embryo, with higher Baz accumulation, in contrast to 0.6 TCs in the WT (n = 80 GB TCs).

(T and U) Tip of tracheal GBs at embryonic stage 16 displaying the tip and stalk *CycA* mutant cells stained for lumen (with CBP in red) in (T and U) and *btl>GFP* in (U) to visualize tracheal cells (green) and DSRF to show the TC nucleus (green in T and blue in U). *CycA* mutant TCs show subcellular lumen bifurcations. Scale bars, 5 μm.

(V) Quantitation of the population of embryos that show luminal bifurcations in *Rca1* (n = 52) in comparison with *CycA* mutant embryos (n = 45).

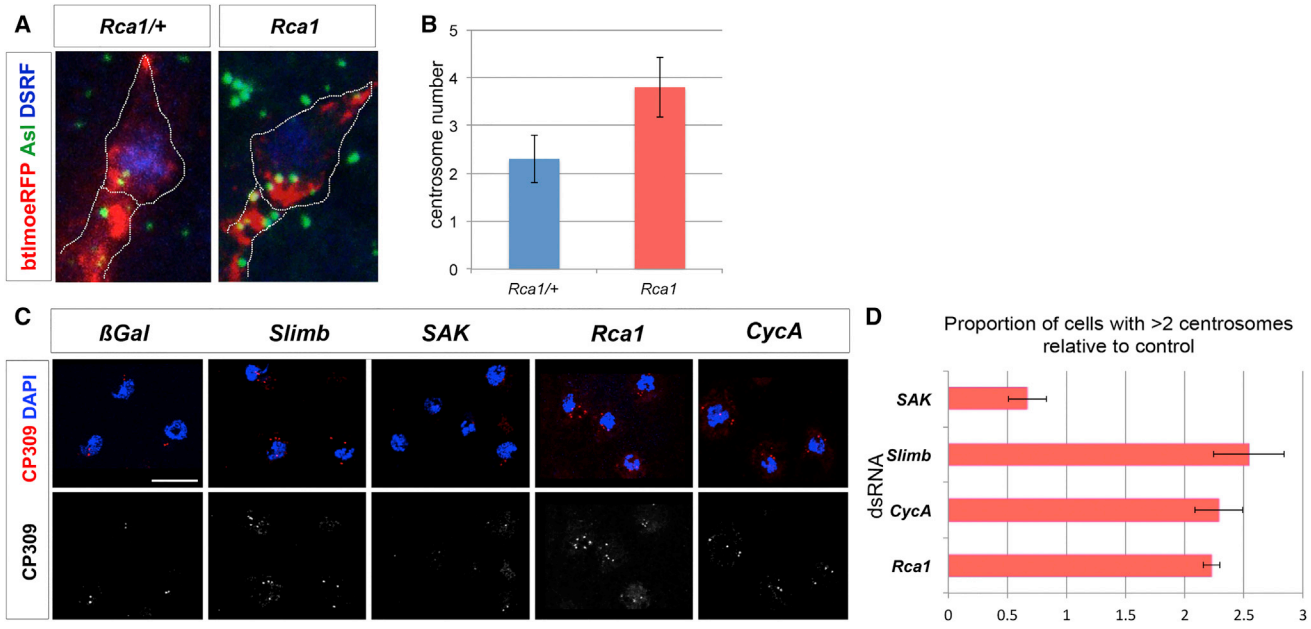

Figure 2. Centriole Amplification in *Rca1* and *CycA* Mutant Cells

(A and B) Centrioles observed in tracheal TCs at the stage of initiation of luminal elongation. (A) *Rca1* heterozygote and homozygote TCs stained for Asl to mark centrioles (green), btl::moeRFP to mark tracheal cells (red), and DSRF to visualize the nucleus of the TC (blue); the white line marks the borders of the TC and the junction of the TC with the stalk cell. Note the higher numbers of centrioles in both *Rca1* mutant tracheal cells and in the surrounding tissues. (B) Quantitation of centrioles in heterozygote (±SEM; n = 33) and mutant *Rca1* (±SEM; n = 42) TCs.

(C and D) Centriole amplification observed after depletion of *Rca1* and *CycA* is at the same level as the one produced by depletion of *slmb*. (C) Cells were treated with double-stranded RNA (dsRNA; indicated) and assayed for centriole numbers. Red indicates CP309, and blue indicates DNA. Scale bar represents 5 μm. (D) Quantitation of supernumerary centrioles after RNAi. Results were normalized relative to controls; ratio is equal to 1 in β-galactosidase (βGal) controls. Data are the average of three RNAi experiments ± SEM (n = 200 cells in each experiment).

Centrosome Amplification Leads to Extra Subcellular Branching

To examine whether the supernumerary centrosomes in *Rca1* and *CycA* mutants might be the cause leading to extra subcellular branching, we asked whether we could get a similar phenotype by changing centrosome numbers by a different mechanism.

We first examined subcellular branching in *slimb* (*slmb*) embryos. Slmb is directly involved in centrosome amplification through the degradation of SAK/Plk4 [23, 25]. In *slmb* loss-of-function conditions, there is a high proportion of cells with more than two centrosomes [23]. The same effect is achieved when a non-degradable form of SAK, SAK-ND, is expressed in *Drosophila* cells [23]. We detected extra subcellular branching in *slmb* tracheal TCs (Figures 3B and 3G; Figures S2B and S2F), thereby corroborating our hypothesis that higher numbers of centrosomes lead to extra subcellular branching events. In addition, we observed extra subcellular branching in TCs expressing SAK-ND (Figures 3C and 3G; Figures S2C and S2F). Of note, although SAK-ND was overexpressed in all tracheal cells by means of a *btl* driver, we detected luminal bifurcations only in the TCs. This result is similar to that obtained by overexpressing SAK-ND only in tracheal TCs (Figures S2D and S2E).

Since branching is physiologically induced upon overactivation of the fibroblast growth factor (FGF) pathway, we also addressed whether centrosome amplification was required in these conditions. However, under conditions of FGF receptor (FGFR) overactivation, we mainly found GB branching as a result of higher numbers of TCs and not as a result of more subcellular lumina generation (Figure S3A). In addition, in all TCs analyzed under conditions of FGFR overactivation (n = 16), we could not detect any supernumerary centrosomes (Figures S3D and S3E). This suggests that subcellular lumen branching upon overactivation of FGFR does not seem to be dependent on centrosome amplification, at least during embryonic stages.

If extra centrosomes lead to luminal bifurcations in tracheal TCs, then a reduction in centrosome number might impair TC subcellular lumen formation. Sas-4 protein is essential for centriole replication in *Drosophila* [26]. *Sas-4* mutants gradually lose centrioles during embryonic development, such that by stages 15–16, centrioles are no longer detected in 50%–80% of cells [26]. According to our hypothesis that centrosomes play a role in subcellular lumen formation, we detected that 88% of *sas*-4 mutants analyzed had defects in TC subcellular lumen generation, quantified as at least one TC without subcellular lumen, despite high variability in the penetrance of the phenotypes (n = 17 embryos; Figure 3E; Figures S2G and S2I–S2L). Indeed, in *sas-4* mutant embryos, we could detect TCs with 0, 1, and 2 centrosomes (Figures S2J–S2L and S2P), and we could correlate the formation of a subcellular TC lumen only with the presence of two centrosomes (n = 29; Figures S2L and S2Q). Furthermore, *sas-4* mutations rescued the *Rca1* bifurcation phenotype (Figures 3F and 3G; Figures S2F, S2H, and S2M–S2O), despite the same variability in centrosome

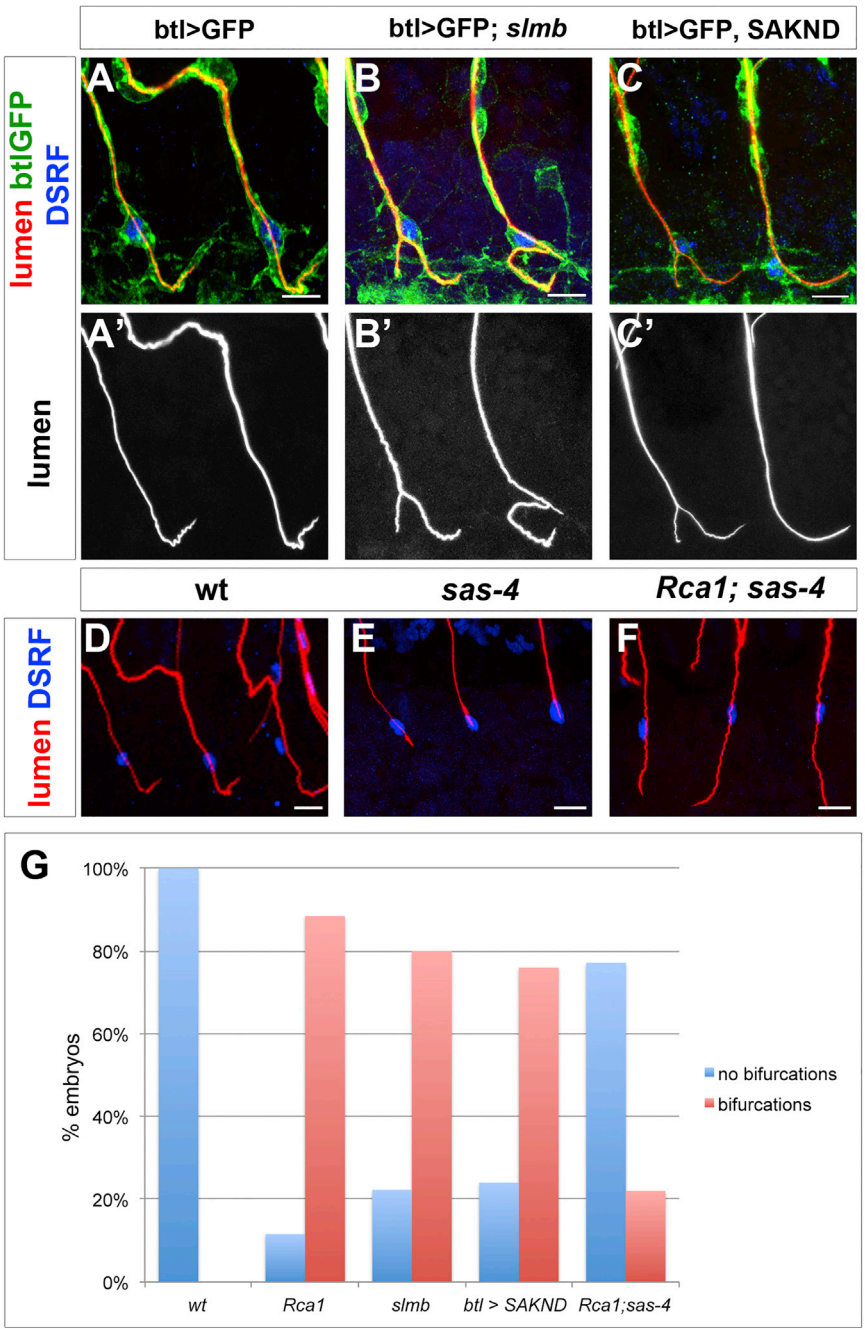

Figure 3. Centriole Numbers Affect Subcellular Lumen Formation

(A–C) Tip of tracheal GBs at embryonic stage 16 displaying the tip and two to three stalk cells and their lumen and stained with GFP to visualize tracheal cells (green), CBP to stain the tracheal chitinous lumen (red), and DSRF to show the TC nucleus (blue). (A) WT TCs with a single lumen each. (B) *slmb* mutant TCs showing subcellular lumen bifurcations. (C) *btl>SAKND*/SAKOE tracheal cells showing one cell with a luminal bifurcation and one WT TC lumen. See also Figure S2.

(D–F) *sas-4* mutant (E) and *Rca1;sas-4* double mutant (F) GB TCs compared to WT (D) TCs; stained with CBP to reveal the tracheal chitinous lumen (red) and DSRF to show the TC nucleus (blue). (E) *sas-4* mutant TCs have defects in subcellular lumen formation in 88% of all GB TCs (n = 19 embryos). (F) *sas-4* removal rescues the luminal bifurcation phenotype of *Rca1* mutant TCs. See also Figure S2.

(G) Quantitation of the population of embryos with bifurcations in the distinct genotypes. WT, n = 41; $Rca1^{G012}$, n = 52; *slmb*, n = 46; *btl>SAKND*, n = 50; $Rca1^{G012}$;*sas-4*, n = 35. See also Figure S2.

number (Figure S2P), suggesting that *sas-4* mutations prevent the generation of supernumerary centrosomes in *Rca1* mutant TCs. Taken together, these data support a direct role for centrosomes in subcellular lumen formation.

Centrosomes Are MTOCs during TC Lumen Initiation

We detected that centrosomes localize apically, near the cell-cell junction, in both WT and *Rca1* mutant TCs (Figures 4A–4F; Figures S4C and S4D; Movie S3). In addition, there is a close relationship between localization of the centrosome pair in the WT and the site of initiation of luminal extension (Figure 4E; Movie S3). In *Rca1* mutant TCs, the supernumerary centrosomes also localize apically in close contact with the extending bifurcated lumina (Figure 4F, inset; Movie S3).

The centrosome is the major MTOC in dividing and many postmitotic differentiated cells. However, in other cell types, MTOC function is reassigned from the centrosome to non-centrosomal sites [27]. In particular, in tracheal multicellular tubes, MT reorganization is coupled to relocalization of the MTOC components from the centrosome to the apical luminal cell domain [28]. We therefore questioned whether TC centrosomes were active as MTOCs. We observed stable acetylated MTs extending from these centrosomes (Figure 4G). In the WT, MT bundles emanate from near the cell-cell apical junction to the periphery of the TC [5]. We detected that these MTs emanate from the centrosomal site (Figure 4G). In *Rca1* TCs, the supranumerary centrosomes were also observed in apical positions, where they associated with MTs (Figure 4H). MTs are nucleated and anchored by the MT nucleator γ-tubulin (γ-tub), which is embedded within the pericentriolar material (PCM) of the centrosome [29]. We found that the apically localized centrosomes of WT and *Rca1* TCs accumulated γ-tub, thereby confirming their role as active MTOCs during subcellular lumen initiation (Figures 4I and 4J). We complemented these results with time-lapse imaging of EB1 and asterless (Asl) in WT TCs (Figure S4E; Movie S4). In a second approach, we used a cold treatment assay, which is reversible and allows the evaluation of both MT disassembly and reassembly [28]. After 6 hr at

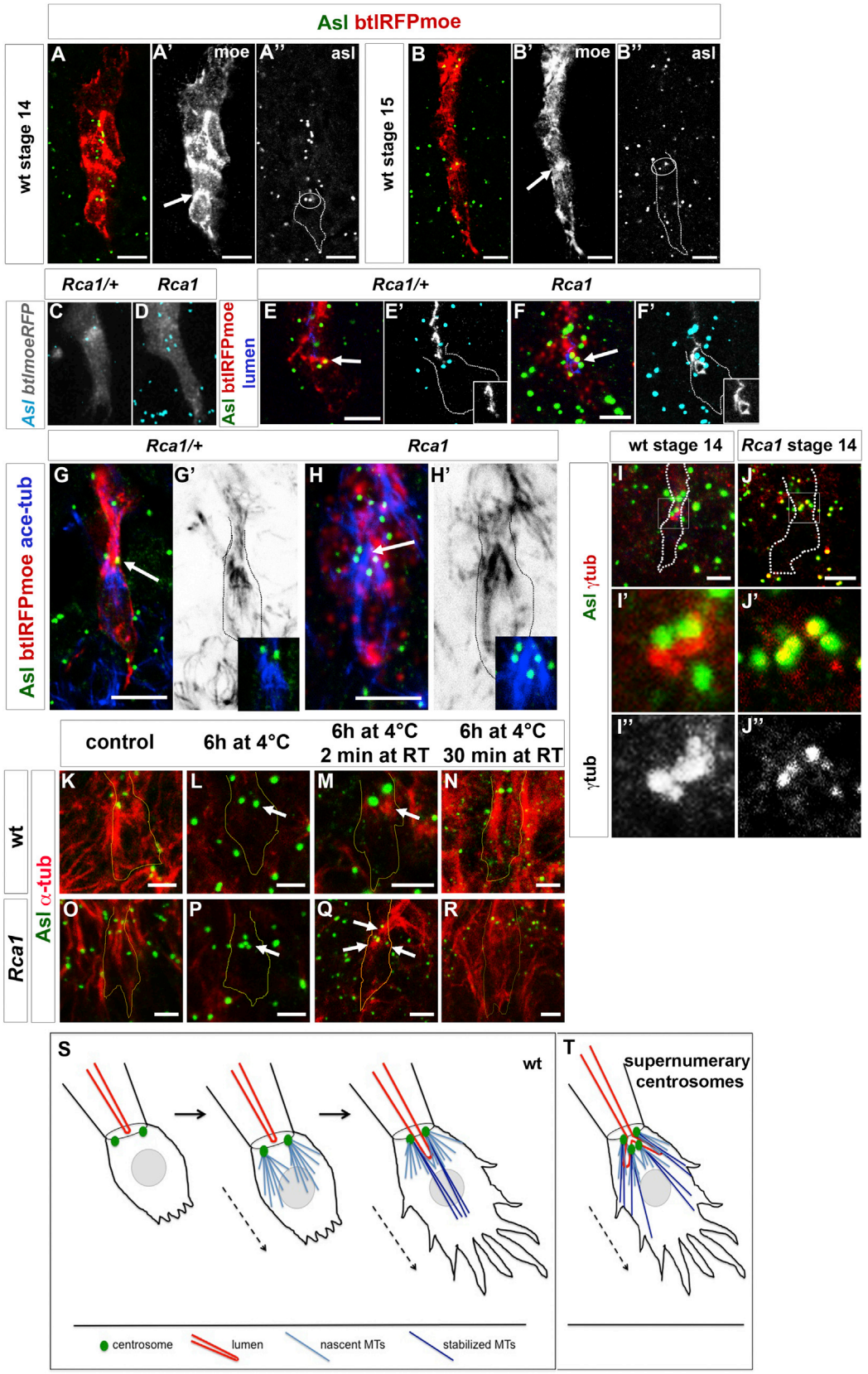

(legend on next page)

4°C, MT fibers are depolymerized in the TCs of WT and *Rca1* mutants (Figures 4L and 4P). Upon recovery for 2 min at room temperature (RT), MTs can be detected at the centrosomal sites (Figures 4M and 4Q). Together, these results suggest that TC centrosomes are active MTOCs during subcellular lumen initiation.

DISCUSSION

Here, we report a new role for the centrosome in cytoskeletal remodeling during subcellular lumen formation. Our findings demonstrate that centrosomes are essential for the formation of tracheal TC subcellular lumina and that centrosome number is a key determinant of the number of subcellular lumina.

The graphical representation of our findings on the involvement of centrosomes in subcellular lumen formation in tracheal TCs is shown in Figures 4S and 4T. In WT TCs, two centrosomes localize apically to the junction of the TC with the stalk cell. There, they become MTOCs and provide the cytoskeletal structure necessary to start forming the ingrowing subcellular lumen (Figure 4S). The MTs that emanate from this centrosome pair grow toward the basolateral membrane (tip) of the TC, forming two tracks through which membrane can be delivered and the new lumen can be built (Figure 4S; Figures S4A and S4B). In TCs with supernumerary centrosomes, extra apically localized MTOCs are active, leading to extra growing MT tracks and the consequent formation of luminal bifurcations (Figure 4T).

We observed higher levels of apical complex proteins such as Baz and aPKC in *Rca1* mutant TCs (Figures 1Q and 1R), and these TCs had supernumerary centrosomes that localized apically (Figures 4D and 4F). Therefore, our data suggest that a higher order complex formed by centrosomes and apical complex proteins is required to achieve the polarization event that triggers subcellular lumen initiation. Accordingly, previous studies have shown a close association between Baz, aPKC, and centrosomal proteins during cytoplasmic polarization events [30–33]. We propose that the structure formed by the centrosome pair, which localizes apically in WT TCs, is necessary for the organized expansion of the apical plasma membrane toward the tip of the cell. This notion is in agreement with our observations that subcellular lumina in cells lacking this centrosome pair do not extend within the TC (Figure 3E; Figure S2J). On the basis of our results and observations reported in cells with similar subcellular lumina, we propose that this model can be generalized to other species such as *C. elegans* [34] and mouse [35].

We show that centrosome amplification in all tracheal cells increases branching of only the TCs. This suggests that centrosomes are particularly important as MTOCs in single-cell de novo lumen formation. The main difference between these and non-centrosomal complex arrangements of MTs, such as those present in *Drosophila* embryonic tracheal cells with non-subcellular lumina [28] or *C. elegans* embryonic intestinal cells [36], is the necessity for symmetry breaking within the cytoplasm, the need for rapid and radical cytoskeletal remodeling, and the generation of new intracellular structures. This is particularly important during periods in which rapid subcellular lumen formation is required, such as rapid organ growth or angiogenesis.

Many studies have noted a positive correlation between centrosome amplification and advanced tumors, recurrence, and poor survival [1, 2]. However, the molecular basis for this has remained elusive. Very few studies have analyzed the consequences of centrosome amplification in vivo in the context of a whole organism. In addition, the results reported were related to cell proliferation and survival and not to the consequences of centrosome amplification in differentiated cells of specific tissues [37–41]. Using cell-culture systems, Godinho and coworkers have recently shown that centrosome amplification promotes cellular invasion, concluding that centrosome amplification can promote features of malignant transformation by altering the cytoskeleton [42]. Here, we report that centrosome amplification increases branching in epithelial cells within

Figure 4. Centrosomes Are MTOCs during the Initiation of Subcellular Lumen Formation

(A and B) Tracheal GBs at embryonic stage 14 (A) and stage 16 (B) showing the tip cells and their lumina and stained with anti-GFP to visualize YFP centrioles (green) and *btl::moeRFP* to mark tracheal cells and the junction (arrow) between the tip and stalk cells (red). The two centrosomes in the TC localize near the junction between tip cell and stalk cell (circles in A'' and B''). *AslYFP* is expressed in all cells in the embryo and not just in the tracheal cells. Images are single confocal scans or projections of only two to three scans to include the whole TC. Scale bars, 5 μm.

(C and D) Live frames showing *Rca1* heterozygous (C) and homozygous (D) embryos carrying constructs expressing Moe in all tracheal cells (*btl::moerfp*) and AslYFP in all cells. (C) *Rca1* heterozygous TC with two centrosomes near the apical cell-cell junction; (D) *Rca1* homozygous TC with four centrosomes localized apically.

(E and F) Progression of early stages of lumen formation in *Rca1* heterozygous (E) and homozygous (F) TCs carrying constructs expressing Moe (stained red), AslYFP (stained green), and stained for chitin to mark the growing lumen in blue. (E' and F') Confocal scans depicting only the lumen in white and centrosomes in cyan to show the relative positions of the centrosomes to the lumen; dotted white line marks the TC borders; insets show only the lumen. Scale bars, 5 μm.

(G and H) Stable MTs in *Rca1* heterozygous (G) and homozygous (H) TCs carrying constructs expressing Moe (stained red), AslYFP (stained green) and stained acetylated MTs in blue. (G' and H') Confocal scans depicting only the MT bundles; dotted black line marks the TC borders; insets show MTs and centrosomes. Scale bars, 5 μm. See also Figure S4.

(I and J) WT (I) and *Rca1* (J) TCs carrying the AslYFP construct and stained for YFP and γ-tub to show whether the apical TC centrosomes are active MTOCs. (I' and J') show higher magnifications of (I and J) depicting how centrosomes colocalize with γ-tub. (I'' and J'') show only γ-tub staining. Note that the centrosome outside the TC does not colocalize with γ-tub in (I'). Scale bars, 5 μm. See also Figure S4.

(K–R) MT depolymerization-repolymerization assay in WT (K–N) and *Rca1* (O–R) mutant embryos. After a 6-hr incubation at 4°C (L and P), MTs are depolymerized (compare K and O with L and P, respectively); after 2 min at room temperature (RT) (M and Q), MTs start regrowing from the centrosome pair in the WT and the four centrosomes in *Rca1*, near the apical junction of the TC; after 30 min at RT (N and R), MTs have fully regrown from the centrosomes. Centrioles are detected by the AslYFP transgene, and MTs are detected by an α-tubulin antibody. Scale bars, 2 μm.

(S) Graphical representation of our findings and the involvement of centrosomes in subcellular lumen formation in WT tracheal TCs. Straight arrows indicate time progression and dotted arrows indicate cell migration.

(T) Graphical representation of our findings and the involvement of centrosomes in subcellular lumen formation in tracheal TCs with supernumerary centrosomes.

a whole living organism. This occurs during a process similar to capillary sprouting of blood vessels during angiogenesis. Therefore, our findings shed more light on the consequences of centrosome amplification in differentiated cell behavior and further strengthen the importance of cytoskeletal regulation during subcellular lumen formation, a process involved in angiogenic sprouting.

SUPPLEMENTAL INFORMATION

Supplemental Information includes Supplemental Experimental Procedures, four figures, and four movies and can be found with this article online at http://dx.doi.org/10.1016/j.cub.2016.08.020.

AUTHOR CONTRIBUTIONS

D.R., M.D., and S.J.A. performed all of the experiments. D.R. and S.J.A. designed the experiments and analyzed the data. J.C. provided expertise and feedback. S.J.A. conceived the study and wrote the paper.

ACKNOWLEDGMENTS

We are grateful to M. Llimargas, V. Brodu, and C. Gonzalez for comments on the manuscript. We thank F. Sprenger, M. Bettencourt-Dias, C. González, and the Bloomington Drosophila Stock Center for fly stocks and reagents. Thanks also go to the IRB-ADMF for assistance and advice with confocal microscopy and software; E. Fuentes, Y. Rivera, and N. Martin for technical assistance; and G. Lebreton and L. Gervais for help and advice during the early stages of this project. S.J.A. is a Ramon y Cajal Researcher (RYC-2007-00417); D.R. is the recipient of an FPU PhD fellowship from the Spanish Ministerio de Educación (FPU12/O5765); M.D. was supported by the Erasmus Programme. This work was supported by the Generalitat de Catalunya and grants from the Spanish Ministerio de Ciencia e Innovación/Ministerio de Economia y Competitividad (BFU2009-07629 and BFU2012-32115). IRB Barcelona is the recipient of a Severo Ochoa Award of Excellence from MINECO (Spanish Government).

Received: April 10, 2016
Revised: July 22, 2016
Accepted: August 3, 2016
Published: September 29, 2016

REFERENCES

1. Chan, J.Y. (2011). A clinical overview of centrosome amplification in human cancers. Int. J. Biol. Sci. *7*, 1122–1144.
2. Godinho, S.A., and Pellman, D. (2014). Causes and consequences of centrosome abnormalities in cancer. Philos. Trans. R. Soc. Lond. B Biol. Sci. *369*, 20130467.
3. Sigurbjörnsdóttir, S., Mathew, R., and Leptin, M. (2014). Molecular mechanisms of de novo lumen formation. Nat. Rev. Mol. Cell Biol. *15*, 665–676.
4. Samakovlis, C., Hacohen, N., Manning, G., Sutherland, D.C., Guillemin, K., and Krasnow, M.A. (1996). Development of the Drosophila tracheal system occurs by a series of morphologically distinct but genetically coupled branching events. Development *122*, 1395–1407.
5. Gervais, L., and Casanova, J. (2010). In vivo coupling of cell elongation and lumen formation in a single cell. Curr. Biol. *20*, 359–366.
6. Schottenfeld-Roames, J., and Ghabrial, A.S. (2012). Whacked and Rab35 polarize dynein-motor-complex-dependent seamless tube growth. Nat. Cell Biol. *14*, 386–393.
7. Schottenfeld-Roames, J., Rosa, J.B., and Ghabrial, A.S. (2014). Seamless tube shape is constrained by endocytosis-dependent regulation of active Moesin. Curr. Biol. *24*, 1756–1764.
8. Araújo, S.J., and Casanova, J. (2011). Sequoia establishes tip-cell number in Drosophila trachea by regulating FGF levels. J. Cell Sci. *124*, 2335–2340.
9. Grosskortenhaus, R., and Sprenger, F. (2002). Rca1 inhibits APC-Cdh1(Fzr) and is required to prevent cyclin degradation in G2. Dev. Cell *2*, 29–40.
10. Tanaka-Matakatsu, M., Thomas, B.J., and Du, W. (2007). Mutation of the Apc1 homologue shattered disrupts normal eye development by disrupting G1 cell cycle arrest and progression through mitosis. Dev. Biol. *309*, 222–235.
11. Reimann, J.D., Freed, E., Hsu, J.Y., Kramer, E.R., Peters, J.M., and Jackson, P.K. (2001). Emi1 is a mitotic regulator that interacts with Cdc20 and inhibits the anaphase promoting complex. Cell *105*, 645–655.
12. Dong, X., Zavitz, K.H., Thomas, B.J., Lin, M., Campbell, S., and Zipursky, S.L. (1997). Control of G1 in the developing Drosophila eye: rca1 regulates Cyclin A. Genes Dev. *11*, 94–105.
13. Celniker, S.E., Dillon, L.A.L., Gerstein, M.B., Gunsalus, K.C., Henikoff, S., Karpen, G.H., Kellis, M., Lai, E.C., Lieb, J.D., MacAlpine, D.M., et al.; modENCODE Consortium (2009). Unlocking the secrets of the genome. Nature *459*, 927–930.
14. Sigrist, S.J., and Lehner, C.F. (1997). Drosophila fizzy-related down-regulates mitotic cyclins and is required for cell proliferation arrest and entry into endocycles. Cell *90*, 671–681.
15. Butí, E., Mesquita, D., and Araújo, S.J. (2014). Hedgehog is a positive regulator of FGF signalling during embryonic tracheal cell migration. PLoS ONE *9*, e92682.
16. Beitel, G.J., and Krasnow, M.A. (2000). Genetic control of epithelial tube size in the Drosophila tracheal system. Development *127*, 3271–3282.
17. Kondo, T., and Hayashi, S. (2013). Mitotic cell rounding accelerates epithelial invagination. Nature *494*, 125–129.
18. Prosser, S.L., Samant, M.D., Baxter, J.E., Morrison, C.G., and Fry, A.M. (2012). Oscillation of APC/C activity during cell cycle arrest promotes centrosome amplification. J. Cell Sci. *125*, 5353–5368.
19. Dienemann, A., and Sprenger, F. (2004). Requirements of cyclin a for mitosis are independent of its subcellular localization. Curr. Biol. *14*, 1117–1123.
20. Erhardt, S., Mellone, B.G., Betts, C.M., Zhang, W., Karpen, G.H., and Straight, A.F. (2008). Genome-wide analysis reveals a cell cycle-dependent mechanism controlling centromere propagation. J. Cell Biol. *183*, 805–818.
21. Bornens, M. (2012). The centrosome in cells and organisms. Science *335*, 422–426.
22. Bettencourt-Dias, M., Rodrigues-Martins, A., Carpenter, L., Riparbelli, M., Lehmann, L., Gatt, M.K., Carmo, N., Balloux, F., Callaini, G., and Glover, D.M. (2005). SAK/PLK4 is required for centriole duplication and flagella development. Curr. Biol. *15*, 2199–2207.
23. Cunha-Ferreira, I., Rodrigues-Martins, A., Bento, I., Riparbelli, M., Zhang, W., Laue, E., Callaini, G., Glover, D.M., and Bettencourt-Dias, M. (2009). The SCF/Slimb ubiquitin ligase limits centrosome amplification through degradation of SAK/PLK4. Curr. Biol. *19*, 43–49.
24. Rogers, G.C., Rusan, N.M., Roberts, D.M., Peifer, M., and Rogers, S.L. (2009). The SCF Slimb ubiquitin ligase regulates Plk4/Sak levels to block centriole reduplication. J. Cell Biol. *184*, 225–239.
25. Wojcik, E.J., Glover, D.M., and Hays, T.S. (2000). The SCF ubiquitin ligase protein slimb regulates centrosome duplication in Drosophila. Curr. Biol. *10*, 1131–1134.
26. Basto, R., Lau, J., Vinogradova, T., Gardiol, A., Woods, C.G., Khodjakov, A., and Raff, J.W. (2006). Flies without centrioles. Cell *125*, 1375–1386.
27. Wiese, C., and Zheng, Y. (2006). Microtubule nucleation: gamma-tubulin and beyond. J. Cell Sci. *119*, 4143–4153.
28. Brodu, V., Baffet, A.D., Le Droguen, P.-M., Casanova, J., and Guichet, A. (2010). A developmentally regulated two-step process generates a non-centrosomal microtubule network in Drosophila tracheal cells. Dev. Cell *18*, 790–801.
29. Lin, T.C., Neuner, A., and Schiebel, E. (2015). Targeting of γ-tubulin complexes to microtubule organizing centers: conservation and divergence. Trends Cell Biol. *25*, 296–307.

30. Chen, G., Rogers, A.K., League, G.P., and Nam, S.-C. (2011). Genetic interaction of centrosomin and bazooka in apical domain regulation in Drosophila photoreceptor. PLoS ONE *6*, e16127.

31. de Anda, F.C., Pollarolo, G., Da Silva, J.S., Camoletto, P.G., Feiguin, F., and Dotti, C.G. (2005). Centrosome localization determines neuronal polarity. Nature *436*, 704–708.

32. Pollarolo, G., Schulz, J.G., Munck, S., and Dotti, C.G. (2011). Cytokinesis remnants define first neuronal asymmetry in vivo. Nat. Neurosci. *14*, 1525–1533.

33. Inaba, M., Venkei, Z.G., and Yamashita, Y.M. (2015). The polarity protein Baz forms a platform for the centrosome orientation during asymmetric stem cell division in the Drosophila male germline. eLife *4*, e04960.

34. Shaye, D.D., and Greenwald, I. (2015). The disease-associated formin INF2/EXC-6 organizes lumen and cell outgrowth during tubulogenesis by regulating F-actin and microtubule cytoskeletons. Dev. Cell *32*, 743–755.

35. Shi, X., Liu, M., Li, D., Wang, J., Aneja, R., and Zhou, J. (2012). Cep70 contributes to angiogenesis by modulating microtubule rearrangement and stimulating cell polarization and migration. Cell Cycle *11*, 1554–1563.

36. Yang, R., and Feldman, J.L. (2015). SPD-2/CEP192 and CDK are limiting for microtubule-organizing center function at the centrosome. Curr. Biol. *25*, 1924–1931.

37. Basto, R., Brunk, K., Vinadogrova, T., Peel, N., Franz, A., Khodjakov, A., and Raff, J.W. (2008). Centrosome amplification can initiate tumorigenesis in flies. Cell *133*, 1032–1042.

38. Dzafic, E., Strzyz, P.J., Wilsch-Bräuninger, M., and Norden, C. (2015). Centriole amplification in zebrafish affects proliferation and survival but not differentiation of neural progenitor cells. Cell Rep. *13*, 168–182.

39. Kulukian, A., Holland, A.J., Vitre, B., Naik, S., Cleveland, D.W., and Fuchs, E. (2015). Epidermal development, growth control, and homeostasis in the face of centrosome amplification. Proc. Natl. Acad. Sci. USA *112*, E6311–E6320.

40. Vitre, B., Holland, A.J., Kulukian, A., Shoshani, O., Hirai, M., Wang, Y., Maldonado, M., Cho, T., Boubaker, J., Swing, D.A., et al. (2015). Chronic centrosome amplification without tumorigenesis. Proc. Natl. Acad. Sci. USA *112*, E6321–E6330.

41. Marthiens, V., Rujano, M.A., Pennetier, C., Tessier, S., Paul-Gilloteaux, P., and Basto, R. (2013). Centrosome amplification causes microcephaly. Nat. Cell Biol. *15*, 731–740.

42. Godinho, S.A., Picone, R., Burute, M., Dagher, R., Su, Y., Leung, C.T., Polyak, K., Brugge, J.S., Théry, M., and Pellman, D. (2014). Oncogene-like induction of cellular invasion from centrosome amplification. Nature *510*, 167–171.